

# Cerebrovascular Dysfunction in the Presence of Chronic Inflammation

---

By: Amy Randell

A thesis submitted to the School of Graduate Studies in partial fulfillment of the requirements for the degree of Masters of Science in Pharmacy.

School of Pharmacy

Memorial University of Newfoundland

St. John's, NL

April 2016

## **Abstract**

*Background:* Patients with autoimmune disease have increased incidence of stroke. Hemorrhagic stroke (HS) is associated with loss of cerebrovascular function, leading to micro-vessel burst, and hemorrhage. We believe chronic inflammation is involved in loss of cerebrovascular function and HS. We established a hypertensive-arthritis model in spontaneously hypertensive rats (SHR) fed either standard rodent diet (0.59% NaCl) (RD) or high salt diet (4% NaCl) (HSD) and compared them to non-inflamed SHR. *Methods:* Complete Freund's adjuvant (CFA) was injected into the left paw to induce mono-arthritis. Blood pressure and inflammation was monitored. At endpoint, animals were sacrificed and evaluated for HS while middle cerebral artery (MCA) was isolated for functional studies. *Results:* HS was observed in 90% of CFA-treated groups. The MCA of arthritic RD-SHR exhibited decreased ability to undergo pressure dependent constriction (PDC). All HSD-SHR showed a decreased response to PDC. However, arthritic HSD-SHR also demonstrated a diminished response to vasoactive peptides. *Conclusion:* HS occurring with CFA injection corresponds with loss of MCA function. Chronic HSD appears to further exacerbate vascular dysfunction in the MCA.

## **Acknowledgements**

I would like to first thank my father, whose passion for research inspired me to pursue graduate studies. It was his gentle encouragement and timely advice that helped me through many a frustrating day in the lab. I would also like to thank my mom who sat through many rants about why I thought science hated me but was always there cheering me on in the good times and bad throughout these past few years of my master's degree.

Secondly, I would like to thank my supervisor, Dr. Daneshtalab, who taught me more than I thought possible in a few short years. She was always patient while I was learning new techniques and clumsily breaking 80% of the lab's glassware. She was always available for a chat when I was having technical issues in the lab or if I needed someone to bounce ideas off of or just general advice about life decisions. She consistently tried to do everything she could to help her students succeed - and for that, I am very grateful for the opportunity to work under her supervision during my master's studies.

I would also like to thank my past/present lab mates, Jocelyn, Killol, Mercy and Kaetan. It was a pleasure working with all of you - and your help at some point or another with my project was invaluable.

I owe a very special thank you to Dr. Smeda who helped me troubleshoot some of my techniques and was always willing to share his wealth of knowledge about how I could streamline my lab techniques. His lab door was always open to me when I needed to borrow anything from bradykinin to pipette tips. He certainly saved the day on more than one occasion.

## Table of Contents

Abstract	1
Acknowledgements	2
Table of Contents	3
List of Figures	6
Abbreviations	7
Chapter One – Introduction and Statement of Problem	9
Chapter Two – Review of Literature	12
2.1    Inflammatory Arthritis	12
2.1.1    Rheumatoid Arthritis: Clinical Definition and Prevalence	12
2.1.2    Pathophysiology of Rheumatoid Arthritis	14
2.1.3    Animal Models of Rheumatoid Arthritis	19
2.2    Rheumatoid Arthritis and Cardiovascular Disease	22
2.2.1    Rheumatoid Arthritis and Hypertension	22
2.2.2    Rheumatoid Arthritis and Stroke	23
2.2.3    Interleukin-17 and Cardiovascular Disease	24
2.3    Dietary Sodium and Cardiovascular Disease	24
2.4    Cerebral Vascular Function	26
2.4.1    Endothelial Function	27
2.4.2    Vascular Smooth Muscle Control	33
2.4.3    Cerebral Blood Flow Autoregulation	37
2.4.4    Pressure Dependent Constriction	38
2.5    Hemorrhagic Stroke	39
2.5.1    Clinical Definition and Prevalence	40
2.5.2    Pathophysiology and Risk Factors	40

2.5.3	Animal Models of Hypertension and Stroke	42
2.5.3.1	SHR	42
2.5.3.2	SHRsp	43
2.6	General Hypothesis	45
Chapter Three – Materials and Methods		47
3.1:	Animals	47
3.2:	Experimental Design	47
3.3:	Preparation of Complete Freund’s Adjuvant	50
3.4:	Induction of Adjuvant Induced Mono-arthritis (AIA)	50
3.5:	Monitoring of Development and Progression of AIA	50
3.6:	Blood Pressure Measurement	51
3.7:	Identification of Cerebral Hemorrhage	51
3.8:	Sample Isolation, Tissue Processing and Histological Staining	52
3.9:	TNF alpha analysis	53
3.10:	Pressure Myograph Experiments	53
3.11:	Evaluation of acute IL-17a exposure (preliminary)	55
3.12:	Statistical Analysis	55
Chapter Four – Results		56
4.1:	Effect of diet and treatment on body weight	56
4.2:	Visual Determination of Mono-arthritis development	56
4.3	Histological Determination of Mono-arthritis	63
4.4	Quantitative progression of mono-arthritis and inflammation	63
4.5	Systolic blood pressure	67
4.6	Plasma TNFalpha levels	67

4.7 Determination of Cerebral Hemorrhage	75
4.8 Effects of Diet and Inflammation on Vascular Function in the MCA	75
4.8.1 Pressure Dependent Constriction	75
4.8.2 Endothelium-Mediated Vasodilation: Bradykinin Response	75
4.8.3 NOS Inhibition: L-NAME Response	76
4.8.4 Intracellular Ca <sup>2+</sup> Release: Vasopressin Response	76
4.8.5 PKC Activation – Phorbol Dibutyrate	76
4.9 Effects of Diet and Acute IL-17a Incubation on Vascular Function in the MCA	88
4.10 The Effect of Chronic Inflammation and Diet on MCA Response in the Presence of IL-17a	88
Chapter Five – Discussion	99
5.1 Limitations and Future Directions	110
References	113

## List of Figures

- Figure 2.1: Pathogenesis of Bone Destruction in Rheumatoid Arthritis
- Figure 2.2: Schematic Diagram of Endothelial-Mediated Vasodilation
- Figure 2.3: Schematic Diagram of Vascular Smooth Muscle Contraction
- Figure 3.1: Animal experimental timeline
- Figure 4.1: Change in weight of the groups expressed as change in weight from baseline.
- Figure 4.2: Hind paws of saline and CFA animals
- Figure 4.3: Arthritic index scores for saline vs CFA throughout experimental timeline
- Figure 4.4: Quantitative measurement of mono-arthritis using caliper measurements and water displacement
- Figure 4.5: Percent change from baseline of systolic blood pressures of SHR-SAL vs. SHR-CFAs on either HSD or RD
- Figure 4.6: Plasma concentration of TNF- $\alpha$  (pg/mL) per experimental group during the experimental period
- Figure 4.7: Evans Blue Dye Infusion
- Figure 4.8: Pressure dependent constriction in regular and high salt diet fed groups.
- Figure 4.9: Bradykinin response in regular and high salt diet fed CFA and SAL groups.
- Figure 4.10: L-NAME response in regular and high salt diet fed CFA and SAL groups.
- Figure 4.11: Vasopressin response in regular and high salt diet fed CFA and SAL groups.
- Figure 4.12: Response to PKC activation in regular and high salt diet fed CFA and SAL groups.
- Figure 4.13: Acute effects of IL-17a on pressure dependent constriction
- Figure 4.14: Acute effects of IL-17a on bradykinin response.
- Figure 4.15: Acute effects of IL-17a on L-NAME response
- Figure 4.16: Acute effects of IL-17a on vasopressin response.
- Figure 4.17: Acute effects of IL-17a on PKC activation

## Abbreviations

Ach	Acetylcholine	MI	Myocardial infarction
ACPA	anti-citrullinated protein antibody	MLC	Myosin light chain
AIA	Adjuvant induced arthritis	MLCK	Myosin light chain kinase
APC	Antigen presenting cell	mmHg	Millimeters of mercury
ATP	Adenosine triphosphate	MMP	Matrix metalloprotease
BBB	Blood brain barrier	NO	Nitric oxide
CaM	Calmodulin	NOS	Nitric oxide synthase
cAMP	Cyclic adenosine monophosphate	nNOS	Neuronal nitric oxide synthase
CFA	Complete freunds adjuvant	NOX-4	NADPH oxidase-4
cGMP	cyclic guanine monophosphate	PDC	Pressure dependent constriction
CRP	c-reactive protein	PGI <sub>2</sub>	Prostaglandin I <sub>2</sub>
<i>CTLA4</i>	cytotoxic T lymphocyte antigen 4	PIP <sub>2</sub>	phosphatidylinositol 4,5-bisphosphate
CV	Cardiovascular	PKC	Protein kinase C
CVA	Cardiovascular accident	PKG	Protein kinase G
CVD	Cardiovascular disease	PLC	Phospholipase C
DAG	Diacyl glycerol	<i>PTPN22</i>	protein tyrosine phosphatase, non-receptor type 22
EAE	experimental autoimmune encephalomyelitis	RA	Rheumatoid arthritis
EB	Evans blue	RANKL	receptor activator of nuclear factor kappa B ligand
EDHF	endothelial derived hyperpolarizing factor	RD	Regular Diet
ELISA	enzyme-linked immunosorbent assay	RF	Rheumatoid factor
EnNaC	endothelial sodium channel	ROS	Reactive Oxygen Species
eNOS	Endothelial nitric oxide synthase	RVLM	rostral ventral lateral medulla
ESR	Erythrocyte Sedimentation Rate	SAL	Saline
GTP	Guanine triphosphate	SDR	Sprague-Dawley Rat
H&E	hematoxylin and eosin	Ser19	Serine 19

<i>HLADRBI</i>	Human Leukocyte Antigen class II antigen DR $\beta$ 1	SHR	Spontaneously hypertensive rat (stroke resistant)
HS	Hemorrhagic Stroke	SHRsp	Spontaneously hypertensive rat (stroke prone)
HSD	4% NaCl High Salt Diet	SR	Sarcoplasmic reticulum
ICH	Intracerebral hemorrhage	T-reg	Regulatory T-cell
IgG	Immunoglobulin G	TGF- $\beta$	transforming growth factor beta
IL	Interleukin	Thr495	Threonine 495
IL-17R	Interleukin-17 receptor	TNF- $\alpha$	tumor necrosis factor alpha
IFN- $\gamma$	Interferon gamma	TRPC	Transient Receptor Potential Canonical Channel
iNOS	Inducible nitric oxide synthase	TRPV	Transient Receptor Potential Vallinoid Channel
L-NAME	<i>N</i> <sub>ω</sub> -nitro-L-arginine methyl-ester	VECM	Vascular Extracellular Matrix
m-BSA	Methylated bovine serum albumin	VOC	Voltage-operated Calcium channel
MCA	Middle cerebral artery	WKY	Wistar-Kyoto Rat

## **1.0: Introduction and Statement of Problem**

Arthritis is a long term, physically debilitating disease that is the second most common chronic condition in Canada, with an annual cost of \$33 billion in related health care costs (1). Rheumatoid arthritis (RA) is one of the more severe forms of arthritis. As a chronically progressive inflammatory disease, it can attack one or more joints, leading to joint degradation and loss of mobility. In addition to the destruction of joints and cartilage, the pathology of arthritic disease takes a progressive toll on many other tissues in the body as it produces diffuse inflammation in the lungs, pleura, pericardium, and sclera (2). The leading cause of death in RA patients is not due to the arthritis itself however, but due to cardiovascular (CV) complications, leading to a 3-fold increase in associated mortality compared to the general population (3-5).

The risk of ischemic heart disease and myocardial infarction has been extensively studied in RA, but more recent and fundamental studies indicate significant risk of stroke in autoimmune arthritis, with patients with RA having a 30% increase in stroke over age-matched controls (6, 7). Of all stroke subtypes, hemorrhagic stroke (HS) has the highest mortality rate, approaching 50% within the first month (8, 9). The risk of death from the first incidence of stroke has also been shown to be significantly higher for RA patients compared to non-arthritic subjects (3, 10, 11). Evidence suggests that traditional risk factors of cardiovascular disease (CVD), (hypertension, smoking, dyslipidemia, and insulin resistance) are more prevalent in the RA population (12). There is also an increased risk of myocardial infarction, CV morbidity, and CV mortality in RA patients (13). The evidence in the literature suggests that approximately two-thirds of patients with primary cerebral hemorrhage have pre-existing or newly diagnosed hypertension (8, 14). The presence of hypertension, either salt-sensitive or not, is in itself a key risk factor for HS and may therefore be a key component in the likelihood of RA patients developing fatal HS.

Animal models have been used for decades to study the pathogenesis of arthritis akin to RA (the adjuvant induced arthritis rats; AIA rats) (15-17). Similarly, the stroke-prone spontaneously hypertensive rat (SHRsp) is widely used to study HS (18). However, there is currently no model that exemplifies the chronic development of HS subsequent to chronic systemic inflammation induced by mono-arthritis and longstanding hypertension. Although, chronic hypertension and chronic inflammation have both been independently linked to various degrees of vascular dysfunction (19-21), the impact of both of these factors together on vascular function has not yet been investigated. In particular, functional studies of the MCA in a chronically inflamed spontaneously hypertensive rat (SHR), has not yet been studied.

Autoregulation of cerebral blood flow is governed by a variety of physical cues (including shear stress and pressure) and endogenous chemical stimuli (such as peptides, nucleotides and cytokines)(22, 23). Pressure dependent constriction (PDC) is one such mechanism by which the cerebral vasculature ensures adequate and controlled perfusion of the small arteries feeding the brain (24). As perfusion pressures increase, the blood vessel reflexively constricts to prevent over-perfusion of the downstream vasculature and maintains a constant flow. Studies in pre- and post-stroke SHRsp have revealed that after hemorrhagic stroke has occurred, the PDC mechanism is lost in the middle cerebral artery (MCA) along with signs of renal failure (18).

Cytokines and growth factors are able to genetically alter the functioning of the vascular endothelium, directly affecting the expression of various activators of endothelial function over a sustained period. This can potentially lead to the modulation of local second messengers such as changes in intracellular  $Ca^{2+}$  concentrations and cyclic nucleotides (23). As a result, vascular functioning becomes altered. Kessler et al showed that proinflammatory cytokines (interleukin-

1 $\beta$ , and tumor necrosis factor- $\alpha$  (TNF- $\alpha$ ) and lipopolysaccharide decreased endothelial-mediated vascular relaxation through decreased production of endothelial derived hyperpolarizing factor (EDHF). Interestingly, this coincided with increased expression of nitric oxide synthase (NOS), resulting in increased nitric oxide (NO) production (25). In this way, the surge of circulating pro-inflammatory cytokines can possibly have a profound impact on the cerebral vascular functioning, leading to vasoconstriction or vasodilation.

Our objective was to address this gap in knowledge by creating a hypertensive-arthritic animal model with the induction of adjuvant mono-arthritis in the stroke-resistant SHR, a strain unique in that it normally develops spontaneous hypertension but does not spontaneously develop stroke. We planned to determine whether induction of monoarthritis increases the propensity for HS in the SHR strain. We also chose to investigate the impact of high salt diet (4% NaCl) on the severity of systemic inflammation and HS. We further examined the impact of chronic inflammation and concurrent hypertension on the ability of the MCA to perform PDC and its responsiveness to vasoactive peptides (bradykinin, vasopressin), NOS inhibition (*N*<sub>ω</sub>-nitro-L-arginine methyl-ester; L-NAME) and protein kinase C (PKC) activation (phorbol dibutyrate) in order to elucidate underlying mechanisms of vascular dysfunction in the hypertensive arthritic rat model.

## **2.0: Review of Literature**

### ***2.1: Inflammatory Arthritis***

In Canada, more than 4.6 million people have reported that they suffer from one or more of the various types of arthritis. Although two-thirds of the people who are affected are women, it is the third most common cause of disability in the country among men (26). Inflammatory arthritis is recognized by the surge in migration of immune cells including monocytes/macrophages, lymphocytes and granulocytes to the synovial lining of the affected joint (27). Enhanced proliferation of synovial fibroblasts at the affected joint(s) also sustains the inflammatory process and helps to initiate and perpetuate joint degeneration (27, 28). This process translates to pain, redness and swelling of the joint(s) which then eventually results in decreased mobility and joint degradation (29). In spite of the fact that the joint inflammation is often fully reversible, the resulting damage and degeneration of the joint is not, making inflammatory arthritis a chronically progressive degenerative disease (29-31). While 115-271 in every 100,000 people are diagnosed with inflammatory arthritis each year, 70% of these go on to receive a diagnosis of Rheumatoid Arthritis (32).

#### *2.1.1: Rheumatoid Arthritis: Clinical Definition and Prevalence*

Rheumatoid Arthritis (RA) affects approximately 300,000 Canadians with a frequency of about 1 in 100 people (26). Women are more than twice as likely as men to develop RA, and around 30% of patients will stop working within two years after the onset of disease, mainly due to the physically debilitating and rapidly progressing effects of this condition (33). This leads to a large economic impact due to costs to the healthcare system as well as lost productivity. RA can present at any age, but the majority of patients will present between the ages of 40-60 (26).

RA is most commonly recognized as being a chronic, symmetrical inflammatory condition of the joints that can also affect various other organ systems over time (2). It is characterized by three main changes within the affected joints; inflammation and proliferation of the synovial tissue (ie; pannus formation), thinning of the articular cartilage, and subsequent focal erosion of the subchondral bone (34). It is the pannus, a highly proliferative cellular membrane of granulation-reactive fibrovascular tissue, that extends into the articular cartilage of the joint and proceeds to break down the bone. Subsequent structural damage to the joint itself is carried out by osteoclasts, multinucleated giant cells that are specially designed to degrade the mineralized components of the cartilage and underlying bone, where they localize to the pannus-bone interface (34). The inflammatory infiltrate of the pannus is comprised of six main types of immune cells; namely T cells, B cells, plasma cells, dendritic cells, mast cells and granulocytes (34). Precipitating factors that trigger this dysfunctional burst of inflammatory activity synchronized with diminished self-tolerance are widely unknown. However, genetics, environmental factors such as cigarette smoking and immunologic factors are assumed to play a role (26).

As such, RA still presents as a highly heterogenous disease with largely unknown etiology. Diagnosis is made based on a number of criteria evaluating the number of joints affected (with at least one joint showing signs of clinical synovitis which can not be explained by other causes), and the presence or absence of certain serological markers such as Rheumatoid Factor (RF) and Anti-Citrullinated Protein Antibody (ACPA) (35). The duration of symptoms (being greater than six weeks) and elevations in circulating acute phase reactants such as C-reactive Protein (CRP) and Erythrocyte Sedimentation Rate (ESR) (35) are also used as indicators of severity of the disease. It is classified as an autoimmune disease due to the presence

of RF, which serves as an autoantibody to the Fc fragment of immunoglobulin G (IgG). However, research shows that increased ACPA activity is more relevant to the autoimmune disease process than RF (36). Citrullination, the enzymatic conversion of the amino acid arginine to citrulline, is a critical step in development of autoimmunity as this leads to the recognition of several highly expressed proteins of the synovium (fibronectin, collagen type II, vimentin, fibrin) by ACPA during the inflammatory process (37). Therefore the disease development can be characterized in three separate phases starting with immune sensitization, proceeding to an inflammatory response which ends in bone and joint erosion (37). In some cases, the initial phase (lymphoid/pre-articular phase) of disease development may present 10-15 years before clinical signs and symptoms of RA become apparent (36, 38).

### *2.1.2: Pathophysiology of Rheumatoid Arthritis*

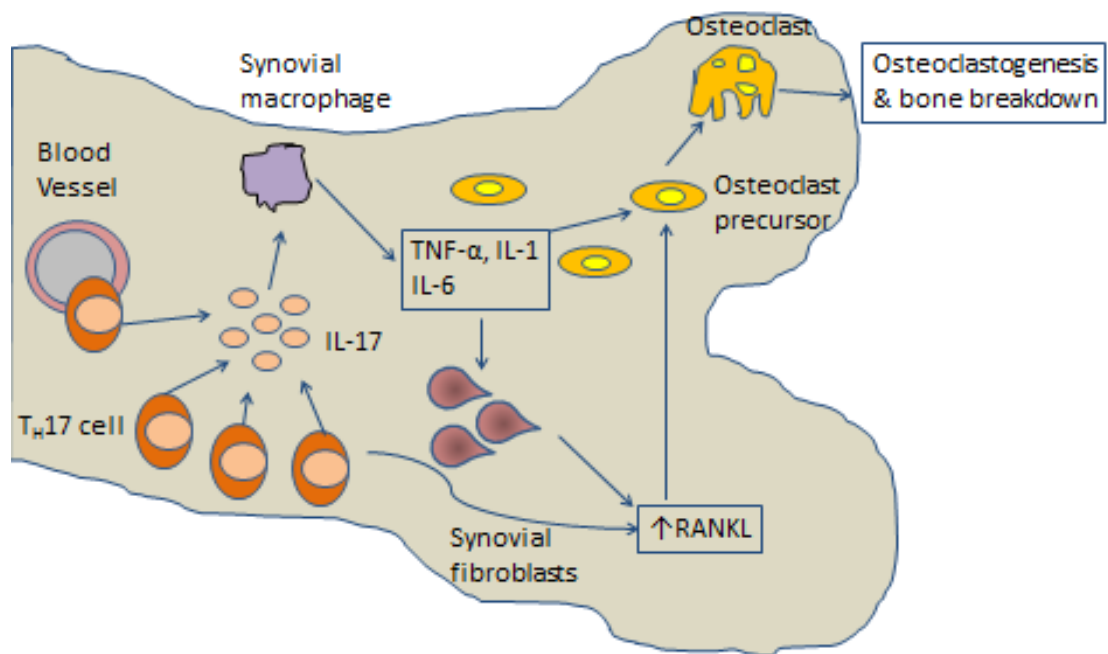
Predisposition to the development of RA has been linked to several genetic susceptibility loci (such as *HLADRB1* (Human Leukocyte Antigen class II antigen DR $\beta$ 1), *PTPN22* (protein tyrosine phosphatase, non-receptor type 22) and *CTLA4* (cytotoxic T lymphocyte antigen 4), some of which are immune-regulated (39). Environmental factors that have been correlated to increased risk of RA development are cigarette smoking (40), caffeine consumption, and obesity (41) while a Mediterranean Diet and diets rich in antioxidants seem to have protective effects (42). Circulating levels of RF and/or ACPA have been shown to be increased for several years prior to the development of symptoms, leading to increased levels of acute phase reactants and inflammatory mediators such as cytokines and chemokines. While the final culmination of events that leads to arthritic symptoms are largely unknown, retrospective studies have identified infection, trauma and stress to be triggers prior to clinical manifestation (38).

Following immune activation, the innate and acquired immune systems work concurrently to perpetuate the inflammatory process. Dendritic cells in the joint become activated by exogenous and autologous antigens while antigen presenting cells (APC's) (including dendritic cells, macrophages and activated B cells) start binding to arthritis-associated antigens (43, 44). Meanwhile, CD<sup>+</sup> T cells located in the synovium begin secreting IL-2 and IFN- $\gamma$  locally. Once activation of B-cells and T-cells has occurred, a large amount of inflammatory cytokines (such as IL-12, 15, 18 and 23) (37) and CC and CXC chemokines are produced which further feeds back into the cycle to increase T-cell, B-cell and macrophage activation. The increased activation further drives the inflammatory response by production of IFN- $\gamma$ , IL-2, 12, 18 and granulocyte macrophage-colony stimulating factor (43, 44). Another important function of activated macrophages and dendritic cells is to provide the necessary inflammatory setting to trigger activation of the Th17 pathway. This is initiated by a surge in production of TGF- $\beta$ , IL-1 $\beta$ , 6, 21 and 23 which together cause a shift in T-cell homeostasis to diminish production of regulatory T-cells (Tregs) and increase differentiation of the Th17 subtype, shifting the balance towards an inflammatory milieu (37).

Figure 2.1: Pathogenesis of Bone Destruction in Rheumatoid Arthritis. In RA, the synovium of the joint becomes inflamed and begins to destroy the underlying bone. Bone destruction is mediated by osteoclasts. Increased levels of RANKL in the synovium causes the induction of osteoclasts. Th17-cell infiltration into the joint produces IL-17 which activates synovial macrophages to produce several other pro-inflammatory cytokines such as TNF- $\alpha$ , IL-1 and IL-6, which also increase proliferation of osteoclasts. IL-17 also triggers the activation of synovial fibroblasts which further increases expression of RANKL, further perpetuating bone degeneration.

*Adapted from Takayanagi, 2007.*

Figure 2.1: Pathogenesis of Bone Destruction in Rheumatoid Arthritis



In RA, the Th17 pathway is responsible for the production of IL-17A, -17F, -21 and -22 as well as TNF- $\alpha$  to perpetuate the inflammatory process and exacerbate bone erosion and joint degeneration (45, 46). The IL-17 receptor (IL-17R) is widely expressed on many of the immune cells involved in RA pathology including fibroblasts, endothelial cells, epithelial cells and neutrophils, lending evidence to the ubiquitous role of this cytokine in the inflammatory disease process (47). IL-17A acts synergistically with TNF- $\alpha$  to further activate synovial fibroblasts, chondrocytes and osteoblasts and suppress differentiation of Tregs (46, 48). Aside from the diffuse production of pro-inflammatory mediators, the Th17 pathway is critical in joint degeneration. IL-17 produced in the synovium serves to activate receptor activator of nuclear factor kappa B ligand (RANKL) signaling in multiple ways. RANKL activity is important because it is the main mechanism by which osteoclast progenitor cells become activated to produce osteoclasts, which actively mediate bone destruction (37, 48). Although Th17 cells express RANKL on their cellular membrane, the main mechanism by which signaling through this ligand is initiated is through the actions of activated synovial fibroblasts. IL-1, -6 and -17, as well as the actions of TNF- $\alpha$  (among other pro-inflammatory cytokines) are able to directly induce RANKL signaling to cause joint damage although IL-1, -6 and TNF- $\alpha$  are also able to activate osteoclast progenitor cells independent of RANKL signaling (37). These pro-inflammatory cytokines also promote the continuing differentiation of B-cells and cause release of several different matrix metalloproteases (primarily MMP-1, -3, -8, -13, -14 and -16) (37) which can also activate osteoclasts but serve to degrade the cartilage in the inflamed joints (49). As Th-17 cells do not synthesize IFN- $\gamma$ , a suppressor of RANKL signaling, bone metabolism and osteoclastogenesis is further enhanced (50) (Figure 2.1).

### *2.1.3: Animal Models of Rheumatoid Arthritis*

Animal models are widely used in the investigation of multiple types of arthritis. They are an invaluable tool in the study of the pathogenesis of various aspects of arthritic disease but are also commonly used to test treatments for these same conditions. Rodent models of arthritis have two main limitations; 1) rodent arthritic process progresses more rapidly than human arthritic disease necessitating caution when interpreting results of acute pathological changes as opposed to chronic changes and 2) joint inflammation in rodents is often characterized by bone resorption and formation, which is not consistent with human inflammatory arthritic disease, as it is characterized by bone erosion only (51). The most common types of RA animal models include adjuvant arthritis (AA), rat type II collagen arthritis and antigen arthritis (51).

Adjuvant arthritis is one of the most common experimental modalities for studying RA disease progression and experimental treatments. Adjuvant injection results in a reproducibly rapid and robust, polyarthritic immune response with mild cartilage erosion and significant bone resorption (51-53). Although the exact mechanism of pathological response has not been fully elucidated, data suggests that the immune response may involve reactivity to proteoglycans produced in cartilage, heatshock proteins or even the rodent's intestinal bacterial flora (54-56). The most commonly used rat strain in adjuvant arthritis is the male Lewis rat. Female Lewis rats are also commonly used, however they produce a more variable disease progression (57). Male Sprague Dawley and Wistar rats are also frequently used in this model (58). Arthritis induction is initiated by either tail-base or footpad injection of Complete Freund's Adjuvant (CFA) containing mycobacterium suspended in an oily vehicle or a synthetic compound, N,N-dioctadecyl-N',N'-bis(2-hydroxyethyl) propanediamine, suspended in mineral oil or olive oil (59). Adjuvant activity is a result of sustained release of antigen from the oily deposit and stimulation of a local

innate immune response resulting in enhanced adaptive immunity. Footpad injection may be preferred to tail-base injection as it represents a moderate arthritic response, compared to the more severe inflammatory response produced by tail-base injection (60). Additionally, it allows monitoring of the initial acute local inflammatory response as well as the tracking of arthritic changes as the inflammation transitions to a chronic, systemic inflammatory response (51). Monitoring of inflammatory changes to the hind paw are typically conducted every second day starting at baseline by caliper measurements at the ankle joint, and/or water volume displacement measurement of the entire paw. Signs of clinical, systemic disease are usually apparent by Day 9 of the experimental protocol (51).

Rat collagen-induced arthritis (CIA) is commonly induced by footpad or tail-base injection with homologous or heterologous type II collagen emulsified in incomplete Freund's adjuvant (IFA), producing an inflammatory process that mimics the joint degradation present in human RA more closely than adjuvant arthritis. Polyarthritis progression is characterized by diffuse cartilage degeneration, localization and deposition of immune complexes at the joint surface, moderate to severe synovitis and osteodegeneration (51, 61, 62). In this model, females tend to be more susceptible to arthritis development (as in human RA) with a severe-erosive poly-arthritic syndrome developing 14-21 days post-injection due to the self-sensitization to articular collagen (61, 63). As such, articular cartilage degeneration is the primary target of the disease process, with significant bone damage but minimal loss in paw volume (64).

CIA differs from AA in that the immunogenic response is primarily mediated by B-cell activation to a greater extent than adjuvant arthritis (61). Also, the more extensive pannus formation at the articular sites correlates better to human RA as well. In spite of this, the AA method has been favored in the past due to the wealth of data that already exists with this model

(51). Regarding arthritis induction protocols, the AA model frequently only involves a single injection while CIA requires a booster injection on the seventh day of the experimental timeline (64). In spite of this, AA exhibits an earlier onset and more rapid plateau of inflammation than CIA, which may take up to 21 days to see a maximal inflammatory response (64). Although polyarthritis is evident in both models, only the inflammation in the injected paw is relevant in the AA model whereas inflammation of both ankles and knees of CIA rats are considered significant (64). This may cause undue discomfort and stress to the rats, from an animal welfare point of view, especially since both models produce similar pathology scores (64). Both CIA and AA rats have shown to have similar levels of circulating (serum) pro-inflammatory mediators (such as IL-1 $\beta$ , TNF- $\alpha$ , IL-6, iNOS and MMP-13) however mRNA for cytokine levels in the joint are significantly elevated in the AA model compared to CIA (64). Additionally, total neutrophil counts are 5-7-fold higher in AA rats (compared to control) whereas the CIA model produces a more modest increase in neutrophils at 3-4 times that of control (64). Therefore, both methods are commonly used, but there are several distinct differences between the AA and CIA models.

Antigen arthritis is a mechanism of arthritis induction that is amenable to virtually any animal model. It involves the subcutaneous or intradermal injection of a positively charged antigen that binds to negatively charged cartilage and remains present in the joint. Most commonly the cationic antigen used is methylated-bovine serum albumin (m-BSA), which after binding to the cartilage, elicits binding of antibody complexes which then causes complement activation and local cartilage degeneration (51, 57). This model is commonly used in various mouse strains (65) but also in rats (66), guinea pigs (67) and rabbits (68). Some protocols require habitual injection at weekly or twice-weekly intervals as well as combination of m-BSA

with CFA for injection directly into the selected joint. By the end of two weeks, severe cartilage destruction has already occurred due to pannus formation (51).

## ***2.2: Rheumatoid Arthritis and Cardiovascular Disease***

One of the leading causes of death among individuals with RA is due to cardiovascular disease (69). RA patients have an increased risk of myocardial infarction (MI), heart failure, stroke and peripheral vascular disease (69-72). Although non-steroidal anti-inflammatory drug (NSAID) use in the RA population has been associated with significant cardiovascular toxicity and associated MI risk (73), it is becoming more commonly accepted that increased CV morbidity and mortality rates in this population are likely not completely attributable to RA treatments (73, 74). After controlling for other modifiable and non-modifiable traditional risk factors such as increased body mass index, diabetes, smoking, diet and gender, multiple large-scale trials still showed an increased risk for CV events in the RA population that was not otherwise explained (75-78). This suggests that there is an increased risk of CV disease conferred by the presence of RA itself. It has been proposed that the actions of high levels of circulating pro-inflammatory cytokines linked to RA pathogenesis (IL-6 and TNF- $\alpha$ ) may be partially responsible for this increased risk. IL-6 is involved in increasing levels of acute phase reactants and is blamed, along with TNF- $\alpha$ , for altering the composition of circulating lipid particles contributing to dyslipidemia and atherosclerotic plaque destabilization (37, 79).

### ***2.2.1: Rheumatoid Arthritis and Hypertension***

A recent study examined CV risk factors present in a group of 73 RA patients and found that hypertension was present in more than 50% of these individuals (80). Another observational study from the United Kingdom, showed hypertension (defined as systolic blood pressure of  $\geq$

140 mmHg and/or diastolic blood pressure of  $\geq 90$  mmHg) was identified in 70.5% of the 400 RA participants. Of those identified as being hypertensive, only 60.6% were treated with anti-hypertensive medications and only 21.8% of those treated were meeting their blood pressure target (81). Lack of appropriate blood pressure control was attributed to both poor medication adherence and a lack of anti-hypertensive therapy optimization (such as, sub-therapeutic dosing or inappropriate drug selection). This demonstrates the high level of prevalence of hypertension among the RA population. Although many other investigators have confirmed that hypertension is highly prevalent in RA (82-84), the incidence of hypertension compared to the general population is also greater in RA (84). Proposed mechanisms of this increased risk include increased arterial stiffness (85), anti-rheumatic drug therapy (including NSAIDs, corticosteroids and some disease-modifying anti-rheumatic drugs) and abnormal vascular function characterized by decreased elasticity in small and large arteries associated with increased vascular resistance (86).

### *2.2.2: Rheumatoid Arthritis and Stroke*

Multiple epidemiological studies have shown that risks for cerebrovascular accidents (CVA) are also increased in RA patients (77, 87). This data can be partially explained by the high prevalence of hypertension in RA populations, which is the most important modifiable cerebrovascular risk factor for stroke development (88). RA has also recently been identified as an independent risk factor for accelerated atherosclerosis, which is a major risk factor for ischemic stroke (77, 89, 90). Along with increased risk of stroke, there is a 50% greater chance of case fatality associated with stroke development in the RA cohort (89). Although approximately 80% of stroke are of the ischemic subtype and strongly linked to atherosclerotic pathology, around 20% of stroke are hemorrhagic which are characterized by cerebral vessel

burst and high mortality (91). The etiology of hemorrhagic stroke is largely unknown, especially in the setting of RA.

### *2.2.3: Interleukin-17 and Cardiovascular Disease*

While the link between cardiovascular disease and endothelial dysfunction and inflammation has already been well established, the exact role of individual circulating cytokines in CV disease remains largely unknown (92, 93). Reports have indicated that high circulating levels of TNF- $\alpha$  and IL-6, as seen in RA, are associated with the progression in cardiovascular damage after controlling for traditional cardiovascular risk factors (19, 94). However, it is unclear whether these cytokines play a role in the development of primary vascular dysfunction. Recently, the role of IL-17 in RA progression as well as CV disorders has received much attention (95-97). In non-RA animal models, IL-17 has been associated with accelerated myocardial fibrosis, atherosclerosis, endothelial dysfunction and increased superoxide formation (97-99). It has been observed that IL-17 may induce the phosphorylation of Thr495 of eNOS at its inhibitory site, causing a conformational change in the enzyme which interferes with calmodulin binding and diminishes enzyme activity (100, 101). This is one proposed mechanism by which IL-17 may play a role in endothelial dysfunction. However, more information is needed regarding the direct vascular effects of IL-17.

### *2.3: Dietary Sodium and Cardiovascular Disease*

The deleterious effect of high dietary sodium intake on the cardiovascular system has been widely accepted (102, 103). In salt-sensitive individuals, it plays a role in hypertension development (102, 104) through several mechanisms including extracellular volume increase, increased cardiac output (105), activation of the sympathetic nervous system (104) and impaired

hormonal responses through the renin-angiotensin-aldosterone system (106, 107). However, in normotensive individuals high salt diets can also cause target organ damage to the heart, kidneys, arteries and the rostral ventral lateral medulla (RVLM - the area of the brain that mediates sympathetic outflow to regulate blood pressure) (108). High salt intake is correlated to increased left ventricular wall thickness and mass, regardless of whether the patient is hypertensive or normotensive (109) and reduced renal function (110). Studies using rodents have shown that high salt diet can increase the sensitivity of excitatory neurons in the RVLM, increasing sympathetic response to various stimuli (111), including exercise (112). This leads to greater variability in blood pressure, which is also a risk factor for target organ damage and CV events (113, 114).

Increased vascular and arterial stiffness is another predictor of CV events which has been correlated to a high sodium diet (115). Vascular stiffening is the result of vascular remodeling that becomes augmented in the presence of various external stimuli, including a high sodium diet, certain comorbidities such as hypertension and dyslipidemia, and the normal aging process (115, 116). This remodeling is characterized by vascular hypertrophy (inward remodeling) and altered composition of the VECM leading to more collagen deposition and decreased presence of elastin (117, 118). This results in decreased vascular compliance and vascular dysfunction.

There are several mechanisms by which increased sodium intake is proposed to cause generalized vascular dysfunction. Numerous studies using rodents, possibly including our own, have linked endothelial dysfunction to elevated dietary sodium (119-122), irrespective of blood pressure. Increased generation of ROS (including superoxide) leading to diminished NO bioavailability are the most commonly proposed mechanisms (119-122). In addition, studies using cell culture techniques have also demonstrated that small increases in intracellular sodium

concentrations can alter the fundamental mechanics of the endothelial cell, causing stiffening of the endothelial cortex, by changing the cell's transcriptome (123-125). This leads to decreased NO production, and altered barrier functions, resulting in increased flux of plasma across the microvascular endothelial barrier (126). This process is thought to be fed by the endothelial sodium channel (EnNaC) which is involved in a “feed-forward” loop with extracellular Na<sup>+</sup> concentration. In the setting of high extracellular Na<sup>+</sup> concentrations, the EnNaC becomes more abundantly expressed on the cell surface, thus allowing increased Na<sup>+</sup> influx into the cell (127). This in turn increases intracellular Na<sup>+</sup> levels which stabilizes the interaction between certain cortical cytoskeletal proteins (actins) leading to the stiffening of the cell (128). In this way, increased plasma Na<sup>+</sup> concentrations are able to have damaging effects on the vasculature of individuals, regardless of their level of salt sensitivity or salt resistance.

#### ***2.4: Cerebral Vascular Function***

Due to the critical functions of the brain and fragility of cerebral blood vessels, blood flow must be tightly regulated. In humans, the brain requires 15% of cardiac output and 25% of total body glucose in order to maintain day-to-day functions. In addition, the brain receives nearly one fifth of total body oxygen, extracting about 50% of the oxygen carried in arterial blood (129). This large blood flow requirement is proportional to the constant amount of oxygen and glucose required for brain mitochondrial cells to carry out oxidative phosphorylation to produce adenosine triphosphate (ATP), generating the energy required to maintain normal brain function (130). There are a number of factors that directly affect cerebral circulation including metabolic and chemical (CO<sub>2</sub> and O<sub>2</sub>) needs of the brain as well as pressure mediated autoregulatory functions (131). In the setting of high neuronal activity, the brain's metabolic needs increase, leading to increased blood flow to the higher activity regions of the brain in a

process called functional hyperemia (132). Chemical influences such as hypocapnia (low CO<sub>2</sub>, leading to tissue alkalosis) caused by hyperventilation or hypoxia (low O<sub>2</sub>, leading to tissue acidosis) caused by respiratory depression can also lead to a decrease or increase in cerebral blood flow respectively, in order to maintain homeostasis (131). Finally, pressure-mediated autoregulation refers to the ability of the certain vascular beds (including the cerebral vasculature) to maintain constant blood flow to downstream arterioles in the setting of pressure variations. In the setting of low perfusion pressures, cerebral arteries will reflexively dilate and alternatively constrict in times of pressure surges (133). The evidence in the literature suggests that a combination of neuronal, astrocytic and vascular signaling patterns allow the brain to maintain hemodynamic stability and respond to the brain's changing needs for nutrients and oxygen (134). However, the remainder of this section will focus solely on the cerebral vascular function as it pertains to pressure mediated blood flow autoregulation.

#### *2.4.1: Endothelial Function*

The vascular endothelium is a dynamic layer of cells that is crucial in the control of vascular tone. Originally, the critical significance of the vascular endothelium was somewhat serendipitously discovered by Furchgott and Zawadski, who noted that helical strips of rabbit thoracic aorta produced a graded contractile response to increasing concentrations of acetylcholine (ACh) (135). However, when using a ring preparation of the same thoracic aorta, they observed a rapid and potent vasodilatory response, realizing that when producing their helical strip of aorta, they had been accidentally rubbing off the endothelial layer. This led them to acknowledge the importance of the endothelium in vascular relaxation responses (135). The study also concluded that activation of muscarinic receptors on the endothelium by ACh triggered the release of a diffusible substance which caused smooth muscle relaxation. Later

work by Furchgott, Ignarro and Murad identified this diffusible substance as nitric oxide (NO), later earning them a Nobel Prize (136). Over time, the identification of several other endothelial-derived mediators of vascular tone have been described, including various prostaglandins/prostanoids (prostacyclin and thromboxane A<sub>2</sub> being the most commonly recognized), endothelial derived hyperpolarizing factor (EDHF), endothelin (a powerful vasoconstrictor) and reactive oxygen species (ROS) (137-141). However, to date, NO is the most well studied and prominent endothelial modulator of vascular tone (136).

Nitric oxide is synthesized in the vascular endothelium as a derivative of L-arginine by the enzyme, Nitric Oxide Synthase (NOS). It is primarily responsible for maintaining vasodilation within blood vessels. However, it also prevents platelet and leukocyte adhesion, and may even play a role in the prevention of hyper-proliferation of smooth muscle cells (142). Within the body, there exists three main types of NOS; neuronal NOS (nNOS), inducible NOS (iNOS) and endothelial NOS (eNOS). Within the vasculature, eNOS is the most diffusely expressed NOS isoform and is constantly producing a baseline amount of NO. Enzymatic activity is positively regulated in a Ca<sup>2+</sup>-calmodulin-dependent manner by shear stress and by various receptor-bound agonists (143). Activation of protein kinase C (PKC) inhibits this Ca<sup>2+</sup>-calmodulin-mediated activation of eNOS (144). In addition, certain cytokines are also able to diminish mRNA expression and enzymatic activity of eNOS as well modulate the production of various endothelial agonists (142).

Stimuli including shear stress, hypoxia, pressure, and numerous chemical mediators such as catecholamines, nucleotides (eg. adenosine, adenosine triphosphate), peptides (eg. bradykinin, vasopressin, endothelin), fatty acids, proteases (eg. thrombin, trypsin) growth factors and cytokines can directly activate the vascular endothelium to produce endothelial modulators that

may increase or decrease endothelial-mediated relaxation (23). Alternatively, cytokines and growth factors are also able to modulate the expression of some of the above mentioned chemical mediators. To activate NO release, some of these chemical agonists bind to their respective G-protein-linked receptors on the vascular endothelium. The downstream signaling pathway includes G-protein coupling to phospholipase C (PLC) which activates inositol trisphosphate (IP<sub>3</sub>) and diacylglycerol (DAG) leading to intracellular and extracellular Ca<sup>2+</sup> mobilization and Ca<sup>2+</sup> influx through nonselective cationic channels. This intracellular Ca<sup>2+</sup> increase allows Ca<sup>2+</sup>-calmodulin binding, which is a critical step in the activation of eNOS and thus the production of NO (23).

Production of NO by NOS enzymes requires nicotinamide adenine dinucleotide phosphate (NADPH) as an electron donor to convert L-arginine to N<sup>o</sup>-hydroxyl-L-arginine. Further oxidation yields NO and L-citrulline. Cofactors required for this enzymatic conversion include tetrahydrobiopterin, flavin adenine dinucleotide (FAD), flavin mononucleotide (FMN), and heme (142). Due to the highly soluble nature of NO, it readily diffuses across the cell membranes and binds to soluble guanylate cyclase to catalyze the conversion of cyclic glutamyl-monophosphate (cGMP) to glutamyl-5'-triphosphate (GTP), activating protein kinase G (PKG). PKG initiates the phosphorylation of a series of cellular targets which causes a decrease in [Ca<sup>2+</sup>]<sub>i</sub> which produces vasodilation (145). Alternatively, NO has also been shown to cause hyperpolarization of vascular smooth muscle through the direct activation of Ca<sup>2+</sup>-dependent K<sup>+</sup>-channels (K<sup>+</sup><sub>Ca</sub>), independent of cGMP (146).

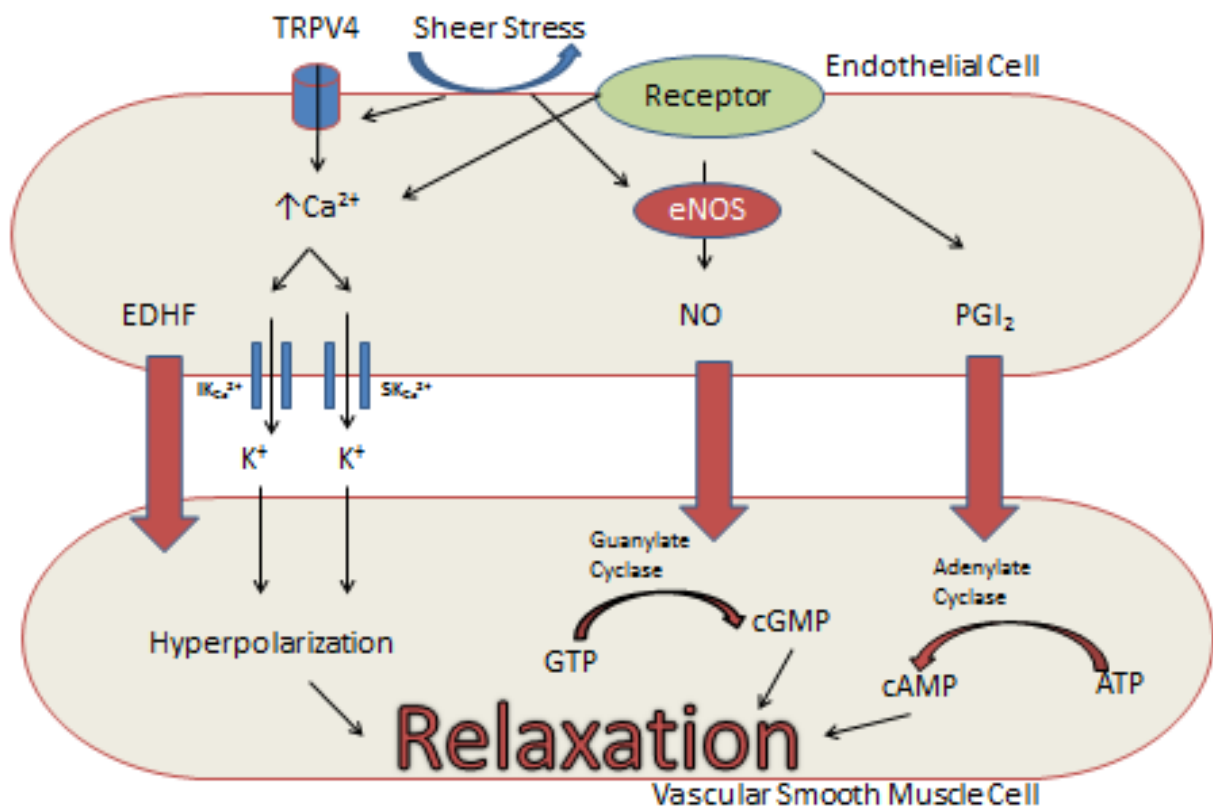
Another pathway of endothelial-dependent relaxation that does not lead to the release of intermediate factors such as EDHF, NO or PGI<sub>2</sub> is through various cation channels expressed on the vascular endothelium, but can be found on the vascular smooth muscle as well (147).

Transient receptor potential (TRP) channels are a family of  $\text{Ca}^{2+}$  permeable ion channels that regulate  $[\text{Ca}^{2+}]_i$  and cell membrane potential (148). As such, activation of these channels leads to an increase in  $[\text{Ca}^{2+}]_i$  which can then trigger changes in vascular tone, permeability, and even remodeling (148). Activation of these channels occurs through both capacitative (decrease in  $[\text{Ca}^{2+}]_i$  stores) and non-capacitative (signaling mediators including DAG, and 5,6-epoxyeicosatrienoic acid, independent of intracellular  $\text{Ca}^{2+}$  stores) mechanisms in endothelial cells increasing vasodilation (148). Alternatively, in certain TRP channels (TRPV4), mechanotransduction of activation signals can lead to vascular smooth muscle hyperpolarization and consequently vasodilation. This response is thought to be attributed to the stimulation of  $\text{Ca}^{2+}$ -sensitive  $\text{K}^+$  channels in vascular smooth muscle, while the same signaling mechanism is thought to occur in the vascular endothelium as well (149) (Figure 2.2).

Figure 2.2: Schematic Diagram of Endothelial-Mediated Vasodilation: Endothelial receptor activation and/or sheer stress can cause the endothelium to generate several vasodilatory mediators including EDHF, NO and PGI<sub>2</sub>. Release of these mediators causes vascular smooth muscle relaxation. In addition, activation of TRP channels located on the vascular endothelium increases intracellular calcium which triggers the opening of various ion channels, causing vascular smooth muscle hyperpolarization, also resulting in a relaxation response.

TRPV4 – Transient Receptor Potential Vallinoid 4 Channel, EDHF – Endothelial Derived Hyperpolarizing Factor, eNOS – endothelial nitric oxide synthase, NO – nitric oxide, PGI<sub>2</sub> – Prostaglandin I<sub>2</sub>, GTP – Guanine triphosphate, cGMP – cyclic guanine monophosphate, cAMP – cyclic adenosine monophosphate, ATP – adenosine triphosphate

*Adapted from Félétou & Vanhoutte (2009)*



#### 2.4.2: Vascular Smooth Muscle Control

Vascular tone within the vasculature is maintained through the cooperation between the vascular endothelium and the smooth muscle. Therefore within the brain, the primary purpose of vascular smooth muscle is to generate and maintain vasoconstriction or facilitate vasorelaxation with the end goal of controlling blood flow. The processes of vasoconstriction and vasodilation are primarily (although not entirely) controlled by the respective increases and decreases in intracellular  $\text{Ca}^{2+}$  concentrations (150). When  $[\text{Ca}^{2+}]_i$  increases, it binds to calmodulin. This complex then activates myosin light-chain kinase (MLCK) which then leads to the phosphorylation of Ser19 on myosin at the regulatory site. Actin can then activate myosin ATPase leading to muscle contraction (150). In the case of endothelial-mediated vasodilation, activated endothelial cells become hyperpolarized (according to the mechanism previously described in section 2.4.1), spreading the wave of hyperpolarization along the length of the vessel and into the vascular smooth muscle cells through myoendothelial gap junctions. The resulting current then causes a decrease in the number of open L-type  $\text{Ca}^{2+}$  channels which leads to a fall in intracellular  $\text{Ca}^{2+}$  concentrations (151). This drop in  $[\text{Ca}^{2+}]_i$  deactivates MLCK, leading to dephosphorylation of myosin light-chain Ser19 by MLC phosphatase and deactivation of actin-myosin ATPase ending in smooth muscle relaxation (150).

The stimulus for smooth muscle constriction is generally incited by receptor activation through G-protein linked pathways or mechanotransduction of signals received based on vessel stretch and stress (ie: stretch-activated cation channels) (152). Receptor agonists include endogenously produced chemicals such as norepinephrine, epinephrine, angiotensin II, vasopressin and endothelin, among others (152). Therefore, ligand binding to cell-surface receptors causes the activation of phospholipase C (PLC) through  $G_{q/11}$  which then catalyzes the

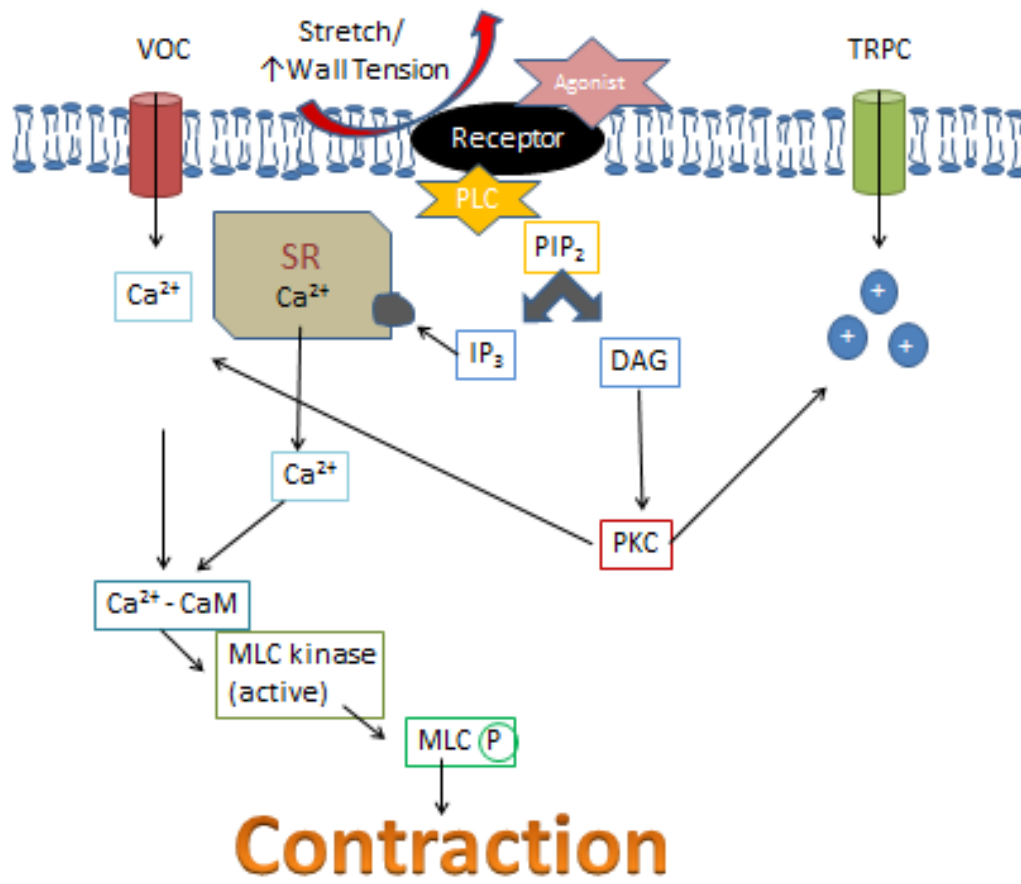
cleavage of phosphatidylinositol 4,5-bisphosphate (PIP<sub>2</sub>) into IP<sub>3</sub> and DAG, who serve as second messengers. Subsequent binding of IP<sub>3</sub> to the IP<sub>3</sub>-receptor (IP<sub>3</sub>R) on the sarcoplasmic reticulum (SR) causes expulsion of Ca<sup>2+</sup> from the SR, increasing [Ca<sup>2+</sup>]<sub>i</sub> causing vascular constriction as described above. In addition, the DAG formed from this receptor-ligand interaction also plays a role in vasoconstriction. PKC, which requires Ca<sup>2+</sup> and DAG for activation, has several downstream effects. It is known to interact with MLCK, ERK1/2, Rho kinase and calmodulin-dependent protein kinase II in addition to membrane channels to elicit vascular smooth muscle contraction (152, 153).

When vascular smooth muscle receptor agonists (vasoconstrictors) bind to receptors, the final result is intracellular calcium release leading to muscle contraction, as described above. This rise in [Ca<sup>2+</sup>]<sub>i</sub> is facilitated by voltage operated calcium (VOC) channels as well as non-specific cation channels, most of which are known as transient receptor potential canonical (TRPC) channels (154). TRPC channels can either be activated by ligand binding to the cell-receptor (as described previously) or by the depletion of internal Ca<sup>2+</sup> stores, referred to as capacitative Ca<sup>2+</sup> entry (155). VOC's commonly found in the cerebral arteries are L-type (Ca<sub>v</sub>1.2) and T-type (Ca<sub>v</sub>3.1 and Ca<sub>v</sub>3.2) Ca<sup>2+</sup> channels (156). Of particular importance, VOC and TRPC channels do not remain static within the plasma membrane. Rather, expression at the cell surface is highly dependent on other intracellular molecules that they associate with, which influences their trafficking and activity in signal transduction processes (154) (Figure 2.3).

Figure 2.3: Schematic Diagram of Vascular Smooth Muscle Contraction. Activation of G-protein coupled receptor on the cell surface occurs when agonist binds to the receptor. This leads to the activation of PLC which catalyzes the cleavage of  $PIP_2$  into  $IP_3$  and DAG.  $IP_3$  triggers intracellular calcium release from the SR. DAG activates PKC which also increases intracellular calcium release through the opening of VOC's and TRPC channels. An increase in intracellular  $Ca^{2+}$  concentrations allows  $Ca^{2+}$ -CaM binding which activates MLCK, leading to the phosphorylation of MLC and subsequent muscle contraction.

VOC – Voltage-gated  $Ca^{2+}$  Channel, TRPC – Transient Receptor Potential Canonical Channel, SR – Sarcoplasmic Reticulum, PLC – Phospholipase C,  $PIP_2$  - phosphatidylinositol 4,5-bisphosphate,  $IP_3$  - inositol trisphosphate, DAG – diacyl glycerol, PKC – protein kinase C, CaM – Calmodulin, MLC – myosin light chain

*Adapted from Webb (2003)*



### *2.4.3: Cerebral Blood Flow Autoregulation*

The concept of autoregulation was first described by Bayliss in 1902, by demonstrating that vascular tone could in part be modulated by intravascular pressure, through his experiments measuring blood flow in a canine hind limb (157). Currently, the four main regulators of cerebral blood flow have been determined to be 1) partial pressure of CO<sub>2</sub> (PaCO<sub>2</sub>), 2) mean arterial pressure, 3) metabolic needs of the brain and 4) the autonomic nervous system (158). In 1959, Lassen modeled the data from seven separate studies recording the relationship between arterial blood pressures and corresponding cerebral blood flow using a curve, showing that cerebral blood flow was largely unchanged over a blood pressure range of approximately 60 mmHg-150 mmHg. He termed this static autoregulation (159). As of late, this concept has been criticized and revised based on studies using the Windkessel model. The Windkessel model is a mathematical model that describes hemodynamics in terms of vascular resistance, compliance and impedance (160). Evidence in the literature suggests that due to the compliance of cerebral arteries, it is possible that they are buffering against changes in blood pressure by “storing” blood throughout a cardiac cycle. This process would be dependent on how quickly blood pressure was changing (161, 162). Conversely, in times of hypotension, cerebral blood flow was less effectively maintained than during acute hypertensive episodes (163, 164). At present, the concept of dynamic cerebral autoregulation and the active modulation of cerebral blood flow during perpetual changes in blood pressure (165, 166) is widely accepted. Although many believe that dynamic cerebral autoregulation is achieved primarily by a constant adjustment of arterial resistance within the cerebrovasculature (based on myogenic responses to stretch/stress as described previously) to arterial blood pressure, the precise mechanism by which this occurs

remains not fully defined (166). However, one important component of dynamic cerebral blood flow autoregulation is pressure dependent constriction (PDC).

#### *2.4.4: Pressure Dependent Constriction*

PDC describes the reflexive decrease in lumen diameter of an autoregulatory vessel (such as certain cerebral arteries) in response to an abrupt increase in blood pressure that would otherwise increase blood flow to the brain. This mechanism is believed to be protective during acute hypertensive episodes because when the perfusion pressure rises excessively, the blood vessel constricts, increasing vascular resistance and maintaining constant blood flow to the rest of the brain (24, 167). Studies of the pathogenesis of hemorrhagic stroke in the stroke prone spontaneously hypertensive rat revealed that before cerebral hemorrhage occurs, PDC is lost in the MCA (167) which corresponds to a loss in cerebral blood flow autoregulation to the areas downstream (168). Therefore, in times of acute hypertension, this alteration in vascular function is thought to lead to over-perfusion of vasculature downstream from the MCA, facilitating disruption of the blood-brain barrier and eventually ending in cerebral hemorrhage. Likewise, in chronic hypertensive vascular disease, weakened vessels would be much more prone to rupture in the presence of an acute spike in blood pressure from baseline (169).

Just as the process of dynamic autoregulation of cerebral blood flow is not fully understood, neither is the process by which the MCA loses its ability to perform PDC. However, PDC is known to be dependent on endothelial function (170) as well as vascular smooth muscle function (171, 172). In SHRsp's who are unable to perform PDC (post-stroke), the vasodilatory response to bradykinin is lost as well as the vasoconstrictor response to NOS inhibition (L-NAME), indicating endothelial dysfunction (168). Additionally, various vascular smooth muscle

agonists (that increase  $[Ca^{2+}]_i$  by initiating  $Ca^{2+}$  release from the sarcoplasmic reticulum (173) and opening of receptor-operated  $Ca^{2+}$  channels in the sarcolemma (174)) including serotonin and vasopressin had reduced vasoconstrictor activity in post-stroke SHRsp but were rendered completely ineffective in the presence of L-type  $Ca^{2+}$  channel blockade. This suggested a defect in the ability of the vessel to use intracellular  $Ca^{2+}$  stores (172). Finally, a significant correlation between PDC and vascular response to PKC activation by phorbol dibutyrate (which directly activates PKC and also increases the sensitivity of the contractile pathway to available  $Ca^{2+}$  (175)) in the MCA of pre/post-stroke SHRsp was observed. After stroke development, SHRsp MCA's had lost the ability to respond to PKC-mediated vasoconstriction, indicating a possible role for PKC activity in PDC (171). Therefore, deficits are apparent in various steps of the contractile pathway of the MCA, all of which are correlated to a concurrent loss in PDC and an increased risk of HS.

### ***2.5: Hemorrhagic Stroke***

Stroke remains a significant cause of death worldwide, causing approximately 5.5 million deaths annually (176). According to a recent report from the Heart and Stroke Foundation, the death rate arising from stroke in Canada is 17.9 per 100,000 people (29.9 in Newfoundland and Labrador) with one stroke occurring every 10 minutes (177). Although the most common stroke subtype is ischemic stroke (87%), between 10% and 15% of all strokes are of the intracerebral hemorrhage (ICH) subtype (178, 179), which is caused by the bursting of small cerebral arterioles. In the majority of cases, the trigger for vascular wall rupture is longstanding hypertension (180). Depending on the underlying cause, cerebral hemorrhage is further sub-classified as primary ICH or secondary ICH. Primary ICH (78%-88% of cases) occurs when chronic vascular damage from longstanding hypertension and/or amyloid angiopathy weakens

the small arteries and arterioles in the brain making them susceptible to rupture leading to hemorrhage (181, 182). Alternatively, secondary ICH occurs in patients with underlying vascular anomalies (such as aneurysms), neoplasm or coagulopathies which make them prone to cerebral hemorrhage development (183, 184).

### *2.5.1: Clinical Definition and Prevalence*

Hemorrhagic stroke (HS) is defined as an abrupt disruption in brain function caused by small cerebral vessel burst followed by bleeding into the cerebral parenchyma (178). Worldwide incidence ranges from 10-20 cases per 100,000 people, and increased risk with advancing age (185). Men are more commonly affected than women, especially after 55 years of age. Individuals of African and Japanese descent (50-55 cases per 100,000) have more than twice the risk of developing ICH than Caucasians (186-188). A higher fatality rate is observed in HS compared to the other subtypes of stroke, with 62% of patients dying within the first year post-stroke and high risk of recurrence (189, 190). HS can also be precipitated iatrogenically by treatment with first-line thrombolytic treatments used to dissolve clots in the treatment of myocardial infarction and ischemic stroke (191).

### *2.5.2: Pathophysiology and Risk Factors*

As previously mentioned, chronic hypertension is the most significant risk factor for ICH development (192). A randomized, double-blind, placebo-controlled trial in elderly patients with systolic blood pressures  $\geq 160$  mmHg using anti-hypertensive medication had a five-year incidence rate of ICH of 5.2% compared to the placebo group who had a rate of 8.2% (193). Therefore, appropriate anti-hypertensive treatment in affected individuals is an important intervention in risk management (194, 195). Other modifiable risk factors include high salt

intake (196), excessive alcohol consumption and dyslipidemia (especially in the presence of hypertension) (197). Other non-modifiable risk factors for primary ICH include certain coagulopathies due to genetic mutations (198) and cerebral amyloid angiopathy, characterized by deposition of  $\beta$ -amyloid protein into the walls of cerebral vessels, compromising structure and function (182, 199).

The changes in vascular structure and reactivity immediately prior to stroke in humans are not well elucidated at this time. However, HS development is thought to be precipitated by chronic hypertensive vascular remodeling, reflected by a decrease in the arterial elastic component and the partial replacement of vascular smooth muscle in the tunica media with collagen deposition (200). Because the elastic component of the vessel provides strength, increased collagen ratio renders the wall much more brittle and prone to burst under conditions of stress (200). In addition, Charcot and Bouchard identified isolated areas of cerebral arterioles that were dilated and identified these highly collagenized sites as the most likely points of rupture within the vascular wall. They are now termed Charcot-Bouchard aneurysms and are thought to play a role in cerebral micro-hemorrhage development that precedes gross cerebral hemorrhage resulting in clinical symptoms (178, 200-203). Therefore, due to these structural changes, the cerebrovasculature becomes prone to distension and vulnerable to over-perfusion. As previously described, amyloid angiopathy is also an important contributor to HS, particularly in the elderly. However, these areas of hemorrhage are usually characterized as being located more superficially on the surface of the brain as opposed to hypertensive-induced hemorrhages which tend to appear close to the Circle of Willis. Hypothetically, this is where the greatest amount of hypertension-induced vascular damage would occur due to the high pressures and frequent arterial bifurcations, contributing to turbulent blood flow (200).

Finally, the development of satellite lesions further worsens the disease progression. After the initial cerebral hemorrhage, the body increases production of catecholamines which further increases the blood pressure. Because vascular damage caused by chronic hypertension as well as amyloid angiopathy (when applicable) is widespread and not isolated to a single area, blood flow autoregulatory function is already presumably compromised globally. In the setting of autoregulatory dysfunction and leaking vessels, it has been shown that blood pressures of 150-160 mmHg are key for the promotion of hematoma expansion. Therefore at high pressures, cerebral blood flow is more likely to increase, leaving the patient vulnerable to primary hematoma expansion but also the development of satellite hemorrhages (lesions), further exacerbating bleeding (200, 204, 205). This helps to explain the high case fatality rate in ICH patients. However, more information is needed regarding the molecular mechanisms of autoregulatory failure that plays a role in HS pathology.

### *2.5.3: Animal Models of Hypertension and Stroke*

To date, no effective pharmacological agents have been developed to treat spontaneous ICH. This means stroke prevention is paramount, as supportive care is the only treatment modality initiated post-stroke. As a result, animal models to study ICH are crucial in increasing our understanding of the underlying pathology leading to stroke development as well as the exploration/development of experimental treatment options to improve survival outcomes in this population. The most commonly used genetically hypertensive animal model used in the study of essential hypertension is the stroke-resistant Spontaneously Hypertensive Rat (SHR). Alternatively, an appropriate animal model to study the pathogenesis of HS is the stroke-prone Spontaneously Hypertensive Rat (SHRsp).

### 2.5.3.1: *SHR*

The most widely used genetically hypertensive rat model, the SHR, was developed by Okamoto and Aoki from selective breeding of a spontaneously hypertensive outbred male Wistar Kyoto (WKY) Rat with a slightly hypertensive female. Subsequent inbreeding of sibling pairs lead to the development of the SHR strain (206). Possibly attributable to the increased activity through the renin-angiotensin-aldosterone system, spontaneous hypertension develops at around five weeks of age, yielding systolic blood pressures as high as 200 mmHg by seven to ten weeks of age (207). Compared to normotensive WKY controls, SHR show signs of alterations in cerebral autoregulation linked to increased stiffness in large arteries and increased distensibility of small arterioles (208-210); however regardless of hypertension-related changes to the vasculature, SHR are highly stroke resistant. Due to this and the common genetic lineage, the SHR is commonly used as a stroke-resistant control for the SHRsp.

### 2.5.3.2: *SHRsp*

Originally developed by Okamoto et al, the inbred SHRsp model is an appropriate animal model to study HS-associated pathology as well as novel treatment strategies post-stroke (211). There are a number of strengths to using this model to study hemorrhagic stroke which include the similarity in mechanism and pathology of stroke development to humans and role of genetics in stroke occurrence. The SHRsp strain reliably produce hemorrhagic stroke at a rate of 88-100% by 10-13 weeks of age subsequent to longstanding hypertension when placed on a Japanese style high salt diet (HSD) from five weeks of age (212, 213). This relates well to human disease as chronic hypertension and associated vascular pathology is one of the key contributors to ICH. In our model, we used a 4% NaCl, 0.75% K<sup>+</sup> HSD which typically produces 100% mortality by

around 15 weeks of age (213, 214). In addition, common areas of ICH due to hypertensive vascular disease in humans tends to be near areas of arterial bifurcations (202) which is also consistent in the SHRsp model. Yamori *et al* described the most common areas of cerebral lesion formation in the SHRsp to be the anteromedial cortex, the occipital cortex, and the basal ganglia (215) which share the common physiologic feature of frequent arterial branching. In addition, the frequency of “boundary zone” lesions, located at the areas of the brain supplied by both the posterior and middle cerebral arteries is also consistent with human disease (215). Finally, the genetic predisposition to stroke development in the SHRsp compared to the SHRsr further reinforces the importance of genetics in HS development, a phenomenon also observed in humans. Although both strains exhibit similar levels of hypertension while consuming HSD, only the SHRsp develops predictable HS (207).

The physiological mechanisms leading to HS development in the SHRsp to HS are multifactorial and include severe hypertension, vascular dysfunction leading to loss of autoregulation of cerebral blood flow, and weakening of the blood brain barrier (BBB) leading to cerebral hemorrhage formation (216). Due to the abnormally heightened activation of the renin-angiotensin-aldosterone system in SHRsp, blood pressures in these rats often rise well over 200 mmHg (216) along with cerebral lesion formation in downstream arterioles. A progressive increase in blood pressure leads to dysfunction of the BBB causing leakiness and subsequent extravasation of plasma proteins. Hypertensive vascular remodeling, as described previously damages the endothelial and vascular smooth muscle cell layers. This leaves behind the basal membrane and causes collagen deposition into the vascular walls, producing arteriolar necrosis (217). Subsequent cerebrovascular dysfunction accompanied by functional deficit in cerebral

blood flow autoregulation render the vessel vulnerable to ectasia and eventual rupture (18, 168, 171, 218).

## ***2.6: Hypothesis***

Currently, the main source of data that correlates increased HS risk and RA is population-based epidemiological studies. As such, there is a large knowledge gap surrounding the pathogenesis and mechanism of this relationship. Based on the evidence available with the various autoimmune arthritis, hypertension and hemorrhagic stroke animal models, theories can be generated in an attempt to explain how chronic inflammation leads to cerebral hemorrhage. However, currently there is no multi-disease animal model that allows for the concurrent study of chronic hypertensive disease and chronic systemic inflammation to test these theories. As a result, there is also a lack in appropriate vascular studies in the setting of chronic hypertension and systemic inflammation to test functional aspects of the cerebral vessels.

*Our hypothesis is that chronic inflammation in the setting of longstanding hypertension in an ageing, stroke-resistant spontaneously hypertensive rat (SHR) predisposes the middle cerebral artery (MCA) to lose the ability to respond properly to pressure, leading to increased incidence of HS. In addition, we hypothesize that high salt diet in conjunction with chronic inflammation will further exacerbate dysfunction in the MCA of inflamed, hypertensive SHR.*

*To address our research question, we developed the following study objectives:*

- 1) Create and define the relevant animal model to study the effect of arthritic inflammatory injury and hypertension on cerebral vessel function
- 2) Investigate whether intracerebral hemorrhage occurs in this mono-arthritic, hypertensive animal model

- 3) Investigate the role of HSD on cerebral vascular function in this mono-arthritic, hypertensive animal model.

### **3.0: Materials and Methods**

#### *3.1: Animals*

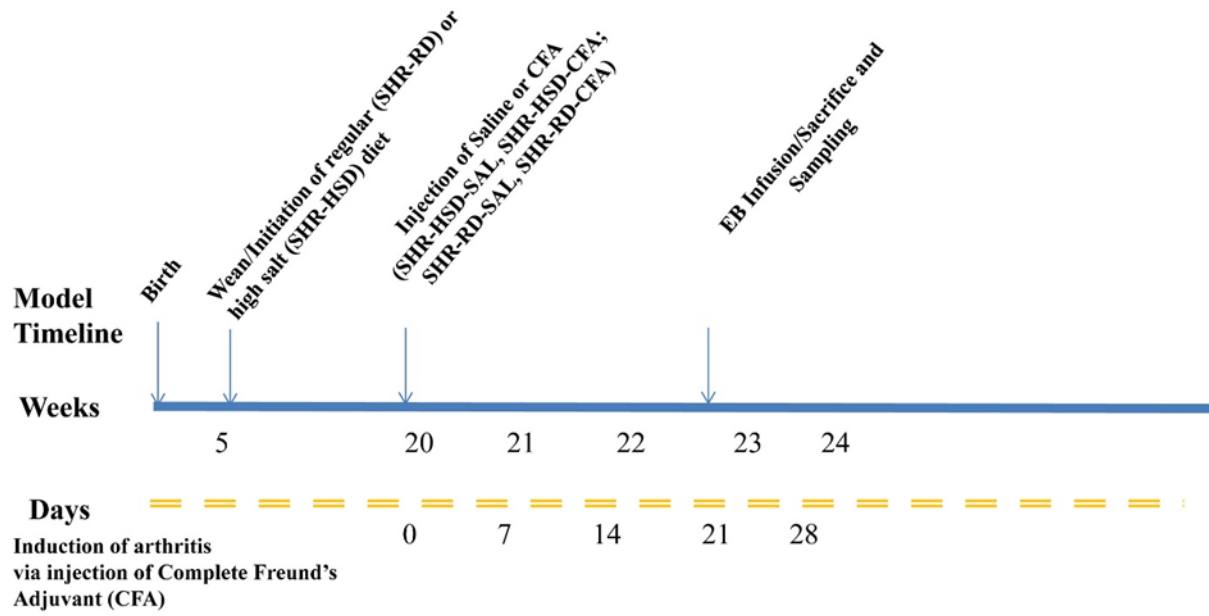
All experimental procedures and animal breeding was carried out at Memorial University of Newfoundland Health Sciences Centre Animal Care Facility and were in compliance with guidelines and recommendations set forth by the Institutional Animal Care ethics committee and the Canadian Council on Animal Care ([Guide to Care and Use of Experimental Animals, vol.1, 2<sup>nd</sup> ed.](#)). In total, 45 male stroke resistant Spontaneously Hypertensive Rats (SHR; Original stock from Charles River Laboratories, Quebec, Canada) were included in the study. The animals were bred in-house and were housed two per cage in ventilated cages under standard light cycle (12 hour light/dark), controlled temperature, and humidity conditions. Experimental design for inducing inflammation was implemented at 20-28 weeks of age. *Ad libitum* access to food and water was permitted.

#### *3.2: Experimental Design*

Rats were divided into four experimental groups based on diet and treatment, and followed the experimental timeline outlined in Figure 3.1. Briefly, SHR-high salt diet (HSD) groups were fed a Japanese-style high salt diet containing 4% NaCl (Zeigler Bros, Gardners, PA, USA) from weaning. SHR-regular diet (RD) groups were maintained on standard rat chow (Laboratory Rodent Diet 500I, Lab Diet, St. Louis, MO, USA; 0.58% NaCl). At 20-28 weeks of age, they were randomly divided into 4 groups based on treatment (Complete Freund's Adjuvant (CFA) model of mono-arthritis or Saline (SAL) injected control) and diet (high salt (HSD), or standard rat chow(RD)), and labelled HSD-SAL (n=10), HSD-CFA (n=14); RD-SAL (n=11), RD-CFA (n=10) (Figure 3.1).

Figure 3.1: Animal experimental timeline. Four experimental groups were followed over the course of 21-23 days, SHR-HSD-SAL, SHR-HSD-CFA; SHR-RD-SAL, SHR-RD-CFA. SHR-HSD groups were weaned and started on Japanese Style High Salt Diet (4% NaCl) while SHR-RD groups were weaned and started on regular purina (0.58% NaCl equivalent) diet at 5 weeks of age. At 20 weeks of age (Experimental Day 0), all groups received an intradermal injection in the left hind paw. Inflamed groups (CFA) received 0.07mL of CFA for the induction of adjuvant arthritis (AA) while control groups (SAL) received the same quantity of sterile saline (0.9%) solution. All groups were monitored for signs of inflammation and hypertension. Broken yellow line represents experimental timeline in days (Day 0-Day 21).

**Figure 3.1: Animal Experimental Timeline**



### *3.3: Preparation of Complete Freund's Adjuvant*

A suspension of *Mycobacterium butyricum* ([10 mg/mL]) in Incomplete Freund's Adjuvant (Sigma, USA; IFA) was prepared according to modified methods for induction of adjuvant induced arthritis (AIA), as commercial sources of CFA have not been found suitable for arthritis induction. In order to insure success of disease induction, heat-killed *M. butyricum* H37RA (Sigma, USA) were ground into smaller particles until fine, using an autoclaved, marble mortar and pestle in a sterile fume hood. IFA was added gradually and grinding continued until thoroughly mixed to make CFA.

### *3.4: Induction of Adjuvant Induced Mono-arthritis (AIA)*

Experimental arthritis was induced by intradermal injection of CFA (0.07 mL of 700 µg *M. butyricum*) into the plantar surface of the left hind paw of SHRs at day 0 of the experimental procedure while the animals were under anesthesia (isoflurane 4% inhalation for induction and 2-2.5% for maintenance). Controls were injected with an equi-volume of sterile 0.9% saline solution under anesthesia.

### *3.5: Monitoring of Development and Progression of AIA*

Animals were assessed for signs of inflammation for 21 days until the end of the experimental period from injection day (day 0). Wellness monitoring of rats was conducted twice daily, in conjunction with staff from the animal care facility according to a standard checklist provided. Animals were inspected for signs of dehydration, facial grimace, self-grooming, presence or absence of vocalizations while handling and mobility and also monitored for ulceration development. When significant vocalization and/or poor mobility were observed, inflamed rats were given 0.03 mg/kg buprenorphine every 12 hours as required for pain management. The dose and the frequency of buprenorphine injections were determined from previous studies

which deemed that the dose would not interfere with the inflammatory process or vascular function (219-221). Caliper measurements were taken every second day to measure hock and paw widths of both hind paws. Water displacement of each hind paw was determined by dipping the ipsilateral paw of the experimental animal up to the ankle in a standard scintillation vial with water (at a consistent weight) in order to gauge swelling of the paw as a whole. The amount of water displaced by the paw was calculated. In addition, animal weights and arthritic index scores were assigned to each rat during monitoring to separately evaluate redness and erythema of the toes, paw, hock and knuckles of the hind paws and forepaws, when applicable. Each area was assigned a score from 0-4, 0 being normal and 4 being severely inflamed. Scores were also assigned for lesion development and rated similarly on a scale of 0-4.

### *3.6: Blood Pressure Measurement*

Blood pressure was recorded by tail-cuff plethysmography (Model 59, IITC Inc., Woodland Hills, CA, USA) at baseline before CFA/Saline injection and weekly thereafter for the 21-24 day experimental period. Experimental time points for measurement of blood pressures were at 0, 7, 14, and 21 days following hind paw injection. Four sequential readings were taken at 4 seconds apart per rat at each time point and the mean (of the systolic blood pressure) was recorded. The percentage change from baseline of systolic blood pressure was calculated.

### *3.7: Identification of Cerebral Hemorrhage*

Upon the day of sacrifice at day 21-24, a random sample from the experimental rats (n=5/group) were anaesthetized with intraperitoneal injection of 50/10 mg/kg of ketamine:xylazine. The hair around the abdomen and hind limbs were shaved and cleaned with alcohol and iodine and the rat placed on a warm board for surgical preparation. The femoral vein at the contralateral side was isolated, and a modified sylastic tube catheter inserted and tied with a 4.0 suture. A 30 mg/kg

bolus dose of Evans-blue dye (Sigma, USA) (15 mg/mL 0.9% saline) was then slowly injected over a 20 second period and allowed to circulate approximately 25-30 minutes. The rats then underwent exsanguination for isolation of their brain and kidneys for further analysis. Because Evans-blue dye binds to plasma albumin, areas of extravasation of Evans-blue dye were deemed indicative of intracerebral hemorrhage based on previously reported data (18, 222). This is because extravasation of dye indicates sufficient disruption of the blood-brain barrier to allow passage of plasma proteins such as albumin. Brains of experimental rats that did not receive Evans-blue dye injection were also investigated to determine level of perfusion, cerebral edema, hemisphere size/symmetry and septal deviation, all indications of brain damage and associated with hemorrhage.

### *3.8: Sample Isolation, Tissue Processing and Histological Staining*

Necropsy was performed on experimental days 21-24 after deeply anesthetizing the animals with intraperitoneal injection of 50/10 mg/kg of ketamine:xylazine. The animals were subsequently exsanguinated by cardiac puncture, using an 18G needle and heparinized 10 mL syringe. Plasma was isolated as described below (See *TNF- $\alpha$  Analysis*). The tibiotarsal joint of the contralateral ankle was removed at the medial and lateral malleolus using a small pair of pruning shears. The digits were then removed, allowing for better penetration of fixative and subsequent decalcifying solution. The ankles were fixed in 10% neutral buffered formalin (Fisher) for 48-92 hours, and further placed into Ca Ex II solution (Fisher), a Fixative/Decalcifier solution of 10% formalin/formic acid solution for decalcification. Completely decalcified samples were embedded in paraffin, and 4  $\mu$ m sections were cut and stained using hemotoxylin and eosin (H&E) by standard procedures for assessment of joint degradation, synovium hyperplasia, angiogenesis, and inflammatory infiltrates.

The brain was removed and placed in oxygenated (95% O<sub>2</sub>, 5% CO<sub>2</sub>) ice-cooled ( $\approx 3^{\circ}\text{C}$ ) HEPES Bicarbonate Buffer (130 mM NaCl, 4.02 mM KCl, 1.22 mM MgSO<sub>4</sub>, 4.05 mM NaHCO<sub>3</sub>, 1.84 mM CaCl<sub>2</sub>, 9.99 mM HEPES, 1.18 mM KH<sub>2</sub>PO<sub>4</sub>, 0.02 mM EDTA, 5.99 mM glucose) which was prepared in-house, adjusted to pH 7.4 and filtered. The right and left MCAs were isolated, starting at the point distal to where it crosses the rhinalis fissure and mounted on a pressure myograph, as described later. The rest of the brain and a kidney were stored in fixative (4% neutral buffered formalin) for later histological examination

### *3.9: TNF- $\alpha$ Analysis*

Tail vein blood samples (0.3-0.5 mL/sampling) were collected using a 25<sup>3/8</sup> G needle and heparinized (1000 IU/mL) syringes under anesthesia (isoflurane 4% inhalation for induction and 2-2.5% for maintenance) at baseline and weekly thereafter (n=5/experimental group). The samples were kept on ice and centrifuged at 45,000 rpm for 10 minutes within 2 hrs of sampling using a cooling centrifuge (Thermo-Fisher, ON, Canada). The supernatant was collected and stored in a -80 °C deep freezer until analysis. Plasma samples were analyzed for TNF- $\alpha$  (standard range 15.6 pg/mL – 1000 pg/mL; sensitivity 2 pg/mL) within the experimental period to determine induction of systemic inflammation using a TNF- $\alpha$  ELISA kit purchased from Biologend (San Diego, CA, USA) as per manufacturer instructions.

### *3.10: Pressure Myograph Experiments*

Isolated MCAs were mounted onto the Single Vessel Chamber component of the Pressure Servo System (Living Systems Instrumentation, VT, USA) for pressure myograph studies. Vascular response was imaged using an inverted microscope and measured using a Video Dimension Analyzer (Living Systems Instrumentation, VT, USA). Mounted vessels were tied off creating a

blind sack and pressurized to 100 mmHg and equilibrated for 30-45 min in an oxygenated (95:5% O<sub>2</sub>:CO<sub>2</sub>), temperature controlled (37 °C) environment. Baumbach *et al* previously described a decrease in blood pressure (BP) of >50% between that measured in the femoral or carotid artery compared to that measured in the distal portions of the middle cerebral vessels (210, 223, 224). As a result, all of the pressure myograph experiments were conducted at a resting pressure of 100 mmHg. We also conducted our myograph experiments in the MCA at resting pressure of 100 mmHg, as we believe the setting accurately models physiological mean BP *in vivo* in the MCA of the SHR, as arterial systolic BP ranges from 200 mmHg to 230 mmHg (225). Pressure Dependent Constriction (PDC) was evaluated first. Following equilibration, the pressure was decreased to 0 mmHg for 6 minutes to disengage PDC (167). After this resting period, the pressure was immediately increased to 100 mmHg and lumen diameter was recorded (at the instant when the vessel experienced maximal pressure-mediated dilation; t=0) and then once more after 6 minutes. Previous work has shown that by 4-6 minutes PDC is re-engaged to control perfusion and maintain a constant lumen diameter in a healthy MCA (18). The effect of Bradykinin (1.6 μM) on the vessel was then tested by measuring the maximal vasodilatory response between 15 seconds and 1 minute. After the preparation was flushed with a sufficient amount of fresh HEPES bicarbonate buffer, the effect of NOS inhibition was then tested (L-NAME (100 μM)). Lumen diameter was recorded at (immediately after the addition to L-NAME) and then again at 5 minutes. A functioning endothelium should elicit a vasoconstrictory response. The contractile response of the vessel to intracellular Ca<sup>2+</sup> release from the SR (vasopressin (1.23x10<sup>-7</sup>M)) and PKC activation (phorbol-dibutyrate (1 μM)) was then investigated from a maximally dilated state by blocking L-type Ca<sup>2+</sup> channels with nifedipine (3 μM). Prior to the addition of vasopressin, the percent reduction in lumen diameter from maximal

vasodilation with nifedipine was first determined (and up to 2 minutes). After washing the preparation, the vessel was maximally dilated with nifedipine as before and then incubated with phorbol-dibutyrate for 5 minutes.

### *3.11: Evaluation of acute IL-17a exposure on MCA function (preliminary)*

One MCA was isolated from a sample (n=4-7/group) of each of the experimental animal groups and incubated with 100 ng/mL of rat IL-17A (Biolegend; San Diego, CA, USA) during the primary equilibration period for 45 minutes. Pressure myograph experiments were then conducted to measure PDC and the effects of vasoactive peptides as described in section 3.10.

### *3.12: Statistical Analysis*

Statistical analysis was performed using SigmaPlot 12.5 (Systat Software Inc., San Jose, CA) and Excel 2010 (Microsoft Corporation, Redmond, WA). Data were analyzed using Analysis of variance (one-way and two-way ANOVA), with either Bonferroni, Tukey, Mann-Whitney Rank or Holm-Sidak post hoc analysis. Values of  $p < 0.05$  were considered statistically significant.

Except where indicated otherwise, all data are expressed as mean  $\pm$  SEM.

## 4.0: Results

### 4.1: *Effect of diet and treatment on body weight*

Over the course of the experimental period, there was a statistically significant reduction in the weight from baseline (expressed as percent change in weight from baseline) in CFA compared to SAL treated animals regardless of the diet (Figure 4.1). Baseline weights of all animals were as follows; HSD-CFA:  $339 \pm 23.9$  g, HSD-SAL:  $342 \pm 18.2$  g, RD-CFA:  $337 \pm 22.0$  g, RD-SAL:  $342 \pm 18.2$  g. There was no statistical difference between baseline weight measurements. The difference observed after the start of the treatment protocol is attributed to both the loss of weight in the CFA rats, particularly during the first week of treatment, and a steady increase in weight of the SAL rats over the 21 day period (Figure 4.1).

### 4.2: *Visual Determination of Mono-arthritis development*

CFA-injected animals developed mono-arthritis restricted to the joints of the injected ipsilateral paw within 2 days post-injection, and remained inflamed for the 21 days post-CFA injection (Figure 4.2 A-C). The degree of inflammation did not significantly differ between the HSD-CFA and the RD-CFA groups, and there were no signs of joint inflammation in the SAL-injected rats. Visual inspection of the CFA-injected animals revealed diffuse soft tissue swelling that included the digits. There was also visual evidence of joint damage with joint space narrowing of the intertarsal joints, and joint deformity by 21 days of CFA injection. In spite of the diffuse swelling covering the area from the toes up to the hock, many CFA-injected rats were still walking on the inflamed paw, with minimal evidence of pain. Some CFA animals showed minor inflammation at other sites including the contralateral, non-injected paw and/or one or both forepaws or the

tail, however this observation was not reliably seen at Day 21 and was commonly isolated to the early stages of inflammation (Days 1-7- Figure 4.3 ).

Figure 4.1: Change in weight of the groups expressed as change in weight from baseline. Shown above is the averaged change from baseline in weight change with respect to time. Data was analysed by two-way ANOVA with Tukey's post-hoc test . \* $p < 0.05$

Figure 4.1: Change in Weight of Regular and High Salt Diet Fed CFA and SAL Groups

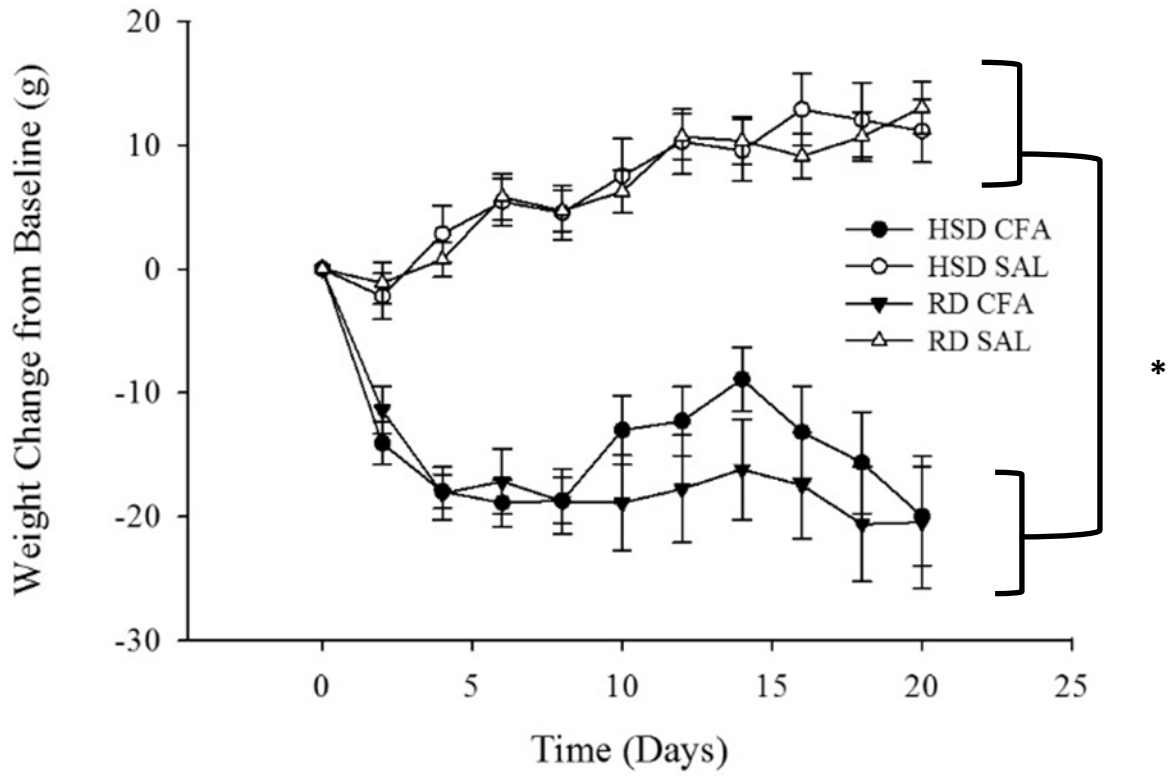


Figure 4.2: Representative images from all the experimental hind paws of Saline and CFA-treated animals. From experimental day 2 to day 21, there was a statistically significant increase in ipsilateral paw circumference and volume in HSD-CFA (B) and RD-CFA (C) compared to SAL controls (A), as reflected in caliper and water displacement values. Representative images of the histological analysis of the paws upon H&E stains are also shown, at 4x and 20 x magnification. Both histological images are representations from the HSD experimental group. Histological analysis of the SAL-injected paws showed normal tissue, synovium, adipocytes, and collagen fibrils populating the joint area (D), with sharp transition between the intima and sub-intima and characteristic morphological details associated with the layer, as seen in higher magnification (E). The sagittal section of CFA-injected paws demonstrates a denuded intimal layer and adipocytes (F), thickened and edemic sub-intima which have been largely replaced by inflammatory cell infiltrates, lymphocytes, and capillaries are congested and wall are thickened, evident in the 20x magnification (G).

Figure 4.2:

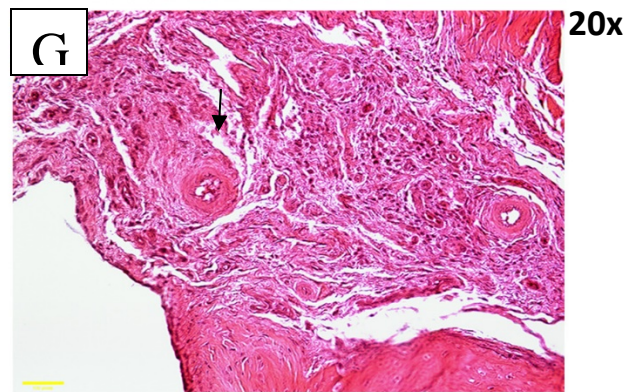
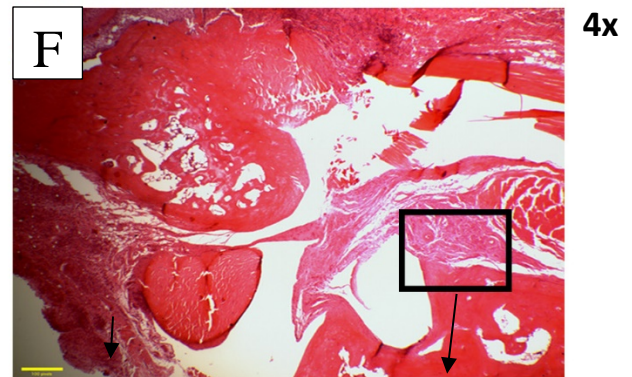
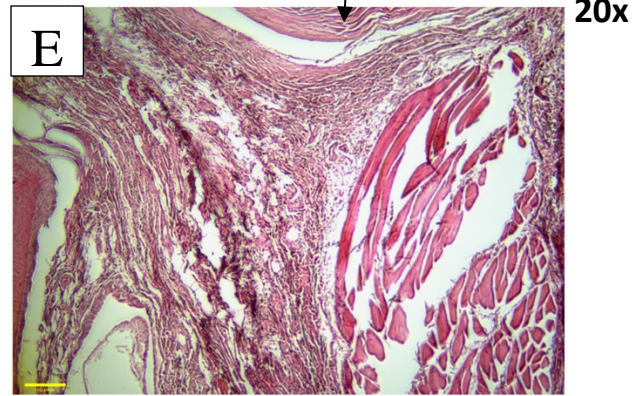
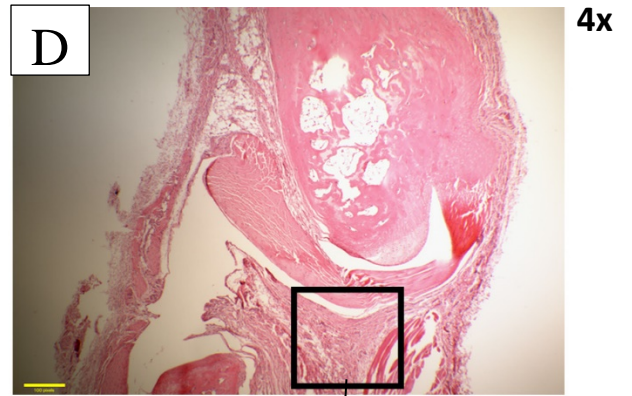
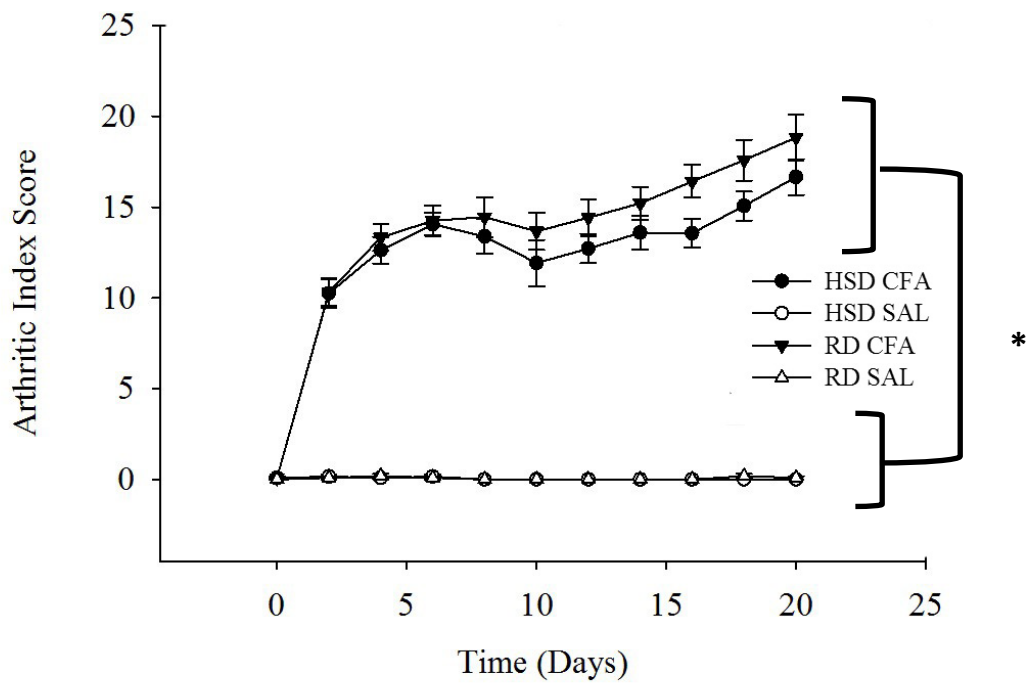


Figure 4.3: Arthritic index scores for saline vs CFA throughout experimental timeline. Data was analyzed by two-way ANOVA using Holm-Sidak method with  $p < 0.001$  for CFA vs SAL in both groups only.

Figure 4.3:  
Arthritic Index Scores for SAL vs CFA throughout Experimental Period



#### *4.3 Histological Determination of Mono-arthritis*

H&E stains were performed on the sagittal sections of the ankles and qualitatively analyzed for cellular infiltration, joint degradation, and changes to the synovial lining (Figure 4.2 D-G).

Sections obtained from saline-treated rats showed normal joint histology with a smooth articular surface and a regular tide mark separating the articular cartilage from the underlying subchondral bone (Figure 4.2 D, E). There was intact morphology of synovium and synovial lining, with no inflammatory cell infiltration, while CFA-injected rats showed a disrupted articular surface with total absence of cartilage in some areas. Both HSD (Figure 4.2 B) and RD (Figure 4.2 C) fed groups exhibited similar degree of inflammation, lesion formation, and the occasional lesions formation at the injection site upon visual inspection of the pad of the inflamed paw. Lesions also appeared at the hock as well, although never progressed to gross ulceration. There was minimal inflammation observed at the contralateral paws. There was no difference in the analysis of the HSD vs. the RD SAL-injected groups with regards to histological comparison. The sagittal section of CFA-injected paws demonstrates a denuded intimal layer and adipocytes (Figure 4.2 F), thickened and edemic sub-intima which have been largely replaced by inflammatory cell infiltrates, lymphocytes, and capillaries are congested and walls are thickened, evident in the 20x magnification (Figure 4.2 G). There was also no difference in the qualitative analysis of the paw joint histology of the HSD vs. RD CFA-injected groups.

#### *4.4 Quantitative progression of mono-arthritis and inflammation*

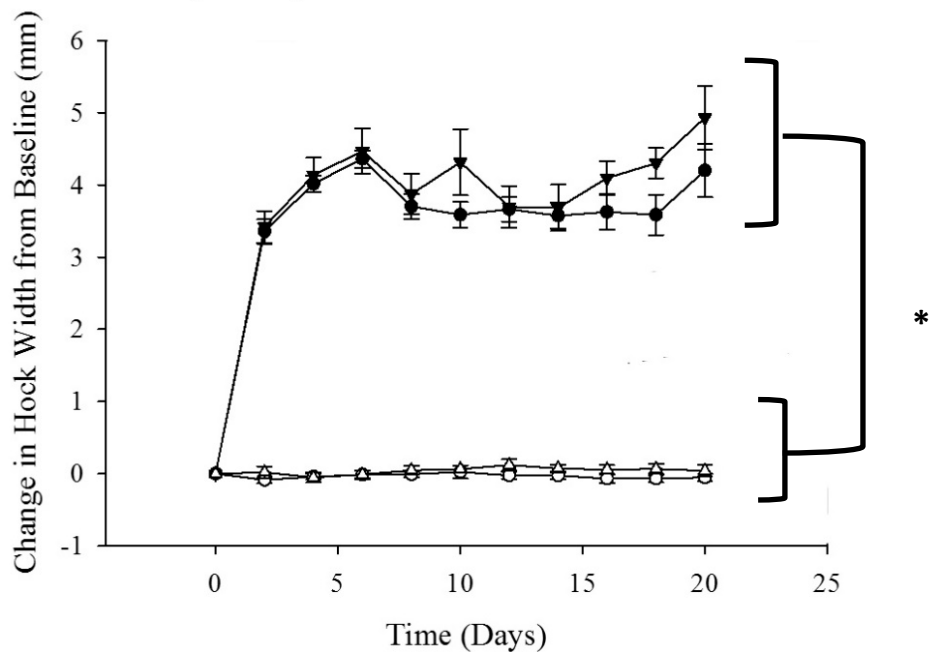
The progression of inflammation from baseline to endpoint is shown in Figure 4.3. All rats were subjectively scored every second day based on level of redness/erythema as well as lesion formation in the toes, foot pad, knuckles and hock on both hind paws. An additional score was

given for redness/erythema or lesion formation in either of the forepaws. Each affected region was scored on a scale of 0-4, 0 being normal and 4 being the maximal severity. The maximum overall score was 20. Caliper measurements (Figure 4.4 A) of the cross-sectional width of the ipsilateral, injected hind paw and hock of the CFA treated animals remained significantly larger throughout the experimental timeline ( $p < 0.05$ ) while no significant change was observed in the size of the left hind paw/hock of SAL-treated controls or in the contralateral hind paw/hock. Water displacement (Figure 4.4 B) of the paws was used to represent overall swelling of the affected foot, including the toes, knuckles, paw, and hock. Although there was no difference in paw volume of the contralateral hind paw for any group ( $p > 0.05$ ), the volume of the ipsilateral hind paw remained significantly elevated in the CFA –treated cohorts ( $p < 0.05$ ) while no change was observed in the SAL-treated animals.

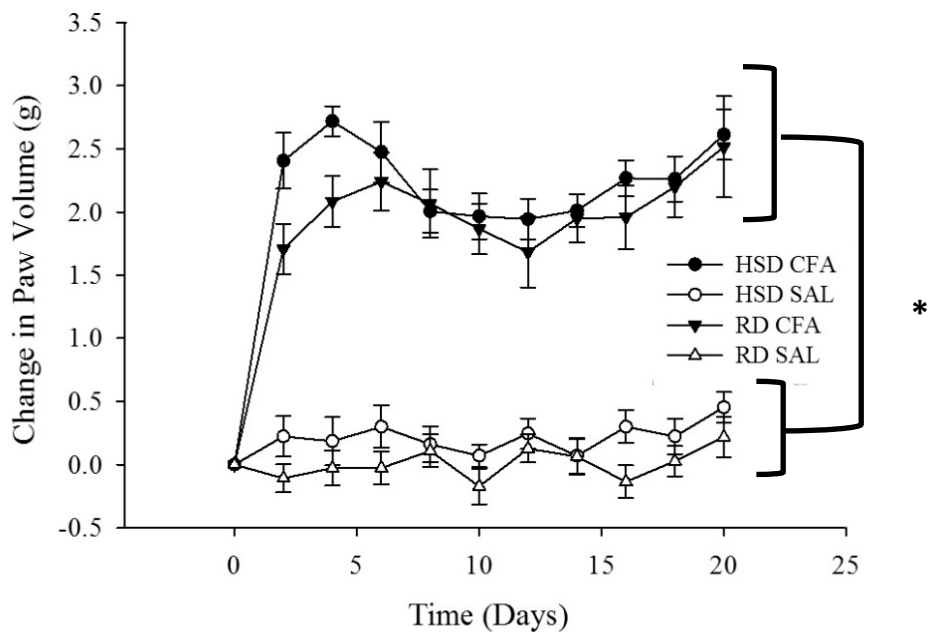
Figure 4.4: Quantitative measurement of mono-arthritis using caliper measurements (A) and water displacement (B). Measurements are expressed as the average change in width of the left hock (A) or change in hind paw volume (B) compared to baseline with respect to time, measured every second day of the experiment. The mean of three measurements of each paw and hock were taken, while the volume displacement was measured only once. Shown above is the change in width of the left hock compared to baseline measurements with respect to time. Data was analyzed using two-way ANOVA using Tukey's post-hoc test. \* $p < 0.05$

Figure 4.4:

**A** Change in Ipsilateral Hock Width Over Time



**B** Change in Ipsilateral Paw Volume Over Time



#### *4.5 Systolic blood pressure*

Weekly blood pressure measurements were recorded from baseline (Day 0) to endpoint at day 21, and the percent change from baseline was calculated and analyzed (Figure 4.5). The SHR<sub>s</sub> all remained hypertensive throughout the experimental period. The mean and standard deviation of the blood pressures at baseline within the groups was as follows; HSD CFA: 227.6 ±31.3 mmHg, HSD SAL: 246 ±23.3 mmHg, RD-CFA: 214±31.1 mmHg, RD-SAL: 224 ±15.4 mmHg. CFA-treated animals had significantly higher blood pressure readings than SAL groups ( $p < 0.05$ ) at day 7. Day 21 readings also indicated significant differences in both diet and treatment induced percent change from baseline systolic blood pressures (HSD vs. RD  $p < 0.05$ ; CFA vs. SAL  $p < 0.001$ ). These results suggest that HSD and CFA effectively induce an increase in systolic blood pressure.

#### *4.6 Plasma TNF alpha levels*

Plasma samples from all treatment groups for Days 0, 7, 14 and 21 were analyzed for levels of TNF- $\alpha$  using a commercially available ELISA kit. The levels of TNF- $\alpha$  remained low at baseline (Day 0) for all treatment groups. Day 7 and 14 yielded statistically significant increase in TNF- $\alpha$  levels in HSD-CFA vs. HSD-SAL and RD-SAL groups. There was no significant difference in the HSD-CFA group compared to the saline controls at day 21 despite an evident numerical increase in TNF- $\alpha$  levels, due to the great variability in samples. TNF- $\alpha$  levels of RD-CFA groups were statistically different only from HSD-SAL group in day 7 and 14. There was no statistical difference in TNF- $\alpha$  levels between the CFA treatment groups, suggesting that HSD does not affect the progression of arthritis development.

Figure 4.5: Percent change from baseline of systolic blood pressures of SHR-SAL vs. SHR-CFAs on either HSD or RD. Four sequential readings were taken at four seconds apart per rat. The SAL and CFA groups were severely hypertensive throughout the experimental timeline at blood pressures above 180 mmHg. The percent change from baseline of the mean values of the systolic blood pressures are depicted (n=8-16/group). Data was analyzed using two-way ANOVA using Holm-Sidak post-hoc test. \* p<0.05, \*\*p<0.001

Figure 4.5:  
% Change in Systolic Blood Pressure over Experimental Timeline

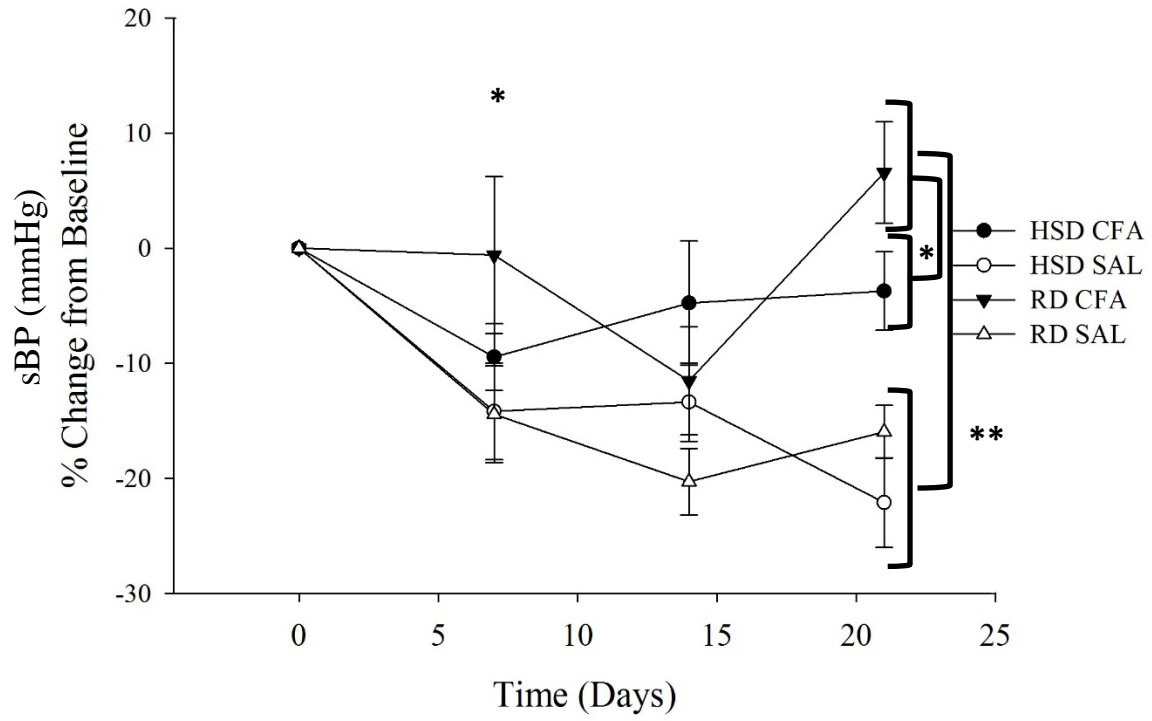
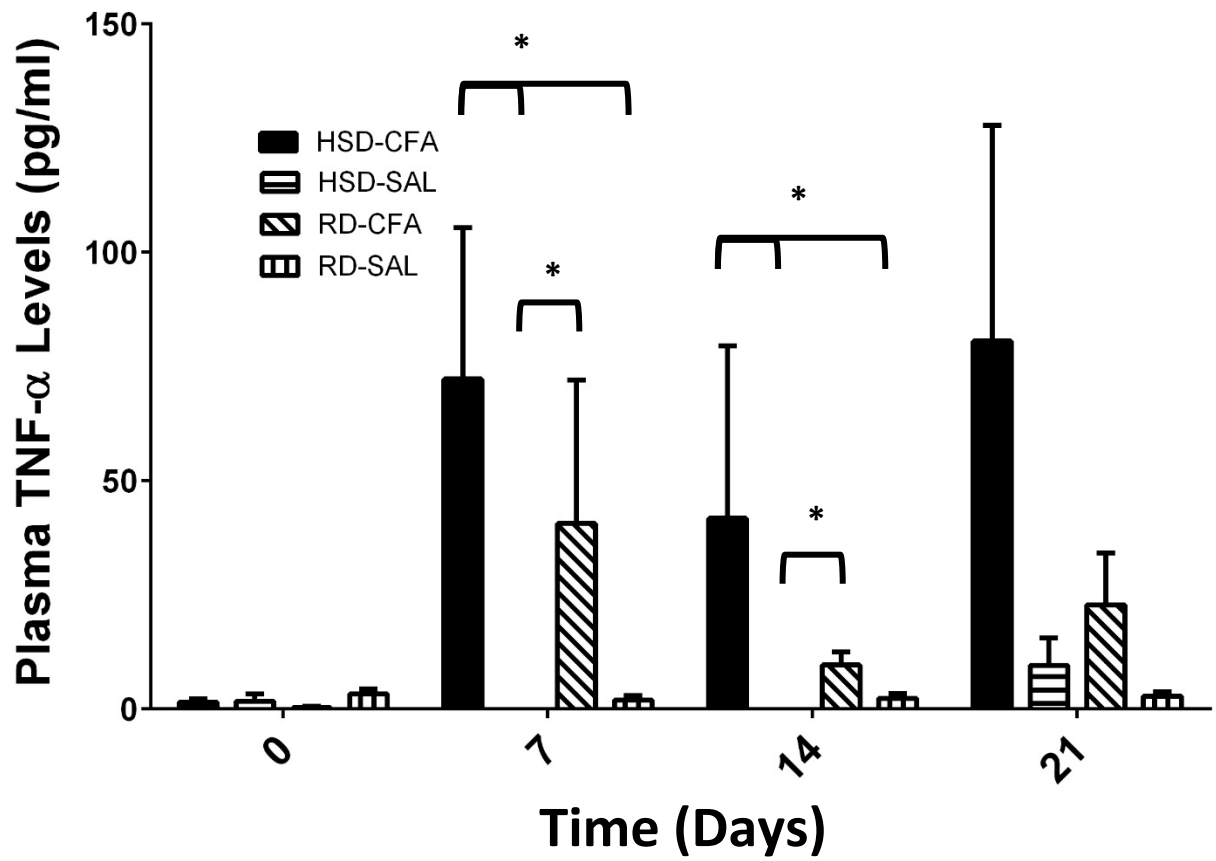


Figure 4.6: Plasma concentration of TNF- $\alpha$  (pg/mL) per experimental group during the experimental period. Plasma samples were taken on day 0, 7, 14 and 21 of experimental period. ELISA analysis of samples was completed for n=5 from each experimental group. The average of the peak TNF- $\alpha$  plasma concentration for all rats in each group was calculated. Data was analyzed using one-way ANOVA using Tukey's t-test for differences in mean values among groups (n=5-8/group). \*p<0.05

Figure 4.6: Average Plasma Concentrations of TNF- $\alpha$

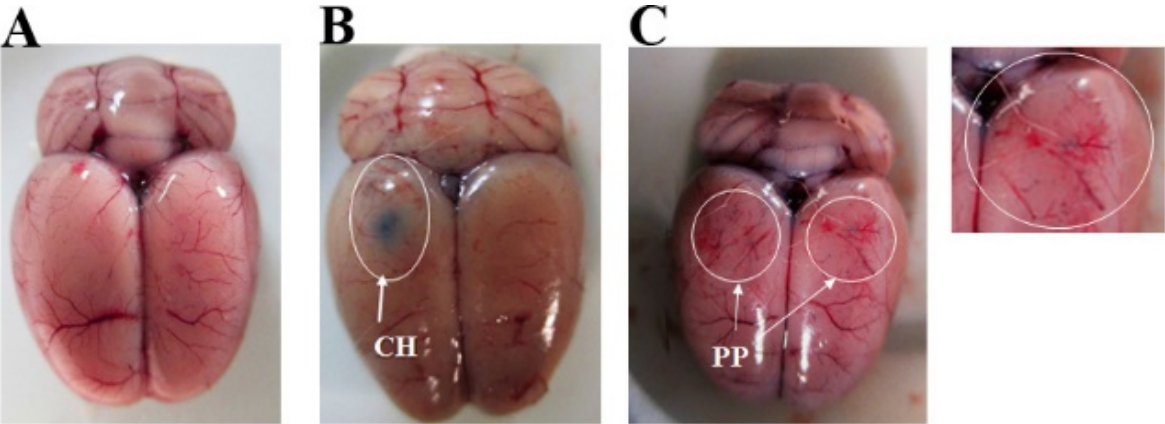


#### *4.7 Determination of Cerebral Hemorrhage*

Experimental animals (n=3-8/group) were randomly selected for Evans-blue dye (EBD) injection at the time of sacrifice in order to identify areas of potential hemorrhage as evidenced by EBD extravasation. Figure 4.7 shows representative images of brains from SHR-SAL (Figure 4.7A) groups compared to CFA-treated animals on HSD (Figure 4.7B) and RD (Figure 4.7C) infused with EBD. Diet had no discriminable effect on SAL treated groups with regards to gross brain morphology. The brains appeared well perfused, with equi-sized hemispheres, a straight and healthy septum, with no evidence of EBD extravasation. EBD extravasation was more evident in all of the HSD-CFA brains (n=8), in forms diffuse and pin point, likely due to larger areas of hemorrhage. Most of the brains from RD-CFA groups (5 out of the 6 experimental animals infused with EBD) exhibited extravasation, as the presence of pin-point hemorrhages (PP). Signs of edema, and decreased cerebral perfusion, and distorted septum were especially apparent in the brains from CFA treated rats, with particularly higher incidence in the HSD-CFA treatment groups. Their brain morphology is akin to the stroke prone spontaneously hypertensive rats (SHRsp) who had developed hemorrhagic stroke, whose brains are characterized by a dysmorphic brain structure and deviated septum due to severe cerebral edema and fluid-filled lesions (169). There was also obvious asymmetry of both left and right hemispheres of the CFA rats compared to controls.

Figure 4.7: Evans-blue dye Infusion. Animals were anaesthetized and Evans Blue Dye was infused over a period of 25-30 minutes at the time of sacrifice. No signs of hemorrhage were apparent in controls (A), while CFA injected animals (HSD: B; RD: C) showed obvious signs of cerebral hemorrhage (circled). Pinpoint hemorrhage (PP); Cerebral hemorrhage (CH)

Figure 4.7: Evans-blue dye Infusion.



## *4.8 Effects of Diet and Inflammation on Vascular Function in the MCA*

### *4.8.1 Pressure Dependent Constriction*

All animals, regardless of diet or treatment, were able to constrict to a degree in response to increased intraluminal pressure, although there were significant variations between the groups with regards to the extent of the PDC response (Figure 4.8). We observed that both diet and CFA treatment affected PDC response. CFA treatment significantly diminished the ability of MCAs to undergo PDC in the RD group compared to SAL controls. However, there was no significant difference in the PDC response of the MCAs in HSD CFA compared to HSD SAL, which was attributable to the effect of the high salt diet on PDC. HSD alone had greatly diminished the PDC response in the vessel, as further evidenced by a significant decrease in PDC response in the HSD SAL group compared to the RD SAL group ( $p=0.01$ ).

### *4.8.2 Endothelium-Mediated Vasodilation: Bradykinin Response*

Figure 4.9 depicts the endothelial vasodilatory response of MCA's to addition of bradykinin (1.6  $\mu\text{M}$ ) (170, 218). The effect of inflammation (induced via CFA; treatment effect) was not evident within MCAs of RD groups (RD CFA vs. RD SAL). However, a significantly diminished response was observed in the MCA's from HSD-fed CFA rats compared to HSD SAL rats ( $p=0.015$ ). There was no difference in vessel response to bradykinin due to the effect of high salt diet (ie. RD SAL vs. HSD SAL). However, comparison between inflamed groups of the different diets indicated a significant decrease in relaxation in the HSD CFA cohort compared to the RD CFA ( $p=0.006$ ), demonstrating the effect of both high salt diet and inflammation on bradykinin response in the MCAs.

#### *4.8.3 NOS Inhibition: L-NAME Response*

Endothelial-mediated relaxation by nitric oxide (NO) was tested by the addition of a non-specific nitric oxide synthase (NOS) inhibitor L-NAME (100  $\mu$ M), eliminating NO-mediated vasodilation. Induction of inflammation via CFA treatment did not significantly decrease response to L-NAME in the RD groups despite a trend in depressed response (RD CFA vs. RD SAL). However, there was a statistically significant decrease observed with CFA treatment in the HSD groups (HSD CFA vs HSD SAL;  $p=0.018$ ) (Figure 4.10). No statistically significant difference was noted in MCA response to L-NAME between diets. As such, the combination of HSD and CFA treatments appears to be detrimental to the NOS system.

#### *4.8.4 Intracellular $Ca^{2+}$ Release: Vasopressin Response*

The contractile response of the MCA to intracellular  $Ca^{2+}$  release by vasopressin ( $1.23 \times 10^{-7}$  M) was evaluated in the presence of nifedipine (L-type calcium channel blocker; 3  $\mu$ M). There was no significant difference in the treatments in the RD group in their response to sarcoplasmic calcium release (RD CFA vs. RD SAL). However, a statistically significant difference was observed in the HSD rats between inflamed and non-inflamed rats, as the MCAs of HSD CFA group had a significant diminished response to vasopressin compared to the HSD SAL group ( $p=0.03$ ) (Figure 4.11). There was no difference in vessel contraction in response to vasopressin between diets (RD SAL vs. HSD SAL). This indicates that in the presence of a HSD, CFA treatment may interfere with intracellular  $Ca^{2+}$  release.

#### *4.8.5 PKC Activation – Phorbol Dibutyrate*

Phorbol Dibutyrate (1  $\mu$ M) was added to the MCAs to evaluate vascular smooth muscle response to PKC activation in the presence of nifedipine (3  $\mu$ M) (Figure 4.12). A significant difference

was observed in the inflammation (CFA) groups compared to SAL of both RD and HSD groups. (p=0.047, RD CFA vs RD SAL; p=0.018, HSD CFA vs. HSD SAL). There was no statistical difference in PKC activation between the diets (RD SAL vs. HSD SAL). This suggests that CFA treatment may interfere with PKC activation within the MCA, regardless of diet.

Figure 4.8: Pressure dependent constriction in regular and high salt diet fed CFA and SAL groups. Comparisons are made in the MCAs isolated from SHR HSD CFA (n=16), HSD SAL (n=13), RD CFA (n=12) and RD SAL (n=11) groups. Ability of the MCA to respond to a 100 mmHg pressure step was evaluated as intraluminal pressure was raised from ~0 mmHg to 100 mmHg. All values represent mean  $\pm$  SEM. Data was analyzed using two-way ANOVA using the Holm-Sidak Method. \*  $p < 0.05$

Figure 4.8: Pressure Dependent Constriction in Regular and High Salt Diet Fed CFA and SAL Groups

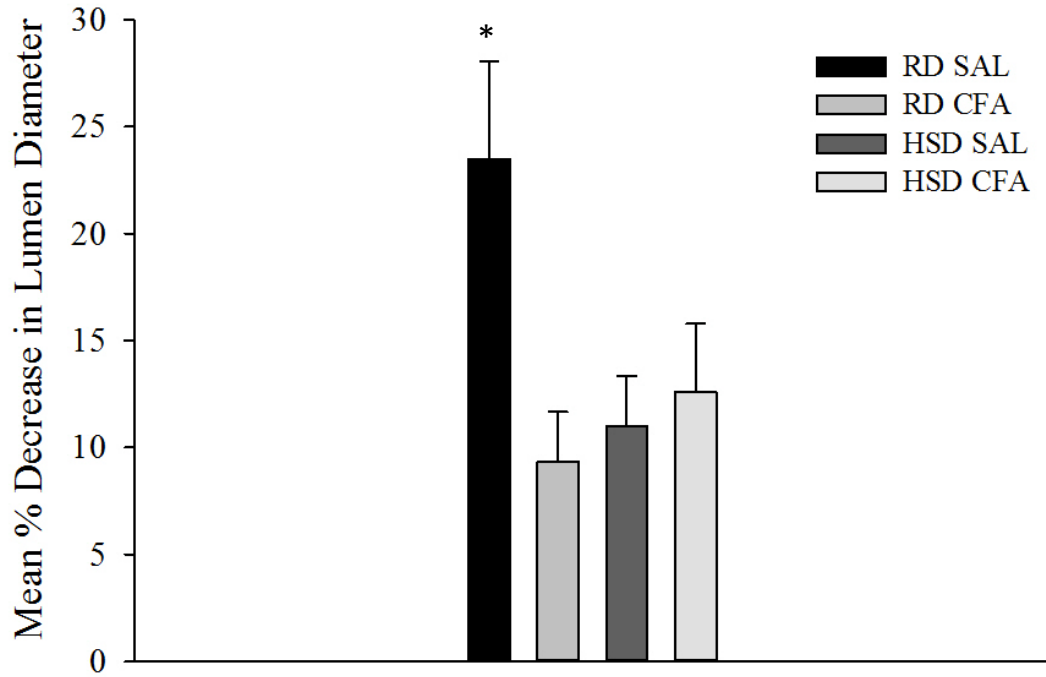


Figure 4.9: Bradykinin-induced relaxation in regular and high salt diet fed CFA and SAL-treated rats. Comparisons are made in the MCAs isolated from SHR HSD CDA (n=9), HSD SAL (n=11), RD CFA (n=10), and RD SAL (n=11) groups. Endothelial response was evaluated by adding 1.6  $\mu$ M bradykinin to the buffer bath and measuring the % maximal dilation of the MCA (compared to dilatory response to 3  $\mu$ M nifedipine). All values represent mean  $\pm$  SEM. Data was analyzed using two-way ANOVA using the Holm-Sidak Method. \*  $p < 0.05$

Figure 4.9: Bradykinin Response in Regular and High Salt Diet Fed CFA and SAL Groups

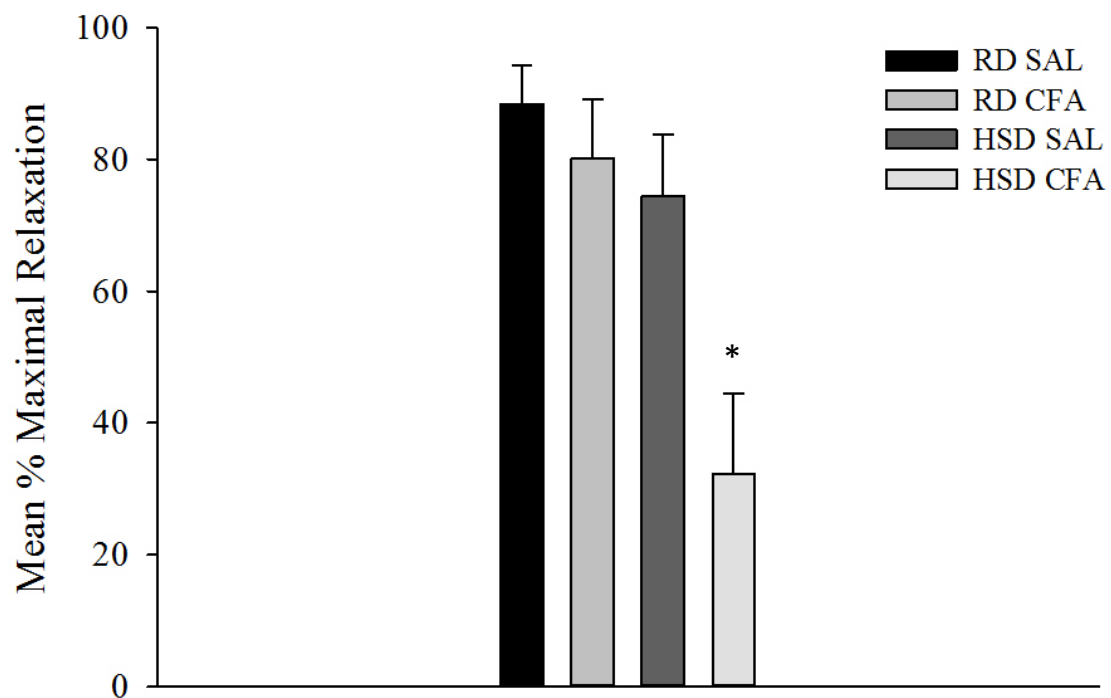


Figure 4.10: L-NAME-mediated vasoconstriction in regular and high salt diet fed CFA and SAL-treated rats. Comparisons are made in the MCAs isolated from SHR HSD CFA (n=16), HSD SAL (n=13), RD CFA (n=11), and RD SAL (n=11) groups. Endothelial response was evaluated by exposing the MCAs to 100  $\mu$ M L-NAME and measuring the % decrease in luminal diameter. All values represent mean  $\pm$  SEM. Data was analyzed using two-way ANOVA using the Holm-Sidak Method. \* p<0.05

Figure 4.10: L-NAME Response in Regular and High Salt Diet Fed CFA and SAL Groups

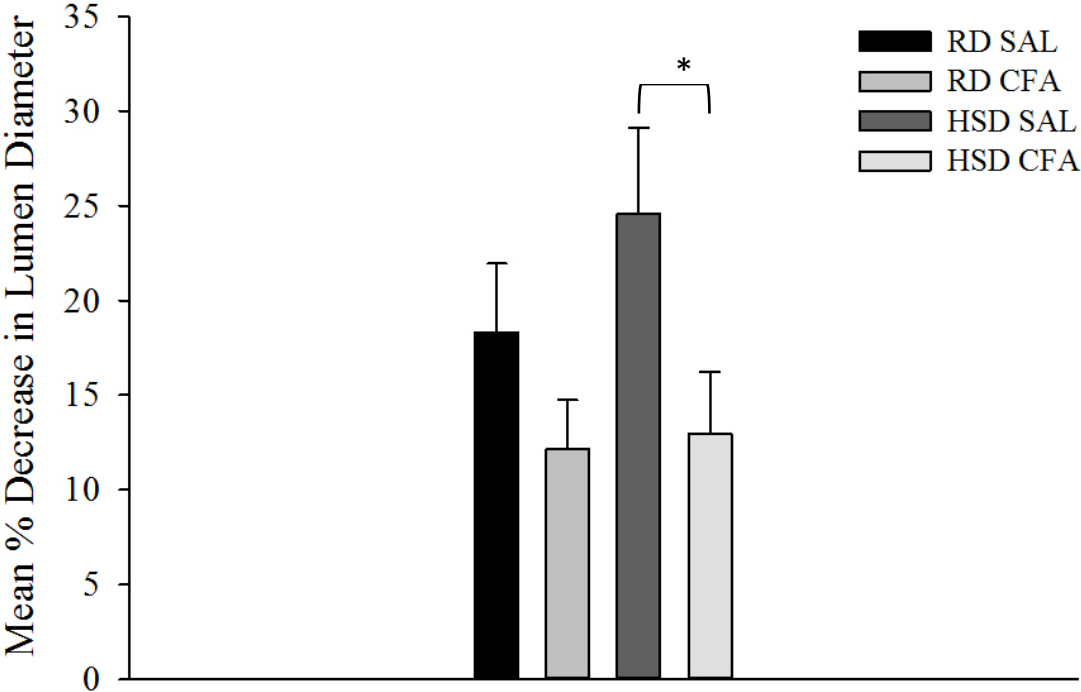


Figure 4.11: Vasopressin-induced vasoconstriction in regular and high salt diet fed CFA and SAL-treated rats. Comparisons are made in the MCAs isolated from SHR HSD CFA (n=16), HSD SAL (n=13), RD CFA (n=12), and RD SAL (n=9) groups. Vascular smooth muscle response to intracellular calcium release was evaluated by exposing the MCA to  $1.23 \times 10^{-7} \text{M}$  vasopressin and measuring the % decrease in luminal diameter from maximal dilation with nifedipine. All values represent mean  $\pm$  SEM. Data was analyzed using two-way ANOVA using the Holm-Sidak Method. \*  $p < 0.05$

Figure 4.11: Vasopressin Response in Regular and High Salt Diet Fed CFA and SAL Groups

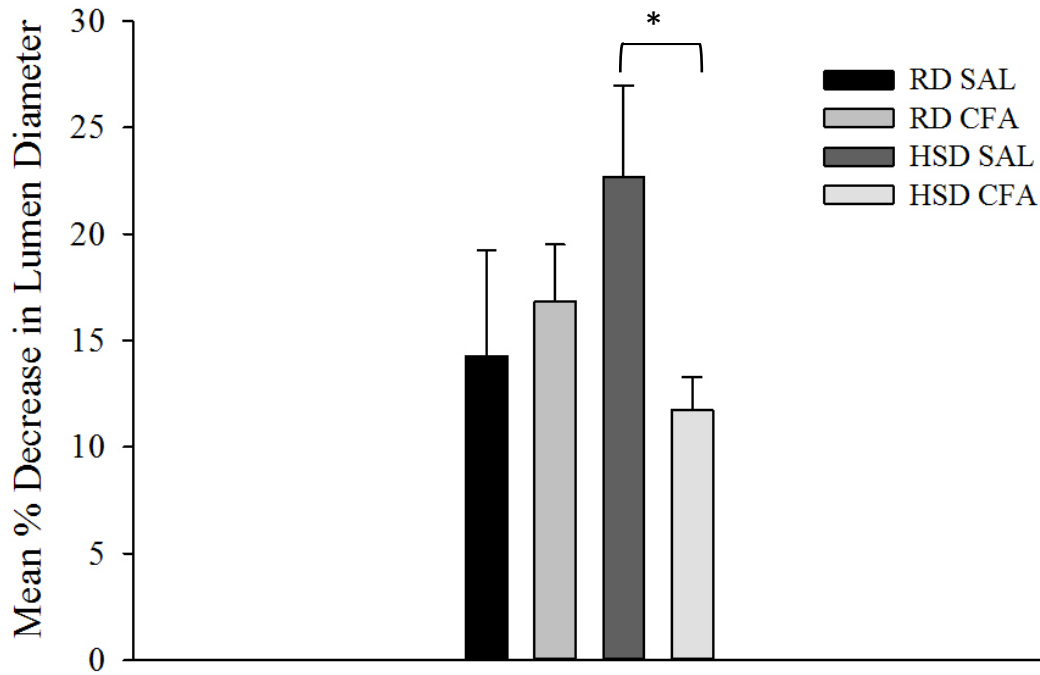
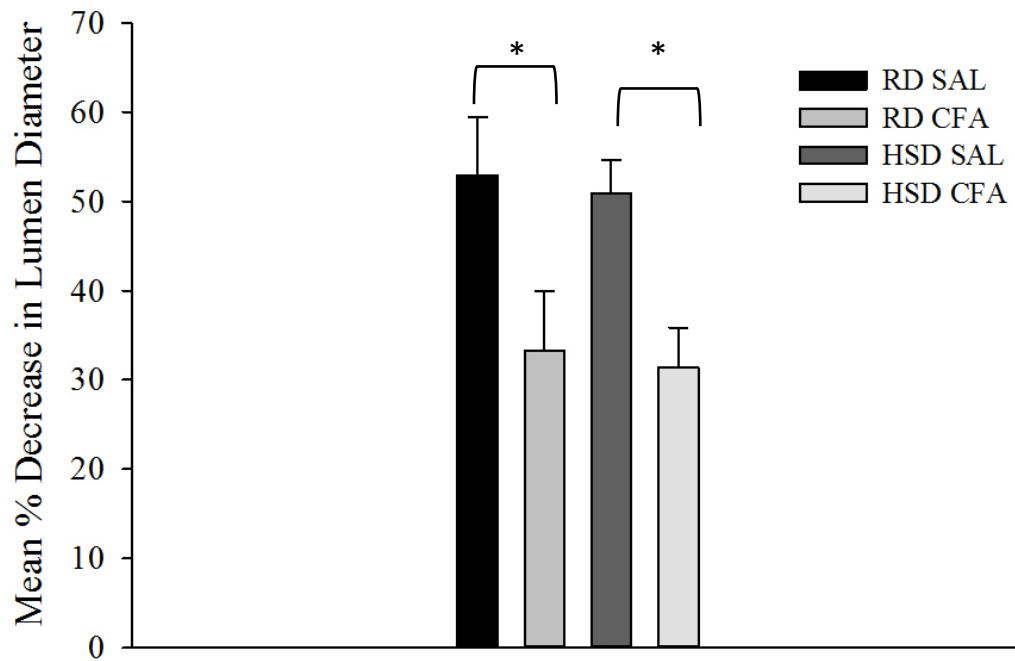


Figure 4.12: Vasoconstriction to PKC activation in regular and high salt diet fed CFA and SAL-treated rats. Comparisons are made in the MCAs isolated from SHR HSD CFA (n=16), HSD SAL (n=13), RD CFA (n=12), and RD SAL (n=9) groups. PKC activation in the vascular smooth muscle was evaluated by exposing the MCA to Phorbol-dibutyrate (1  $\mu$ M) and measuring the % decrease in luminal diameter from maximal dilation with nifedipine. All values represent mean  $\pm$  SEM. Data was analyzed using two-way ANOVA using the Holm-Sidak Method. \*  $p < 0.05$ .

Figure 4.12: Response to PKC Activation in Regular and High Salt Diet Fed CFA and SAL Groups



#### *4.9 The Effect of Diet and Acute IL-17a Incubation on Vascular Function in the MCA (preliminary study)*

To determine whether IL-17a is directly involved in vascular dysfunction induced by CFA treatment and/or HSD regimen, we incubated a sample of MCA's with IL-17a prior to our pressure myograph experiments. IL-17a preincubation significantly decreased PDC (Figure 4.13) and bradykinin-mediated vasodilation (Figure 4.14) in the RD fed animals, while no difference was observed with respect to responses to L-NAME (Figure 4.15), vasopressin (Figure 4.16) and phorbol-dibutyrate (Figure 4.18). In the HSD group, preincubation with IL-17a only affected the L-NAME response (with a significant decrease in constriction) while the MCA's ability to undergo PDC, dilate to bradykinin and constrict in response to vasopressin and phorbol-dibutyrate were unaffected. This suggests that IL-17a may have direct effects on vascular function in the MCA. However, this effect differs based on the diet consumed by the animal.

#### *4.10 The Effect of Chronic Inflammation and Diet on MCA Response in the Presence of IL-17a*

A sample of MCA's from RD CFA and HSD CFA groups were also incubated with IL-17a and evaluated for changes in vascular function (data not shown). Incubation with IL-17a appeared not to alter any parameters of vascular endothelial or smooth muscle function in our MCA's regardless of diet. However, our experiments were insufficiently powered to detect statistical differences due to small sample sizes (n=1-4 per group). Therefore the results are not yet interpretable.

Figure 4.13: Acute effects of IL-17a on pressure dependent constriction. PDC was measured in saline-treated SHR as described previously. Comparisons between RD Reg (n=11) vs RD +IL-17a (n=4) and HSD Reg (n=13) vs HSD +IL-17a (n=7) were made. All values represent mean  $\pm$  SEM. Data was analyzed using one-way ANOVA using Mann-Whitney Rank T-test. \*p<0.05

Figure 4.13: Acute Effects of IL-17a on Pressure Dependent Constriction

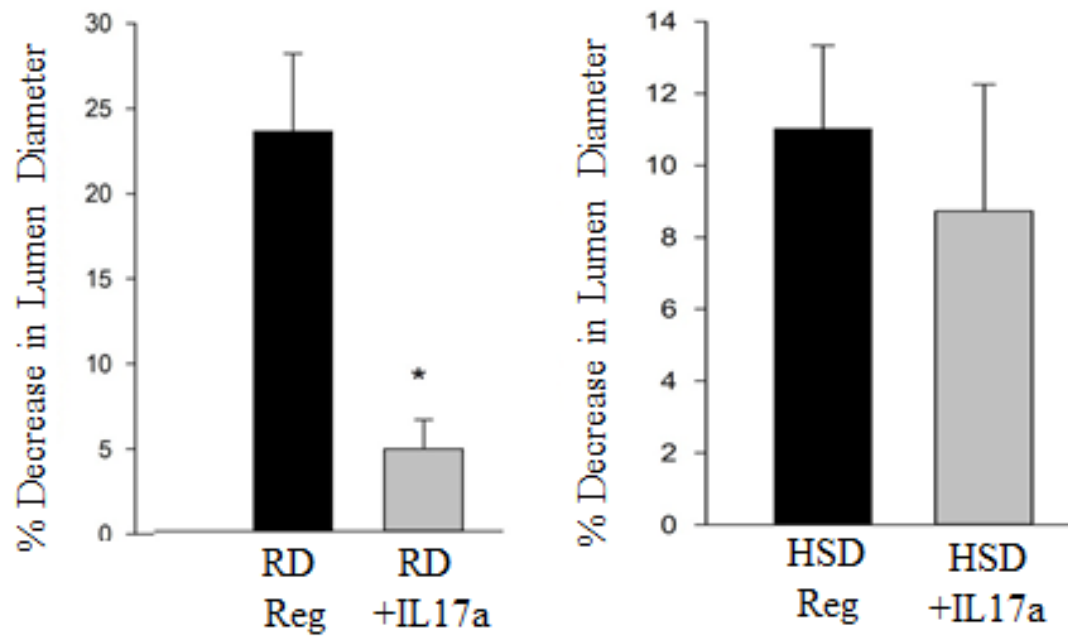


Figure 4.14: Acute effects of IL-17a on bradykinin-mediated vasodilation. Bradykinin-mediated vasodilatory response was measured in saline-treated SHR as described previously. Comparisons between RD Reg (n=11) vs RD +IL-17a (n=4) and HSD Reg (n=11) vs HSD +IL-17a (n=6) were made. All values represent mean  $\pm$  SEM. Data were analyzed using one-way ANOVA using Tukey's T-test. \*p<0.05

Figure 4.14: Acute Effects of IL-17a on Bradykinin Response

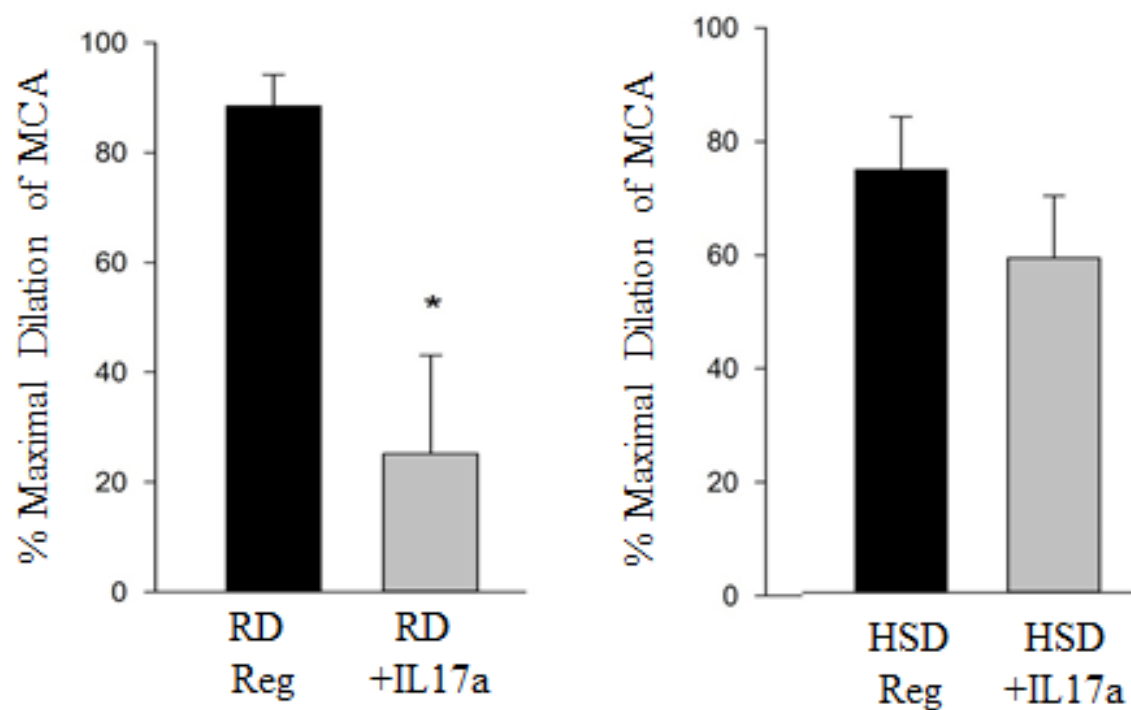


Figure 4.15: Acute effects of IL-17a on L-NAME-mediated vasoconstriction. MCA vasoconstriction to L-NAME was measured in saline-treated SHR as described previously. Comparisons between RD Reg (n=11) vs RD +IL-17a (n=4) and HSD Reg (n=13) vs HSD +IL-17a (n=7) were made. All values represent mean  $\pm$  SEM. Data was analyzed using one-way ANOVA using Tukey's T-test. \*p<0.05.

Figure 4.15: Acute Effects of IL-17a on L-NAME Response

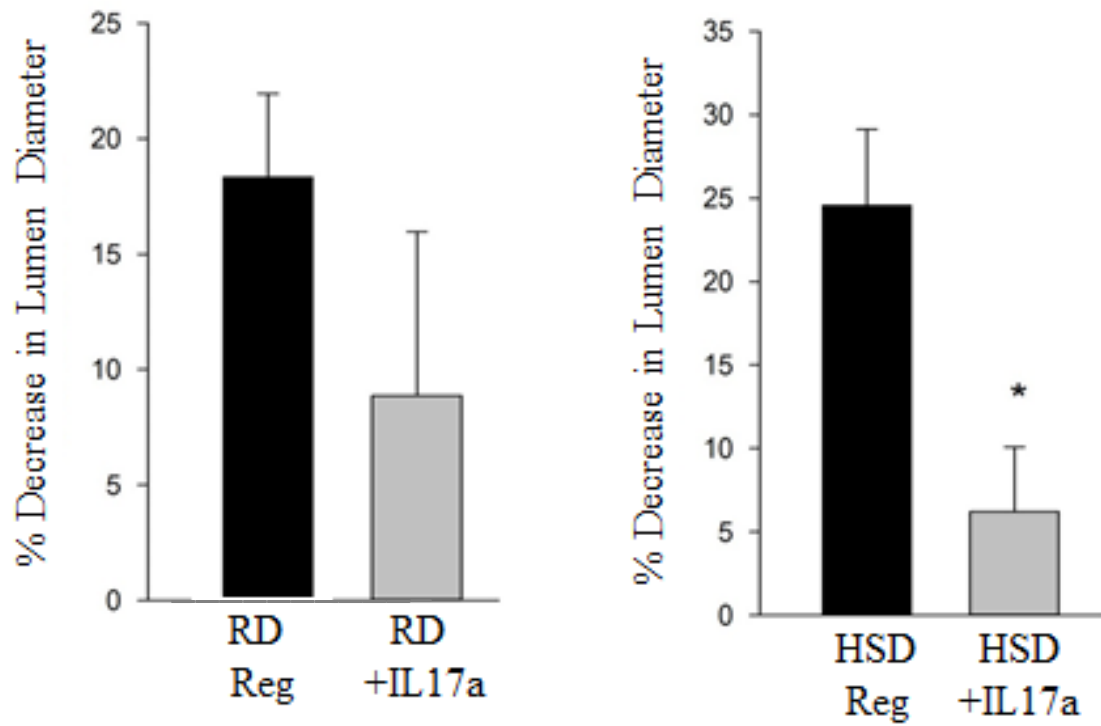


Figure 4.16: Acute effects of IL-17a on vasopressin-induced vasoconstriction. MCA vasoconstrictor response to intracellular calcium release (vasopressin) was measured in saline-treated SHR as described previously. Comparisons between RD Reg (n=11) vs RD +IL-17a (n=4) and HSD Reg (n=13) vs HSD +IL-17a (n=7) are presented here. All values represent mean  $\pm$  SEM. Data was analyzed using one-way ANOVA using Tukey's T-test.

Figure 4.16: Acute Effects of IL-17a on Vasopressin Response

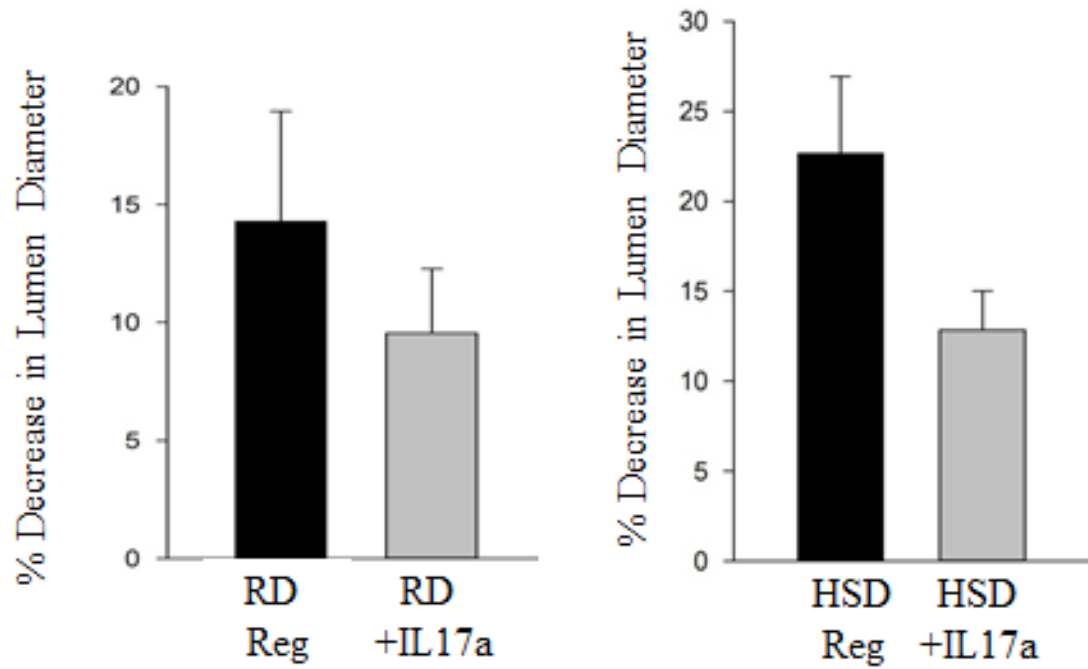
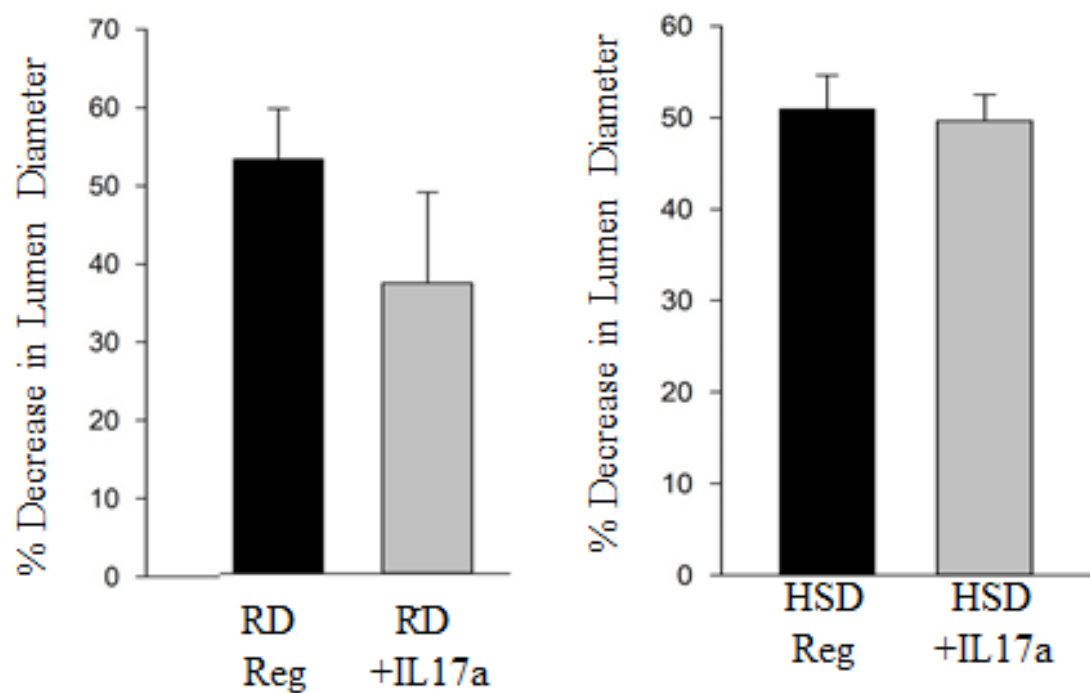


Figure 4.17: Acute effects of IL-17a on vasoconstrictory response to PKC activation. MCA vasoconstriction to activation of PKC (phorbol dibutyrate) was measured in saline-treated SHR as described previously. Comparisons between RD Reg (n=11) vs RD +IL-17a (n=4) and HSD Reg (n=13) vs HSD +IL-17a (n=7) are presented here. All values represent mean  $\pm$  SEM. Data were analyzed using one-way ANOVA using Tukey's T-test.

Figure 4.17: Acute Effects of IL-17a on PKC Activation



## 5.0 Discussion:

Our model is unique in that it is the first animal model in which the induction of mono-arthritis in a stroke-resistant hypertensive rat model potentiates the development of hemorrhagic stroke. This model incorporates the two important aspects in RA conditions which appear to predispose the patient to develop stroke: chronic high blood pressure and chronic inflammatory insult. This study also addresses the impact of high dietary salt content on increasing the systemic inflammatory response, and exacerbating the severity of the hemorrhage in our model.

The CFA-induced mono-arthritis model exemplifies a moderate arthritic response while still inducing systemic inflammation compared to the tail-base, CFA-injected AIA model, which induces severe systemic inflammation, debilitating poly-arthritis, and chronic pain (64). While the latter model often raises concerns for animal welfare and comfort, the former model minimizes animal discomfort and allows for an arthritic injury to develop into polyarthritis as well as systemic inflammation. In our mono-arthritic hypertensive groups, the arthritic index of the forepaws and the contralateral paws rarely exceeded 0, indicating that although systemic inflammation was induced (as observed by increased plasma TNF- $\alpha$  levels), arthritis and joint degradation was likely isolated to the injected paw. Therefore, animals maintained full mobility of most of their limbs, and were able to reach the full 21 day period with minimal buprenorphine administration. The reduced severity of inflammatory response in the SHR strain is not associated with the site of the adjuvant injection (60). The SHR strain itself is deemed to be less prone to inflammation (226). The severity of the AIA model often prevents the experimental protocol from continuing to the full 21 day period and likely increases the need for higher doses (or frequency) of buprenorphine administration, a drug suggested to have variable effects on the vasculature in both chronic and acute administration settings (227, 228).

The joint damage with our mono-arthritis model is reminiscent of the changes that occur with RA (17). There is defined degeneration of the joints and breakdown of cartilage, angiogenesis and vascularizations, and increased levels of cellular infiltrates in the synovium in the CFA-injected paw. The lack of distinction between the intimal and sub-intimal layers may be due to intimal thickening and/or a heavy immune cell infiltration in the subintima, both of which are characteristic of the structural changes to the synovium during progression of arthritis, in addition to synovial villus projections into the joint space (229, 230). These are all changes that are in part attributed to the action of TNF- $\alpha$  (231, 232). However, the systemic response is not as severe in the hypertensive SHR model, possibly due to this strain's immunological resistance to the robust Th1 inflammatory response associated with the injection of CFA. This is due to the general suppression of cell-mediated immunity rendering them "immunologically depressed" compared to commonly used rat strains (226). Classic rat strains including Lewis rats, the Dark Agouti, and the Sprague Dawley rats (SDR) are genetically predisposed to mount a robust systemic inflammatory response to the mycobacterial component of CFA (233-235). Baseline TNF- $\alpha$  levels in the SDR model are approximately 3-fold higher than the SHR strain (data from BioLegend ELISA kit tests, unpublished) and induction of inflammation by CFA injection in the hind paw of the SDR along a similar timeline results in systemic TNF- $\alpha$  of 130-600 pg/ml in comparison to our mean peak levels of 66-200 pg/mL in SHR (236), (unpublished data from Fotso-Soh & Daneshtalab, 2015). While the increase in plasma TNF- $\alpha$  level in our hypertensive mono-arthritic rats are not as high as the SDR models, there is still an increase in the TNF- $\alpha$  in the CFA treated animals compared to the SAL counterparts. The increase in TNF- $\alpha$  level is slight in the RD CFA model, but it is still significantly higher (~3 fold) in the hypertensive-mono-arthritic (HSD CFA) rats on the high salt (4% NaCl) diet (Figure 4.6).

In our model, gross cerebral hemorrhage was not present in the SAL groups, as the SHR strain is deemed to be stroke-resistant (207). It was only in conjunction with the mono-arthritic injury that evidence of gross hemorrhage and altered brain morphology occurred, regardless of the diet. Evidence shows that the loss of MCA's ability to undergo PDC is linked to spontaneous hemorrhagic stroke development in the SHRsp model (169). The loss of MCA function is attributed to changes in endothelial or smooth muscle function in the SHRsp. If the MCA's endothelial and vascular smooth muscle function were damaged, it would prevent the MCAs from undergoing PDC and properly auto-regulating the blood flow. It is possible that inflammatory mediators produced by our current mono-arthritic model, in conjunction with the underlying hypertensive physiology, played a role in the loss of MCA function by affecting various aspects of vessel function. Studies indicate that intracranial aneurysms are associated with physiological vascular remodeling that occurs in conjunction with inflammatory reactions, NOS dysfunction, and extracellular matrix remodeling (237-240). Moreover, there is a shift in the commonly accepted role of salt in potentiating cardiovascular diseases through traditional mechanisms such as hypertension and kidney dysfunction. More studies highlight salt's integral role in impairing endothelial function, increasing arterial stiffness independent of blood pressure (241-243), and changes to the vascular endothelial glycocalyx layer and epithelial sodium channel to alter non-osmotic storage of salt (244). The increase in severity of HS and MCA dysfunction in the HSD CFA groups also suggests salt and inflammatory injury play a cooperative role in increasing cerebral vessel damage, in the presence of hypertension.

The significant increase in TNF- $\alpha$  in our HSD CFA model (Figure 4.6) is reflective of the possible effect of salt in the diet potentiating the initial inflammatory injury by exponentially increasing the inflammatory response. Our results are consistent with ideas originally presented

by Kleinewietfeld et al and others in which sodium chloride drives autoimmune diseases (245-248). Similarly, the activation of the Th17 pathway via sodium chloride was proposed to be involved in increasing the severity of the experimental autoimmune encephalomyelitis (EAE) in mice due to an increase in other pro-inflammatory cytokines such as TNF- $\alpha$  and IL-2. Our HSD CFA model shows similarities to the salt-EAE model previously proposed, as there is exacerbation of the inflammatory response and evidence of severe hemorrhagic stroke development as indicated by intracerebral extravasation of Evans-blue dye and visually apparent altered brain morphology with increasing cerebral edema, regional ischemia, decreased perfusion and deviation in hemisphere size. However, hemorrhagic stroke was also induced, albeit less severely as pin-point hemorrhages, in the RD CFA group who were fed a regular salt diet. Indeed, extravasation of Evans-blue dye was present in 100% of HSD-CFA and 84% of RD-CFA groups investigated. Interestingly, the morphological appearance of the brains of the RD-CFA animals appeared healthy, even with the pinpoint hemorrhages, particularly in comparison to what we have observed in post-stroke SHRsp models and our current HSD-CFA model. Also, as intracerebral hemorrhages do not always appear on the brain surface, the results of the RD-CFA's are not indicative of internal brain damage which requires further investigation. Although the TNF- $\alpha$  level was not statistically higher in the RD CFA compared to the SAL-treated animals, it was approximately 10-fold higher. Therefore, as an adjuvant arthritic model, this is reflective of the immune-complexity and heterogeneity that exists within the pathogenesis of RA, with high interpatient variability (249).

A vast network of immune cells and cytokines are likely involved in the disease progression from the initial inflammatory injury, involving local recruitment and activation of immune cells as well as effector functions (250). The main pro-inflammatory cytokine directly

correlated with joint destruction in RA is TNF- $\alpha$  (251). In addition to its direct effects on joint degeneration, TNF- $\alpha$  induces several other pro-inflammatory cytokines such as interleukin-1 (IL-1), interleukin-8 (IL-8), and granulocyte macrophage-colony stimulating factor (GM-CSF) (252). It mediates the expression, and in some cases amplifies the effects of, inflammatory mediators including IL-1 $\beta$ , PGE<sub>2</sub>, NO (253) and interleukin-6 (IL-6) in peripheral organs (254). Additionally, there is evidence of the involvement of TNF- $\alpha$  in increasing angiotensin II (AGII) levels and activity, and inducing nephron-glomerular damage, increasing urea and uric acid accumulation in plasma, inducing hypertension, and worsening endothelial dysfunction (255-261). Periodic Acid-Schiff (PAS) staining of kidney samples from our animals (performed by Dr. Dickhout's lab (*unpublished*)) revealed signs of inflammatory infiltrates and glomerular sclerosis in both inflamed groups (RD CFA and HSD CFA), although renal damage was more severe in the HSD CFA rats with the appearance of obsolete (non-functional) glomeruli. Although saline-treated controls receiving HSD showed evidence of renal damage and immune cell infiltrates as well, the frequency of obsolete glomeruli and protein casts increased significantly after CFA treatment, as did the occurrence of inflammatory infiltrates. In contrast, the RD SAL cohort showed no signs of renal damage indicating that nephron-glomerular insult was attributed to high dietary salt content and/or inflammatory injury from CFA injection. As such, conditions associated with kidney damage precede the development of hemorrhagic stroke (262), and appears to be occurring in our hypertensive mono-arthritic model, although further investigation into the effect of kidney disease in our model is warranted. It is also likely that increases in various pro-inflammatory cytokines systemically induce central inflammation (in the brain) and cytokine production, promoting intracerebral damage directly and increasing

incidence of hemorrhagic damage in our hypertensive mono-arthritic models, and requires additional scrutiny.

Intracerebral hemorrhages are also characterized by the middle cerebral artery (MCA)'s inability to undergo autoregulation and maintain constant cerebral perfusion, particularly during chronic hypertension. Our animal groups all remained hypertensive (at ~230mmHg compared to the normal blood pressure of less than 140 mmHg for a SDR strain) throughout the experimental period regardless of their treatment. Although there were no significant differences in blood pressure among the groups from baseline, there were variations throughout the experimental timeline associated with the diet or CFA-treatment (Figure 4.5). Regardless of this, the ability of the MCA to undergo PDC was significantly diminished in all groups relative to the RD SAL control (Figure 4.8). The maintenance of high systolic blood pressure is independent of diet among our experimental groups, which allows us to isolate the diet effect on MCA function as well, rather than blood pressure differences. Although Yamori *et al* found that with sustained levels of stress, spontaneous stroke can occur in up to 30% of SHRs (225), no signs of cerebral hemorrhage was observed in any of the SAL-treated SHR.

Evidence in the literature indicates that MCA's isolated from SHRsp prior to signs of stroke showed healthy responses to various vasoactive drugs which affect both endothelial and vascular smooth muscle function. Response to certain vasogenic peptides were all lost in the SHRsp after evidence of stroke, although response to phorbol dibutyrate was maintained to a lesser extent in some. Moreover, PDC was also lost, which indicates dysfunction in various aspects of vascular function as well (18, 168, 171, 218). Due to signs of gross cerebral hemorrhage found in both CFA groups in our study, comparisons between the various indicators of vascular function in our animal models and the pre-stroke and post-stroke SHRsp was

necessary. Our study showed the type of diet (HSD vs RD) and treatment (CFA vs SAL) affected different aspects of the MCA's vascular function. When we compared treatment differences in our RD-fed rats', vascular response to phorbol dibutyrate (Figure 4.12) and PDC (Figure 4.8) were significantly diminished with CFA compared to SAL but responses to bradykinin (Figure 4.9), L-NAME (Figure 4.10) and vasopressin (Figure 4.11) were not affected. In our HSD-fed CFA rats, responses to all indicators of vascular function (bradykinin, L-NAME, vasopressin and phorbol dibutyrate) were significantly diminished with CFA treatment compared to SAL controls. However, there was no significant loss of PDC in the HSD rats between CFA and SAL treatment, which was unexpected. A comparison of the effect of diet (HSD or RD) on PDC showed a significant loss of PDC in the MCA with HSD compared to RD SAL animals, indicating that the diet alone may be causing vascular damage. Interestingly, although the HSD SAL rats had diminished response to PDC compared to their RD SAL controls, there were no signs of gross cerebral hemorrhage in the HSD-SAL group. This suggests that a diminished PDC response may not be sufficient to elicit vessel rupture or signs of gross hemorrhage on its own. However, chronic inflammation may be triggering a sequence of events within the MCA leading to changes in the autoregulatory capacity of the vessel, regardless of diet.

The lack of appropriate autoregulatory function in the MCA of the HSD SAL rats is likely attributed to the effects of chronic high salt diet on the endothelium and its homeostatic functions. Endothelial dysfunction secondary to chronic salt intake has been linked to increased endothelial production of Transforming Growth Factor (TGF)- $\beta$  which in turn increases the production of reactive oxygen species (ROS) through NADPH oxidase-4 (NOX4), leading to decreased NO bioavailability (263, 264). In male SDRs, aortic vascular endothelial  $[Ca^{2+}]_i$  signaling in response to histamine and methacholine was impaired after a short term 8%

NaCl diet (243). Although there was no significant decrease in the ability of the HSD SAL group to respond to bradykinin (Figure 4.9), endothelial dysfunction involving changes in ROS and endothelial  $\text{Ca}^{2+}$  regulation may occur as possible mechanisms of PDC failure. The lack of difference in PDC response between HSD-fed animals may therefore be accounted for by the significantly detrimental effects of the HSD to various aspects of MCA's endothelial function involved in regulating PDC to a point where additional damage caused by inflammatory injury were likely negligible in the HSD CFA group. We can, however, observe the direct effect of inflammatory treatment on MCA function in our RD-fed groups, as evidenced by cerebrovascular function in the RD CFA group.

The RD CFA group had significantly diminished PDC response, indicating that inflammatory pathology may be involved directly in autoregulatory dysfunction. One possible mechanism by which this altered vascular response may have occurred is by the increased expression of specific transient receptor potential (TRP) channels. Recent data is now showing an association between chronic inflammatory conditions such as RA and increased expression of TRP channels at the cell surface (265-267). TRP channel upregulation can be triggered by increased and persistent local production of ROS and pro-inflammatory cytokines, increased kinase activity such as NF- $\kappa$ B (268), and other physical and chemical cell-stress signals (267). Two types of channels that are known to be present in cerebral arteries are TRPV1 and TRPV4. When activated by increased  $[\text{Ca}^{2+}]_i$  in the endothelium, they cause vasodilation (148). It may be that over-expression of TRPV1 occurs in RD CFA due to the increased inflammatory milieu, which could explain why the pressure-induced contractile response was impaired while the bradykinin vasodilatory response remained intact.

The effect of inflammatory mediators on the endothelium has also been studied with the interaction between TNF- $\alpha$  and eNOS. Evidence shows that TNF- $\alpha$  interferes with endothelial nitric oxide (eNOS) production at the mRNA level by inhibiting the eNOS promoter and destabilizing the mRNA. This leads to endothelial dysfunction and vasoconstriction due to a shortage of eNOS (269). In our study, evaluation of the MCA's response to bradykinin (which causes NO release in the vascular endothelium leading to vasodilation) and L-NAME (an inhibitor of NOS, which decreases NO release and leads to vasoconstriction) was performed. The HSD CFA exhibited a significant decrease in response to both bradykinin and L-NAME compared to HSD SAL, whereas no difference was observed between treatments in the RD-fed animals. It appears that endothelial dysfunction is exacerbated by chronic high salt diet and inflammatory insult, leading to the diminished response to bradykinin. Alternatively, bradykinin activates other vasodilatory effectors including endothelial derived hyperpolarizing factor (EDHF) (147). Kessler et al. showed that chronic elevation of pro-inflammatory cytokines such as IL-1 $\beta$  and TNF- $\alpha$  are known to decrease the production of EDHF, leading to diminished EDHF-initiated relaxation of the vascular smooth muscle (25). The degree of systemic inflammation, as observed by the plasma levels of TNF- $\alpha$  were approximately 8-fold higher in the HSD CFA group compared to HSD SAL and 3-fold higher than the RD CFA cohort (Figure 4.6). It is possible that the magnitude of the TNF- $\alpha$ -incited EDHF and eNOS inhibitory effects may be occurring more prominently among HSD-fed, CFA-treated rats, lending evidence to possible interactions between HSD and inflammation to promote further endothelial damage. TNF- $\alpha$  levels were not statistically higher in the RD CFA rats compared to RD SAL rats, which may potentially explain why there was no significant difference in L-NAME or bradykinin response between inflamed and non-inflamed RD-fed SHR.

The evidence of the direct effects of HSD on endothelial response is well-established, as a wealth of literature exists to link dietary sodium chloride to endothelial dysfunction. Chronic high salt intake is correlated to decrease in NO bioavailability, and increased endothelial and arterial stiffness, diminishing vascular integrity and compliance (127, 241, 244, 270). Direct effects of the HSD on cerebral vessels may explain why our RD SAL group had a significantly better vasodilatory response to bradykinin than the HSD SAL group and why observed cerebrovascular damage (particularly on the endothelium) was exponentially increased when HSD was combined with inflammatory injury in the HSD CFA group (as seen in the diminished response to bradykinin).

Our results indicate that there is also a significant degree of vascular smooth muscle dysfunction, which is associated primarily with CFA treatment rather than diet effect. However, there were differences in the degree of vascular smooth muscle damage associated with both diet and inflammation. While the HSD CFA group had a significantly diminished response to both vasopressin and phorbol ester (compared to HSD SAL), the RD-fed CFA group only showed a diminished response to PKC activation (compared to RD SAL). MCA remodeling due to an increase in inflammatory mediators may be accountable for the dysfunctional response to sarcoplasmic calcium release (vasopressin) as well as PKC activation (phorbol dibutyrate) (144, 152, 171). TNF- $\alpha$  is a potent stimulator of vascular remodeling for the smooth muscle cell layer of the vascular wall, increasing matrix metalloproteinase activity and increasing proliferation of vascular smooth muscle cells (271, 272). The impaired response to PKC activation in both inflamed groups is akin to the decrease in PKC observed in the post-stroke SHRsp (171). However, the MCA's of these post-stroke SHRsp were also unable to constrict in response to vasopressin as well, which was only apparent in our HSD-fed CFA group. Binding of

vasopressin to its receptor (V1) activates the vascular contractile response through activation of phospholipase C (PLC) which triggers a series of downstream events leading to release of  $\text{Ca}^{2+}$  from the sarcoplasmic reticulum, secondary to the cleavage of phosphatidylinositol 4,5-bisphosphate ( $\text{PIP}_2$ ) and release of inositol trisphosphate ( $\text{IP}_3$ ) (273). However, this mechanism also releases diacylglycerol (DAG) which additionally translocates and activates PKC (273). In our model, inflammation and HSD may impair both the PLC/  $\text{IP}_3$  along with the PKC system. The RD-fed CFA group on the other hand, only exhibited dysfunction in PKC activation while maintaining PLC/  $\text{IP}_3$  signaling, which appears to occur in spite of the necessary cooperation of the pathways after V1 receptor activation. Interestingly, the RD-fed CFA groups still showed signs of pinpoint hemorrhages despite a functioning MCA. This indicates that although there are absolute signs of vascular dysfunction and stroke-related changes to cerebral vascular function, it is still possible to have hemorrhagic stroke without exhibiting all levels of dysfunction exemplified by the post-stroke SHRsp (ie: lack of response to bradykinin, L-NAME, vasopressin, phorbol dibutyrate and PDC).

In conjunction with the effect of salt and inflammatory injury in promoting intracerebral hemorrhage, the age of the SHRs themselves is also important. Preliminary studies in the SHR to induce HS with CFA injection failed if the animals were younger than 3 months of age. The optimal age for creating the hypertensive mono-arthritic model was 20-28 weeks of age (~5-7 months), equivalent to approximately 20-40 human years (274). We believe the model at this age better reflects the onset and progression of RA; although RA can start at any age, it often peaks between ages of 30-50 years, regardless of genetic predisposition.

Our results indicate that inflammatory injury in the setting of high dietary sodium intake and chronic hypertension leads to a more severe course of inflammatory autoimmune disease and

predisposes the patient to developing an apparently more severe form of hemorrhagic stroke. Based on the presence of inflammatory infiltrates in the kidneys of our HSD-fed, saline controls, it is likely that elevated dietary sodium alone is initiating a type of inflammatory process. *In vitro* and *in vivo* data shows that in the presence of a modest sodium increase, pathogenic Th17 induction occurs, leading to tissue inflammation (275). Subsequent inflammatory insult by way of CFA injection inarguably exacerbates this process, leading to diffuse renal damage and also cerebral hemorrhage. The varying levels of hemorrhage observed in our model, being less severe than what is usually observed in the SHRsp model, allowed us to correlate the subsequent tiers of cerebrovascular dysfunction compared to the SHRsp model.

#### *5.1: Limitations and Future Directions*

Although our goal was to study the mechanism of hemorrhagic stroke in an animal model of RA and chronic hypertension, there are several limitations to our data. We did find signs of cerebral hemorrhage in our inflamed animals on Day 21 however, we do not currently know when stroke occurred, as we did not observe obvious acute signs of stroke (ie: hemi-paralysis, twitching, “slug” behavior associated with stroke occurrence in the SHRsp model), making it difficult to correlate the observed vascular dysfunction with our cytokine assay data. Although TNF $\alpha$  levels seemed to peak at Days 7 and 14 as well, we cannot correlate this to the timing of cerebral hemorrhage or link the acute peak to our vascular function analysis, as cytokine levels had dropped by Day 21 in the RD-fed animals. Although there may be acute vascular effects of these pro-inflammatory cytokines, our study was not appropriately designed to detect these effects. Sacrifice and sampling of our animals at multiple time points (Day 7, 14 and 21) would provide more information to correlate the vascular implications of acute spikes in inflammatory mediators, allowing us to more appropriately narrow down the time frame at which cerebral

hemorrhage is occurring. Additionally, extrapolation of our stroke pathogenesis results to the human RA population is not completely applicable at this time. While it is widely accepted that atherosclerosis is positively correlated to human stroke development, this factor is absent as our rat model does not develop atherosclerosis (276). Therefore, comparison made between our model of hemorrhagic stroke and human disease must be made with caution. Another potential limitation is the apparent decrease in blood pressure in all groups on Day 7 of our experimental timeline. Because animals were not previously acclimatized to being frequently handled or having their blood pressure measured, it is very likely that they were stressed on the day of their baseline reading. This possibly gave a false trend of blood pressure decreasing one week after injection. Therefore, acclimatization of rodents to the blood pressure monitoring protocol as well as regular handling for two weeks prior to the start of experiments would help to avoid misinterpretation of results. Conversely, the use of implantable telemeters would likely yield much more consistent blood pressure monitoring throughout the experimental period, eliminating handling bias.

Evaluation of endothelial function only included analysis of vascular response to bradykinin and NOS inhibition, which does not provide a complete picture of endothelial function as a whole since mediators such as EDHF and PGI<sub>2</sub> also play a role in endothelial-mediated vasodilation. In addition, alterations to vascular response to NOS inhibition only generates partial insight into inflammation-related changes to the MCA. Data suggests that IL-17 may have direct effects on the activity of eNOS (100), requiring appropriate characterization of active versus inactive eNOS expression in the MCA. We also believe that modulation in expression of certain TRP channels may be involved in changes to MCA function. Therefore, characterization of TRP channel expression (especially TRPV4) on the vascular endothelium

would test this hypothesis. It would also be interesting to test expression patterns of the various VOC and TRPC channels in the smooth muscle of the MCA as well.

Of particular importance is the fact that our preliminary data evaluating vascular function in the presence of acute IL-17a exposure is insufficiently powered at this time to detect statistically significant differences in many of our groups. Therefore, these data are not interpretable at this time but rather represent an area for future work. This future work should also include characterization of TRPV4 channel expression pre-and post-incubation with IL-17a to further test our hypothesis that TRP channel expression is playing a role in functional alterations to the MCA.

### *Conclusion*

Essentially, our results demonstrate that the combination of chronic inflammation and high dietary salt intake is detrimental to the mechanical functioning of the cerebrovasculature in the setting of chronic hypertension. This failure is evidenced by not only cerebral vascular dysfunction but ultimately the inability to effectively autoregulate lumen diameter of the MCA leading to over-perfusion and cerebral hemorrhage.

## References:

1. Canada AAo. The Impact of Arthritis in Canada: Today and Over the Next 30 Years. 2011;32(40).
2. Cutolo M, Kitas GD, van Riel PL. Burden of disease in treated rheumatoid arthritis patients: going beyond the joint. *Seminars in arthritis and rheumatism*. 2014;43(4):479-88.
3. Solomon DH, Karlson EW, Rimm EB, Cannuscio CC, Mandl LA, Manson JE, et al. Cardiovascular morbidity and mortality in women diagnosed with rheumatoid arthritis. *Circulation*. 2003;107(9):1303-7.
4. Gonzalez A, Maradit Kremers H, Crowson CS, Ballman KV, Roger VL, Jacobsen SJ, et al. Do cardiovascular risk factors confer the same risk for cardiovascular outcomes in rheumatoid arthritis patients as in non-rheumatoid arthritis patients? *Ann Rheum Dis*. 2008;67(1):64-9.
5. England BR, Sayles H, Michaud K, Caplan L, Davis LA, Cannon GW, et al. Cause-Specific Mortality in Male US Veterans With Rheumatoid Arthritis. *Arthritis care & research*. 2016;68(1):36-45.
6. Lindhardsen J, Ahlehoff O, Gislason GH, Madsen OR, Olesen JB, Svendsen JH, et al. Risk of atrial fibrillation and stroke in rheumatoid arthritis: Danish nationwide cohort study. *Bmj*. 2012;344:e1257.
7. Zoller B, Li X, Sundquist J, Sundquist K. Risk of subsequent ischemic and hemorrhagic stroke in patients hospitalized for immune-mediated diseases: a nationwide follow-up study from Sweden. *BMC Neurol*. 2012;12:41.
8. Thrift AG, McNeil JJ, Forbes A, Donnan GA. Risk factors for cerebral hemorrhage in the era of well-controlled hypertension. Melbourne Risk Factor Study (MERFS) Group. *Stroke*. 1996;27(11):2020-5.
9. Donnan GA, Fisher M, Macleod M, Davis SM. *Stroke*. *Lancet*. 2008;371(9624):1612-23.
10. Book C, Saxne T, Jacobsson LT. Prediction of mortality in rheumatoid arthritis based on disease activity markers. *The Journal of rheumatology*. 2005;32(3):430-4.
11. Sokka T, Abelson B, Pincus T. Mortality in rheumatoid arthritis: 2008 update. *Clinical and experimental rheumatology*. 2008;26(5 Suppl 51):S35-61.
12. Boyer JF, Gourraud PA, Cantagrel A, Davignon JL, Constantin A. Traditional cardiovascular risk factors in rheumatoid arthritis: a meta-analysis. *Joint, bone, spine : revue du rhumatisme*. 2011;78(2):179-83.
13. Baghdadi LR, Woodman RJ, Shanahan EM, Mangoni AA. The impact of traditional cardiovascular risk factors on cardiovascular outcomes in patients with rheumatoid arthritis: a systematic review and meta-analysis. *PloS one*. 2015;10(2):e0117952.
14. Thrift AG, Donnan GA, McNeil JJ. Epidemiology of intracerebral hemorrhage. *Epidemiol Rev*. 1995;17(2):361-81.
15. Williams RO. Rodent models of arthritis: relevance for human disease. *Clin Exp Immunol*. 1998;114(3):330-2.
16. Brahn E. Animal models of rheumatoid arthritis. Clues to etiology and treatment. *Clin Orthop Relat Res*. 1991(265):42-53.
17. Kannan K, Ortmann RA, Kimpel D. Animal models of rheumatoid arthritis and their relevance to human disease. *Pathophysiology*. 2005;12(3):167-81.

18. Smeda JS. Cerebral vascular changes associated with hemorrhagic stroke in hypertension. *Canadian journal of physiology and pharmacology*. 1992;70(4):552-64.
19. Sattar N, McCarey DW, Capell H, McInnes IB. Explaining how "high-grade" systemic inflammation accelerates vascular risk in rheumatoid arthritis. *Circulation*. 2003;108(24):2957-63.
20. Sprague AH, Khalil RA. Inflammatory cytokines in vascular dysfunction and vascular disease. *Biochemical pharmacology*. 2009;78(6):539-52.
21. Vanhoutte PM, Shimokawa H, Feletou M, Tang EH. Endothelial Dysfunction and Vascular Disease - A Thirtieth Anniversary Update. *Acta physiologica (Oxford, England)*. 2015.
22. Bassenge E, Heusch G. Endothelial and neuro-humoral control of coronary blood flow in health and disease. *Reviews of physiology, biochemistry and pharmacology*. 1990;116:77-165.
23. Vanhoutte PM, Mombouli JV. Vascular endothelium: vasoactive mediators. *Progress in cardiovascular diseases*. 1996;39(3):229-38.
24. Johnson PC. Autoregulation of blood flow. *Circ Res*. 1986;59(5):483-95.
25. Kessler P, Popp R, Busse R, Schini-Kerth VB. Proinflammatory mediators chronically downregulate the formation of the endothelium-derived hyperpolarizing factor in arteries via a nitric oxide/cyclic GMP-dependent mechanism. *Circulation*. 1999;99(14):1878-84.
26. (ACREU) ACRaEU. Arthritis in Canada: The Arthritis Society; 2013 [cited 2015 11/27/2015]. Available from: <http://arthritis.ca/understand-arthritis/arthritis-facts-figures>.
27. Undifferentiated early inflammatory arthritis in adults [Internet]. UpToDate. 2015 [cited Oct 2015].
28. McInnes IB, Schett G. Cytokines in the pathogenesis of rheumatoid arthritis. *Nature reviews Immunology*. 2007;7(6):429-42.
29. Aletaha D, Smolen J, Ward MM. Measuring function in rheumatoid arthritis: Identifying reversible and irreversible components. *Arthritis and rheumatism*. 2006;54(9):2784-92.
30. Drossaers-Bakker KW, de Buck M, van Zeben D, Zwinderman AH, Breedveld FC, Hazes JM. Long-term course and outcome of functional capacity in rheumatoid arthritis: the effect of disease activity and radiologic damage over time. *Arthritis and rheumatism*. 1999;42(9):1854-60.
31. Redlich K, Smolen JS. Inflammatory bone loss: pathogenesis and therapeutic intervention. *Nature reviews Drug discovery*. 2012;11(3):234-50.
32. Hazes JM, Luime JJ. The epidemiology of early inflammatory arthritis. *Nature reviews Rheumatology*. 2011;7(7):381-90.
33. Rheumatoid Arthritis [Internet]. 2009.
34. Shah A SCE. Rheumatoid Arthritis. In: Kasper D FA, Hauser S, Longo D, Jameson J, Loscalzo J., editor. *Harrison's Principles of Internal Medicine*. 19 ed. New York, NY: McGraw-Hill; 2015.
35. Mjaavatten MD, Bykerk VP. Early rheumatoid arthritis: the performance of the 2010 ACR/EULAR criteria for diagnosing RA. *Best practice & research Clinical rheumatology*. 2013;27(4):451-66.
36. Chimenti MS, Triggianese P, Conigliaro P, Candi E, Melino G, Perricone R. The interplay between inflammation and metabolism in rheumatoid arthritis. *Cell death & disease*. 2015;6:e1887.

37. McInnes IB, Schett G. The pathogenesis of rheumatoid arthritis. *The New England journal of medicine*. 2011;365(23):2205-19.
38. Isaacs JD. The changing face of rheumatoid arthritis: sustained remission for all? *Nature reviews Immunology*. 2010;10(8):605-11.
39. Barton A, Worthington J. Genetic susceptibility to rheumatoid arthritis: an emerging picture. *Arthritis and rheumatism*. 2009;61(10):1441-6.
40. Kallberg H, Padyukov L, Plenge RM, Ronnelid J, Gregersen PK, van der Helm-van Mil AH, et al. Gene-gene and gene-environment interactions involving HLA-DRB1, PTPN22, and smoking in two subsets of rheumatoid arthritis. *American journal of human genetics*. 2007;80(5):867-75.
41. Oliver JE, Silman AJ. What epidemiology has told us about risk factors and aetiopathogenesis in rheumatic diseases. *Arthritis research & therapy*. 2009;11(3):223.
42. Kallberg H, Jacobsen S, Bengtsson C, Pedersen M, Padyukov L, Garred P, et al. Alcohol consumption is associated with decreased risk of rheumatoid arthritis: results from two Scandinavian case-control studies. *Ann Rheum Dis*. 2009;68(2):222-7.
43. Smolen JS, Steiner G. Therapeutic strategies for rheumatoid arthritis. *Nature reviews Drug discovery*. 2003;2(6):473-88.
44. Smolen JS, Aletaha D, Koeller M, Weisman MH, Emery P. New therapies for treatment of rheumatoid arthritis. *Lancet (London, England)*. 2007;370(9602):1861-74.
45. Chabaud M, Fossiez F, Taupin JL, Miossec P. Enhancing effect of IL-17 on IL-1-induced IL-6 and leukemia inhibitory factor production by rheumatoid arthritis synoviocytes and its regulation by Th2 cytokines. *Journal of immunology (Baltimore, Md : 1950)*. 1998;161(1):409-14.
46. Miossec P, Korn T, Kuchroo VK. Interleukin-17 and type 17 helper T cells. *The New England journal of medicine*. 2009;361(9):888-98.
47. Kolls JK, Linden A. Interleukin-17 family members and inflammation. *Immunity*. 2004;21(4):467-76.
48. Nadkarni S, Mauri C, Ehrenstein MR. Anti-TNF-alpha therapy induces a distinct regulatory T cell population in patients with rheumatoid arthritis via TGF-beta. *J Exp Med*. 2007;204(1):33-9.
49. Steiner G, Tohidast-Akrad M, Witzmann G, Vesely M, Studnicka-Benke A, Gal A, et al. Cytokine production by synovial T cells in rheumatoid arthritis. *Rheumatology (Oxford, England)*. 1999;38(3):202-13.
50. Takayanagi H, Ogasawara K, Hida S, Chiba T, Murata S, Sato K, et al. T-cell-mediated regulation of osteoclastogenesis by signalling cross-talk between RANKL and IFN-gamma. *Nature*. 2000;408(6812):600-5.
51. Bendele A. Animal models of rheumatoid arthritis. *Journal of musculoskeletal & neuronal interactions*. 2001;1(4):377-85.
52. Pearson CM. Development of arthritis, peri-arthritis and periostitis in rats given adjuvants. *Proc Soc Exp Biol Med*. 1956;91(1):95-101.
53. Carlson RP, Datko LJ, O'Neill-Davis L, Blazek EM, DeLustro F, Beideman R, et al. Comparison of inflammatory changes in established type II collagen- and adjuvant-induced arthritis using outbred Wistar rats. *International journal of immunopharmacology*. 1985;7(6):811-26.
54. Van Vollenhoven RF, Soriano A, McCarthy PE, Schwartz RL, Garbrecht FC, Thorbecke GJ, et al. The role of immunity to cartilage proteoglycan in adjuvant arthritis. *Intravenous*

- injection of bovine proteoglycan enhances adjuvant arthritis. *Journal of immunology* (Baltimore, Md : 1950). 1988;141(4):1168-73.
55. Feige U, Schulmeister A, Mollenhauer J, Brune K, Bang H. A constitutive 65 kDa chondrocyte protein as a target antigen in adjuvant arthritis in Lewis rats. *Autoimmunity*. 1994;17(3):233-9.
  56. van de Langerijt AG, van Lent PL, Hermus AR, Sweep CG, Cools AR, van den Berg WB. Susceptibility to adjuvant arthritis: relative importance of adrenal activity and bacterial flora. *Clin Exp Immunol*. 1994;97(1):33-8.
  57. Bendele A, McComb J, Gould T, McAbee T, Sennello G, Chlipala E, et al. Animal models of arthritis: relevance to human disease. *Toxicologic pathology*. 1999;27(1):134-42.
  58. Currey HL. Adjuvant arthritis in the rat. Effect of intraperitoneal injections of either whole dead mycobacteria or tuberculin. *Ann Rheum Dis*. 1970;29(3):314-20.
  59. Chang YH, Pearson CM, Abe C. Adjuvant polyarthritis. IV. Induction by a synthetic adjuvant: immunologic, histopathologic, and other studies. *Arthritis and rheumatism*. 1980;23(1):62-71.
  60. Torres MG, Kwasniewski FH, Scaliante LG, Ishii-Iwamoto EL, Caparroz-Assef SM, Cuman RK, et al. Arthritis induced by adjuvant in spontaneously hypertensive and normotensive rats: endogenous glucocorticoid effects on inflammatory response. *Inflammation*. 2009;32(1):20-6.
  61. Holmdahl R, Lorentzen JC, Lu S, Olofsson P, Wester L, Holmberg J, et al. Arthritis induced in rats with nonimmunogenic adjuvants as models for rheumatoid arthritis. *Immunol Rev*. 2001;184:184-202.
  62. Trentham DE, Townes AS, Kang AH. Autoimmunity to type II collagen an experimental model of arthritis. *J Exp Med*. 1977;146(3):857-68.
  63. Larsson P, Kleinau S, Holmdahl R, Klareskog L. Homologous type II collagen-induced arthritis in rats. Characterization of the disease and demonstration of clinically distinct forms of arthritis in two strains of rats after immunization with the same collagen preparation. *Arthritis and rheumatism*. 1990;33(5):693-701.
  64. Schopf LR AK, Jaffee BD. Rat models of arthritis: Similarities, differences, advantages, and disadvantages in the identification of novel therapeutics. In: Stevenson CS ML, Morgan DW, editor. *In Vivo Models of Inflammation. Progress in Inflammation Research*. 1. 2 ed. Basel, Switzerland: Springer Science+Business Media; 2006. p. 1-34.
  65. Brackertz D, Mitchell GF, Mackay IR. Antigen-induced arthritis in mice. I. Induction of arthritis in various strains of mice. *Arthritis and rheumatism*. 1977;20(3):841-50.
  66. Tiggelman AM, Van Noorden CJ. Mast cells in early stages of antigen-induced arthritis in rat knee joints. *International journal of experimental pathology*. 1990;71(4):455-64.
  67. Brauer R, Kittlick PD, Thoss K, Henzgen S. Different immunological mechanisms contribute to cartilage destruction in antigen-induced arthritis. *Experimental and toxicologic pathology : official journal of the Gesellschaft fur Toxikologische Pathologie*. 1994;46(4-5):383-8.
  68. Henderson B, Thompson RC, Hardingham T, Lewthwaite J. Inhibition of interleukin-1-induced synovitis and articular cartilage proteoglycan loss in the rabbit knee by recombinant human interleukin-1 receptor antagonist. *Cytokine*. 1991;3(3):246-9.
  69. Michaud K, Wolfe F. Comorbidities in rheumatoid arthritis. *Best practice & research Clinical rheumatology*. 2007;21(5):885-906.

70. Nicola PJ, Crowson CS, Maradit-Kremers H, Ballman KV, Roger VL, Jacobsen SJ, et al. Contribution of congestive heart failure and ischemic heart disease to excess mortality in rheumatoid arthritis. *Arthritis and rheumatism*. 2006;54(1):60-7.
71. Gabriel SE. Cardiovascular morbidity and mortality in rheumatoid arthritis. *The American journal of medicine*. 2008;121(10 Suppl 1):S9-14.
72. Goodson N, Marks J, Lunt M, Symmons D. Cardiovascular admissions and mortality in an inception cohort of patients with rheumatoid arthritis with onset in the 1980s and 1990s. *Ann Rheum Dis*. 2005;64(11):1595-601.
73. Atzeni F, Turiel M, Caporali R, Cavagna L, Tomasoni L, Sitia S, et al. The effect of pharmacological therapy on the cardiovascular system of patients with systemic rheumatic diseases. *Autoimmunity reviews*. 2010;9(12):835-9.
74. Sodergren A, Stegmayr B, Lundberg V, Ohman ML, Wallberg-Jonsson S. Increased incidence of and impaired prognosis after acute myocardial infarction among patients with seropositive rheumatoid arthritis. *Ann Rheum Dis*. 2007;66(2):263-6.
75. Crowson CS, Nicola PJ, Kremers HM, O'Fallon WM, Therneau TM, Jacobsen SJ, et al. How much of the increased incidence of heart failure in rheumatoid arthritis is attributable to traditional cardiovascular risk factors and ischemic heart disease? *Arthritis and rheumatism*. 2005;52(10):3039-44.
76. Maradit-Kremers H, Crowson CS, Nicola PJ, Ballman KV, Roger VL, Jacobsen SJ, et al. Increased unrecognized coronary heart disease and sudden deaths in rheumatoid arthritis: a population-based cohort study. *Arthritis and rheumatism*. 2005;52(2):402-11.
77. Solomon DH, Goodson NJ, Katz JN, Weinblatt ME, Avorn J, Setoguchi S, et al. Patterns of cardiovascular risk in rheumatoid arthritis. *Ann Rheum Dis*. 2006;65(12):1608-12.
78. Solomon DH, Curhan GC, Rimm EB, Cannuscio CC, Karlson EW. Cardiovascular risk factors in women with and without rheumatoid arthritis. *Arthritis and rheumatism*. 2004;50(11):3444-9.
79. Sattar N, McInnes IB. Vascular comorbidity in rheumatoid arthritis: potential mechanisms and solutions. *Current opinion in rheumatology*. 2005;17(3):286-92.
80. Deus Junior RS, Ferraz AL, Oesterreich SA, Schmitz WO, Shinzato MM. Risk factors for cardiovascular disease in rheumatoid arthritis patients from Mato Grosso do Sul. *Revista brasileira de reumatologia*. 2015;55(6):493-500.
81. Panoulas VF, Douglas KM, Milionis HJ, Stavropoulos-Kalinglou A, Nightingale P, Kita MD, et al. Prevalence and associations of hypertension and its control in patients with rheumatoid arthritis. *Rheumatology (Oxford, England)*. 2007;46(9):1477-82.
82. Gerli R, Sherer Y, Vaudo G, Schillaci G, Gilburd B, Giordano A, et al. Early atherosclerosis in rheumatoid arthritis: effects of smoking on thickness of the carotid artery intima media. *Annals of the New York Academy of Sciences*. 2005;1051:281-90.
83. McEntegart A, Capell HA, Creran D, Rumley A, Woodward M, Lowe GD. Cardiovascular risk factors, including thrombotic variables, in a population with rheumatoid arthritis. *Rheumatology (Oxford, England)*. 2001;40(6):640-4.
84. Han C, Robinson DW, Jr., Hackett MV, Paramore LC, Fraeman KH, Bala MV. Cardiovascular disease and risk factors in patients with rheumatoid arthritis, psoriatic arthritis, and ankylosing spondylitis. *J Rheumatol*. 2006;33(11):2167-72.
85. Roman MJ, Devereux RB, Schwartz JE, Lockshin MD, Paget SA, Davis A, et al. Arterial stiffness in chronic inflammatory diseases. *Hypertension*. 2005;46(1):194-9.

86. Wong M, Toh L, Wilson A, Rowley K, Karschimkus C, Prior D, et al. Reduced arterial elasticity in rheumatoid arthritis and the relationship to vascular disease risk factors and inflammation. *Arthritis and rheumatism*. 2003;48(1):81-9.
87. Watson DJ, Rhodes T, Guess HA. All-cause mortality and vascular events among patients with rheumatoid arthritis, osteoarthritis, or no arthritis in the UK General Practice Research Database. *J Rheumatol*. 2003;30(6):1196-202.
88. Pinto A, Tuttolomondo A, Di Raimondo D, Fernandez P, Licata G. Cerebrovascular risk factors and clinical classification of strokes. *Seminars in vascular medicine*. 2004;4(3):287-303.
89. Sodergren A, Stegmayr B, Ohman ML, Wallberg-Jonsson S. Increased incidence of stroke and impaired prognosis after stroke among patients with seropositive rheumatoid arthritis. *Clinical and experimental rheumatology*. 2009;27(4):641-4.
90. Bacani AK, Gabriel SE, Crowson CS, Heit JA, Matteson EL. Noncardiac vascular disease in rheumatoid arthritis: increase in venous thromboembolic events? *Arthritis and rheumatism*. 2012;64(1):53-61.
91. Hill MD, Silver FL, Austin PC, Tu JV. Rate of stroke recurrence in patients with primary intracerebral hemorrhage. *Stroke; a journal of cerebral circulation*. 2000;31(1):123-7.
92. Kaplan MJ. Management of cardiovascular disease risk in chronic inflammatory disorders. *Nature reviews Rheumatology*. 2009;5(4):208-17.
93. Warrington KJ, Kent PD, Frye RL, Lymp JF, Kopecky SL, Goronzy JJ, et al. Rheumatoid arthritis is an independent risk factor for multi-vessel coronary artery disease: a case control study. *Arthritis research & therapy*. 2005;7(5):R984-91.
94. Maradit-Kremers H, Nicola PJ, Crowson CS, Ballman KV, Gabriel SE. Cardiovascular death in rheumatoid arthritis: a population-based study. *Arthritis and rheumatism*. 2005;52(3):722-32.
95. Leipe J, Grunke M, Dechant C, Reindl C, Kerzendorf U, Schulze-Koops H, et al. Role of Th17 cells in human autoimmune arthritis. *Arthritis and rheumatism*. 2010;62(10):2876-85.
96. Marder W, Khalatbari S, Myles JD, Hench R, Yalavarthi S, Lustig S, et al. Interleukin 17 as a novel predictor of vascular function in rheumatoid arthritis. *Ann Rheum Dis*. 2011;70(9):1550-5.
97. Madhur MS, Lob HE, McCann LA, Iwakura Y, Blinder Y, Guzik TJ, et al. Interleukin 17 promotes angiotensin II-induced hypertension and vascular dysfunction. *Hypertension*. 2010;55(2):500-7.
98. Feng W, Li W, Liu W, Wang F, Li Y, Yan W. IL-17 induces myocardial fibrosis and enhances RANKL/OPG and MMP/TIMP signaling in isoproterenol-induced heart failure. *Experimental and molecular pathology*. 2009;87(3):212-8.
99. van Es T, van Puijvelde GH, Ramos OH, Segers FM, Joosten LA, van den Berg WB, et al. Attenuated atherosclerosis upon IL-17R signaling disruption in LDLr deficient mice. *Biochemical and biophysical research communications*. 2009;388(2):261-5.
100. Fleming I, Fisslthaler B, Dimmeler S, Kemp BE, Busse R. Phosphorylation of Thr(495) regulates Ca(2+)/calmodulin-dependent endothelial nitric oxide synthase activity. *Circ Res*. 2001;88(11):E68-75.
101. Piazza M, Taiakina V, Guillemette SR, Guillemette JG, Dieckmann T. Solution structure of calmodulin bound to the target peptide of endothelial nitric oxide synthase phosphorylated at Thr495. *Biochemistry*. 2014;53(8):1241-9.

102. Kawasaki T, Delea CS, Bartter FC, Smith H. The effect of high-sodium and low-sodium intakes on blood pressure and other related variables in human subjects with idiopathic hypertension. *The American journal of medicine*. 1978;64(2):193-8.
103. Boegehold MA. The effect of high salt intake on endothelial function: reduced vascular nitric oxide in the absence of hypertension. *Journal of vascular research*. 2013;50(6):458-67.
104. Weinberger MH, Miller JZ, Luft FC, Grim CE, Fineberg NS. Definitions and characteristics of sodium sensitivity and blood pressure resistance. *Hypertension*. 1986;8(6 Pt 2):ii127-34.
105. Schmidlin O, Sebastian AF, Morris RC, Jr. What initiates the pressor effect of salt in salt-sensitive humans? Observations in normotensive blacks. *Hypertension*. 2007;49(5):1032-9.
106. He FJ, Markandu ND, Sagnella GA, MacGregor GA. Importance of the renin system in determining blood pressure fall with salt restriction in black and white hypertensives. *Hypertension*. 1998;32(5):820-4.
107. Crowley SD, Gurley SB, Oliverio MI, Pazmino AK, Griffiths R, Flannery PJ, et al. Distinct roles for the kidney and systemic tissues in blood pressure regulation by the renin-angiotensin system. *The Journal of clinical investigation*. 2005;115(4):1092-9.
108. Kotchen TA, Cowley AW, Jr., Frohlich ED. Salt in health and disease--a delicate balance. *The New England journal of medicine*. 2013;368(26):2531-2.
109. Jin Y, Kuznetsova T, Maillard M, Richart T, Thijs L, Bochud M, et al. Independent relations of left ventricular structure with the 24-hour urinary excretion of sodium and aldosterone. *Hypertension*. 2009;54(3):489-95.
110. Smyth A, O'Donnell MJ, Yusuf S, Clase CM, Teo KK, Canavan M, et al. Sodium intake and renal outcomes: a systematic review. *American journal of hypertension*. 2014;27(10):1277-84.
111. Ito S, Gordon FJ, Sved AF. Dietary salt intake alters cardiovascular responses evoked from the rostral ventrolateral medulla. *The American journal of physiology*. 1999;276(6 Pt 2):R1600-7.
112. Yamauchi K, Tsuchimochi H, Stone AJ, Stocker SD, Kaufman MP. Increased dietary salt intake enhances the exercise pressor reflex. *American journal of physiology Heart and circulatory physiology*. 2014;306(3):H450-4.
113. Chenniappan M. Blood Pressure Variability: Assessment, Prognostic Significance and Management. *The Journal of the Association of Physicians of India*. 2015;63(5):47-53.
114. Parati G, Ochoa JE, Lombardi C, Bilo G. Assessment and management of blood-pressure variability. *Nature reviews Cardiology*. 2013;10(3):143-55.
115. Ziemann SJ, Melenovsky V, Kass DA. Mechanisms, pathophysiology, and therapy of arterial stiffness. *Arteriosclerosis, thrombosis, and vascular biology*. 2005;25(5):932-43.
116. Steppan J, Barodka V, Berkowitz DE, Nyhan D. Vascular stiffness and increased pulse pressure in the aging cardiovascular system. *Cardiology research and practice*. 2011;2011:263585.
117. Et-Taouil K, Schiavi P, Levy BI, Plante GE. Sodium intake, large artery stiffness, and proteoglycans in the spontaneously hypertensive rat. *Hypertension*. 2001;38(5):1172-6.
118. Partovian C, Benetos A, Pommies JP, Mischler W, Safar ME. Effects of a chronic high-salt diet on large artery structure: role of endogenous bradykinin. *The American journal of physiology*. 1998;274(5 Pt 2):H1423-8.

119. Lenda DM, Boegehold MA. Effect of a high-salt diet on oxidant enzyme activity in skeletal muscle microcirculation. *American journal of physiology Heart and circulatory physiology*. 2002;282(2):H395-402.
120. Lenda DM, Sauls BA, Boegehold MA. Reactive oxygen species may contribute to reduced endothelium-dependent dilation in rats fed high salt. *American journal of physiology Heart and circulatory physiology*. 2000;279(1):H7-h14.
121. Nurkiewicz TR, Boegehold MA. High salt intake reduces endothelium-dependent dilation of mouse arterioles via superoxide anion generated from nitric oxide synthase. *American journal of physiology Regulatory, integrative and comparative physiology*. 2007;292(4):R1550-6.
122. Zhu J, Huang T, Lombard JH. Effect of high-salt diet on vascular relaxation and oxidative stress in mesenteric resistance arteries. *Journal of vascular research*. 2007;44(5):382-90.
123. Pesen D, Hoh JH. Micromechanical architecture of the endothelial cell cortex. *Biophysical journal*. 2005;88(1):670-9.
124. Oda T, Makino K, Yamashita I, Namba K, Maeda Y. Distinct structural changes detected by X-ray fiber diffraction in stabilization of F-actin by lowering pH and increasing ionic strength. *Biophysical journal*. 2001;80(2):841-51.
125. Koltsova SV, Trushina Y, Haloui M, Akimova OA, Tremblay J, Hamet P, et al. Ubiquitous [Na<sup>+</sup>]<sub>i</sub>/[K<sup>+</sup>]<sub>i</sub>-sensitive transcriptome in mammalian cells: evidence for Ca<sup>2+</sup><sub>i</sub>-independent excitation-transcription coupling. *PloS one*. 2012;7(5):e38032.
126. Yuan SY, Rigor RR. *Integrated Systems Physiology: From Molecule to Function to Disease. Regulation of Endothelial Barrier Function*. San Rafael (CA): Morgan & Claypool Life Sciences Copyright (c) 2011 by Morgan & Claypool Life Sciences.; 2010.
127. Kusche-Vihrog K, Schmitz B, Brand E. Salt controls endothelial and vascular phenotype. *Pflugers Archiv : European journal of physiology*. 2015;467(3):499-512.
128. Fels J, Jeggle P, Liashkovich I, Peters W, Oberleithner H. Nanomechanics of vascular endothelium. *Cell and tissue research*. 2014;355(3):727-37.
129. Kety SS, Schmidt CF. THE NITROUS OXIDE METHOD FOR THE QUANTITATIVE DETERMINATION OF CEREBRAL BLOOD FLOW IN MAN: THEORY, PROCEDURE AND NORMAL VALUES. *The Journal of clinical investigation*. 1948;27(4):476-83.
130. Zhu XH, Zhang N, Zhang Y, Ugurbil K, Chen W. New insights into central roles of cerebral oxygen metabolism in the resting and stimulus-evoked brain. *J Cereb Blood Flow Metab*. 2009;29(1):10-8.
131. Strandgaard S, Paulson OB. Regulation of cerebral blood flow in health and disease. *Journal of cardiovascular pharmacology*. 1992;19 Suppl 6:S89-93.
132. Howarth C. The contribution of astrocytes to the regulation of cerebral blood flow. *Frontiers in neuroscience*. 2014;8:103.
133. Paulson OB, Strandgaard S, Edvinsson L. Cerebral autoregulation. *Cerebrovascular and brain metabolism reviews*. 1990;2(2):161-92.
134. Muoio V, Persson PB, Sendeski MM. The neurovascular unit - concept review. *Acta physiologica (Oxford, England)*. 2014;210(4):790-8.
135. Furchgott RF, Zawadzki JV. The obligatory role of endothelial cells in the relaxation of arterial smooth muscle by acetylcholine. *Nature*. 1980;288(5789):373-6.

136. Vanhoutte PM. How We Learned to Say NO. *Arteriosclerosis, thrombosis, and vascular biology*. 2009;29(8):1156-60.
137. Moncada S, Gryglewski R, Bunting S, Vane JR. An enzyme isolated from arteries transforms prostaglandin endoperoxides to an unstable substance that inhibits platelet aggregation. *Nature*. 1976;263(5579):663-5.
138. Luscher TF, Vanhoutte PM. Endothelium-dependent contractions to acetylcholine in the aorta of the spontaneously hypertensive rat. *Hypertension*. 1986;8(4):344-8.
139. Feletou M, Vanhoutte PM. Endothelium-dependent hyperpolarization of canine coronary smooth muscle. *British journal of pharmacology*. 1988;93(3):515-24.
140. Yanagisawa M, Kurihara H, Kimura S, Tomobe Y, Kobayashi M, Mitsui Y, et al. A novel potent vasoconstrictor peptide produced by vascular endothelial cells. *Nature*. 1988;332(6163):411-5.
141. Katusic ZS, Vanhoutte PM. Superoxide anion is an endothelium-derived contracting factor. *The American journal of physiology*. 1989;257(1 Pt 2):H33-7.
142. Forstermann U, Closs EI, Pollock JS, Nakane M, Schwarz P, Gath I, et al. Nitric oxide synthase isozymes. Characterization, purification, molecular cloning, and functions. *Hypertension*. 1994;23(6 Pt 2):1121-31.
143. Forstermann U, Pollock JS, Schmidt HH, Heller M, Murad F. Calmodulin-dependent endothelium-derived relaxing factor/nitric oxide synthase activity is present in the particulate and cytosolic fractions of bovine aortic endothelial cells. *Proceedings of the National Academy of Sciences of the United States of America*. 1991;88(5):1788-92.
144. Tsukahara H, Gordienko DV, Goligorsky MS. Continuous monitoring of nitric oxide release from human umbilical vein endothelial cells. *Biochemical and biophysical research communications*. 1993;193(2):722-9.
145. Walter U. Physiological role of cGMP and cGMP-dependent protein kinase in the cardiovascular system. *Reviews of physiology, biochemistry and pharmacology*. 1989;113:41-88.
146. Bolotina VM, Najibi S, Palacino JJ, Pagano PJ, Cohen RA. Nitric oxide directly activates calcium-dependent potassium channels in vascular smooth muscle. *Nature*. 1994;368(6474):850-3.
147. Feletou M, Vanhoutte PM. EDHF: an update. *Clinical science (London, England : 1979)*. 2009;117(4):139-55.
148. Kwan HY, Huang Y, Yao X. TRP channels in endothelial function and dysfunction. *Biochimica et biophysica acta*. 2007;1772(8):907-14.
149. Nilius B, Droogmans G. Ion channels and their functional role in vascular endothelium. *Physiological reviews*. 2001;81(4):1415-59.
150. Somlyo AP, Somlyo AV. Signal transduction and regulation in smooth muscle. *Nature*. 1994;372(6503):231-6.
151. Jensen LJ, Holstein-Rathlou NH. The vascular conducted response in cerebral blood flow regulation. *J Cereb Blood Flow Metab*. 2013;33(5):649-56.
152. Bastin G, Heximer SP. Intracellular regulation of heterotrimeric G-protein signaling modulates vascular smooth muscle cell contraction. *Archives of biochemistry and biophysics*. 2011;510(2):182-9.
153. Babwah AV, Dale LB, Ferguson SS. Protein kinase C isoform-specific differences in the spatial-temporal regulation and decoding of metabotropic glutamate receptor 1a-

- stimulated second messenger responses. *The Journal of biological chemistry*. 2003;278(7):5419-26.
154. Martinsen A, Dessy C, Morel N. Regulation of calcium channels in smooth muscle: new insights into the role of myosin light chain kinase. *Channels (Austin, Tex)*. 2014;8(5):402-13.
  155. Gees M, Colsoul B, Nilius B. The role of transient receptor potential cation channels in Ca<sup>2+</sup> signaling. *Cold Spring Harbor perspectives in biology*. 2010;2(10):a003962.
  156. Abd El-Rahman RR, Harraz OF, Brett SE, Anfinogenova Y, Mufti RE, Goldman D, et al. Identification of L- and T-type Ca<sup>2+</sup> channels in rat cerebral arteries: role in myogenic tone development. *American journal of physiology Heart and circulatory physiology*. 2013;304(1):H58-71.
  157. Bayliss WM. On the local reactions of the arterial wall to changes of internal pressure. *The Journal of physiology*. 1902;28(3):220-31.
  158. Willie CK, Tzeng YC, Fisher JA, Ainslie PN. Integrative regulation of human brain blood flow. *The Journal of physiology*. 2014;592(Pt 5):841-59.
  159. Lassen NA. Cerebral blood flow and oxygen consumption in man. *Physiological reviews*. 1959;39(2):183-238.
  160. Westerhof N, Lankhaar JW, Westerhof BE. The arterial Windkessel. *Medical & biological engineering & computing*. 2009;47(2):131-41.
  161. Zhang R, Behbehani K, Levine BD. Dynamic pressure-flow relationship of the cerebral circulation during acute increase in arterial pressure. *The Journal of physiology*. 2009;587(Pt 11):2567-77.
  162. Chan GS, Ainslie PN, Willie CK, Taylor CE, Atkinson G, Jones H, et al. Contribution of arterial Windkessel in low-frequency cerebral hemodynamics during transient changes in blood pressure. *Journal of applied physiology (Bethesda, Md : 1985)*. 2011;110(4):917-25.
  163. Aaslid R, Blaha M, Svirid G, Douville CM, Newell DW. Asymmetric dynamic cerebral autoregulatory response to cyclic stimuli. *Stroke; a journal of cerebral circulation*. 2007;38(5):1465-9.
  164. Schmidt B, Klingelhofer J, Perkes I, Czosnyka M. Cerebral autoregulatory response depends on the direction of change in perfusion pressure. *Journal of neurotrauma*. 2009;26(5):651-6.
  165. Sorond FA, Serrador JM, Jones RN, Shaffer ML, Lipsitz LA. The sit-to-stand technique for the measurement of dynamic cerebral autoregulation. *Ultrasound in medicine & biology*. 2009;35(1):21-9.
  166. Tzeng YC CG, Willie CK, Ainslie PN. Determinants of human cerebral pressure-flow velocity relationships: new insights from vascular modelling and Ca<sup>2+</sup> channel blockade. *The Journal of physiology*. 2011;Aug 15(589 (Pt 16)).
  167. Smeda JS, King S. Electromechanical alterations in the cerebrovasculature of stroke-prone rats. *Stroke; a journal of cerebral circulation*. 2000;31(3):751-8; discussion 8-9.
  168. Daneshtalab N, Smeda JS. Alterations in the modulation of cerebrovascular tone and blood flow by nitric oxide synthases in SHRsp with stroke. *Cardiovascular research*. 2010;86(1):160-8.
  169. Smeda JS, Daneshtalab N. The effects of poststroke captopril and losartan treatment on cerebral blood flow autoregulation in SHRsp with hemorrhagic stroke. *J Cereb Blood Flow Metab*. 2011;31(2):476-85.

170. Smeda JS, McGuire JJ. Effects of poststroke losartan versus captopril treatment on myogenic and endothelial function in the cerebrovasculature of SHRsp. *Stroke; a journal of cerebral circulation*. 2007;38(5):1590-6.
171. Smeda JS, King S, Harder DR. Cerebrovascular alterations in protein kinase C-mediated constriction in stroke-prone rats. *Stroke*. 1999;30(3):656-61.
172. Smeda JS. Stroke development in stroke-prone spontaneously hypertensive rats alters the ability of cerebrovascular muscle to utilize internal Ca<sup>2+</sup> to elicit constriction. *Stroke; a journal of cerebral circulation*. 2003;34(6):1491-6.
173. Somlyo AV, Somlyo AP. Intracellular signaling in vascular smooth muscle. *Advances in experimental medicine and biology*. 1993;346:31-8.
174. Benham CD, Tsien RW. A novel receptor-operated Ca<sup>2+</sup>-permeable channel activated by ATP in smooth muscle. *Nature*. 1987;328(6127):275-8.
175. Shima H, Blaustein MP. Contrasting effects of phorbol esters on serotonin- and vasopressin-evoked contractions in rat aorta and small mesenteric artery. *Circ Res*. 1992;70(5):978-90.
176. World Health Report 2004: Changing History. Geneva, Switzerland: World Health Organization, 2004.
177. Together Against A Rising Tide: Advancing Stroke Systems of Care. Online: 2014.
178. Elijovich L, Patel PV, Hemphill JC, 3rd. Intracerebral hemorrhage. *Seminars in neurology*. 2008;28(5):657-67.
179. Mozaffarian D, Benjamin EJ, Go AS, Arnett DK, Blaha MJ, Cushman M, et al. Executive Summary: Heart Disease and Stroke Statistics-2016 Update: A Report From the American Heart Association. *Circulation*. 2016;133(4):447-54.
180. McCormick WF, Rosenfield DB. Massive brain hemorrhage: a review of 144 cases and an examination of their causes. *Stroke; a journal of cerebral circulation*. 1973;4(6):946-54.
181. Foulkes MA, Wolf PA, Price TR, Mohr JP, Hier DB. The Stroke Data Bank: design, methods, and baseline characteristics. *Stroke; a journal of cerebral circulation*. 1988;19(5):547-54.
182. O'Donnell HC, Rosand J, Knudsen KA, Furie KL, Segal AZ, Chiu RI, et al. Apolipoprotein E genotype and the risk of recurrent lobar intracerebral hemorrhage. *The New England journal of medicine*. 2000;342(4):240-5.
183. Choi JH, Mohr JP. Brain arteriovenous malformations in adults. *The Lancet Neurology*. 2005;4(5):299-308.
184. Barrow DL. Classification and natural history of cerebral vascular malformations: arteriovenous, cavernous, and venous. *J Stroke Cerebrovasc Dis*. 1997;6(4):264-7.
185. Broderick JP, Brott T, Tomsick T, Huster G, Miller R. The risk of subarachnoid and intracerebral hemorrhages in blacks as compared with whites. *The New England journal of medicine*. 1992;326(11):733-6.
186. Suzuki K, Kutsuzawa T, Takita K, Ito M, Sakamoto T, Hirayama A, et al. Clinico-epidemiologic study of stroke in Akita, Japan. *Stroke; a journal of cerebral circulation*. 1987;18(2):402-6.
187. Qureshi AI, Giles WH, Croft JB. Racial differences in the incidence of intracerebral hemorrhage: effects of blood pressure and education. *Neurology*. 1999;52(8):1617-21.

188. Giroud M, Gras P, Chadan N, Beuriat P, Milan C, Arveux P, et al. Cerebral haemorrhage in a French prospective population study. *Journal of neurology, neurosurgery, and psychiatry*. 1991;54(7):595-8.
189. Qureshi AI, Tuhim S, Broderick JP, Batjer HH, Hondo H, Hanley DF. Spontaneous intracerebral hemorrhage. *The New England journal of medicine*. 2001;344(19):1450-60.
190. Dennis MS, Burn JP, Sandercock PA, Bamford JM, Wade DT, Warlow CP. Long-term survival after first-ever stroke: the Oxfordshire Community Stroke Project. *Stroke; a journal of cerebral circulation*. 1993;24(6):796-800.
191. Broderick JP, Brott TG, Duldner JE, Tomsick T, Huster G. Volume of intracerebral hemorrhage. A powerful and easy-to-use predictor of 30-day mortality. *Stroke; a journal of cerebral circulation*. 1993;24(7):987-93.
192. Brott T, Thalinger K, Hertzberg V. Hypertension as a risk factor for spontaneous intracerebral hemorrhage. *Stroke; a journal of cerebral circulation*. 1986;17(6):1078-83.
193. Prevention of stroke by antihypertensive drug treatment in older persons with isolated systolic hypertension. Final results of the Systolic Hypertension in the Elderly Program (SHEP). SHEP Cooperative Research Group. *Jama*. 1991;265(24):3255-64.
194. Furlan AJ, Whisnant JP, Elveback LR. The decreasing incidence of primary intracerebral hemorrhage: a population study. *Annals of neurology*. 1979;5(4):367-73.
195. Five-year findings of the hypertension detection and follow-up program. III. Reduction in stroke incidence among persons with high blood pressure. Hypertension Detection and Follow-up Program Cooperative Group. *Jama*. 1982;247(5):633-8.
196. Choi-Kwon S, Kim JS. Lifestyle factors and risk of stroke in Seoul, south Korea. *J Stroke Cerebrovasc Dis*. 1998;7(6):414-20.
197. Gorelick PB. Stroke prevention. *Archives of neurology*. 1995;52(4):347-55.
198. Catto AJ, Kohler HP, Bannan S, Stickland M, Carter A, Grant PJ. Factor XIII Val 34 Leu: a novel association with primary intracerebral hemorrhage. *Stroke; a journal of cerebral circulation*. 1998;29(4):813-6.
199. Iso H, Jacobs DR, Jr., Wentworth D, Neaton JD, Cohen JD. Serum cholesterol levels and six-year mortality from stroke in 350,977 men screened for the multiple risk factor intervention trial. *The New England journal of medicine*. 1989;320(14):904-10.
200. Sutherland GR, Auer RN. Primary intracerebral hemorrhage. *Journal of clinical neuroscience : official journal of the Neurosurgical Society of Australasia*. 2006;13(5):511-7.
201. Kim BJ, Lee SH. Cerebral microbleeds: their associated factors, radiologic findings, and clinical implications. *Journal of stroke*. 2013;15(3):153-63.
202. Takebayashi S, Kaneko M. Electron microscopic studies of ruptured arteries in hypertensive intracerebral hemorrhage. *Stroke; a journal of cerebral circulation*. 1983;14(1):28-36.
203. Fisher CM. Pathological observations in hypertensive cerebral hemorrhage. *Journal of neuropathology and experimental neurology*. 1971;30(3):536-50.
204. Ohwaki K, Yano E, Nagashima H, Hirata M, Nakagomi T, Tamura A. Blood pressure management in acute intracerebral hemorrhage: relationship between elevated blood pressure and hematoma enlargement. *Stroke; a journal of cerebral circulation*. 2004;35(6):1364-7.

205. Brott T, Broderick J, Kothari R, Barsan W, Tomsick T, Sauerbeck L, et al. Early hemorrhage growth in patients with intracerebral hemorrhage. *Stroke; a journal of cerebral circulation*. 1997;28(1):1-5.
206. Okamoto K, Aoki K. Development of a strain of spontaneously hypertensive rats. *Japanese circulation journal*. 1963;27:282-93.
207. Yamori Y. Importance of genetic factors in stroke: an evidence obtained by selective breeding of stroke-prone and -resistant SHR. *Japanese circulation journal*. 1974;38(12):1095-100.
208. Harper SL, Bohlen HG. Microvascular adaptation in the cerebral cortex of adult spontaneously hypertensive rats. *Hypertension*. 1984;6(3):408-19.
209. Baumbach GL, Heistad DD. Cerebral circulation in chronic arterial hypertension. *Hypertension*. 1988;12(2):89-95.
210. Baumbach GL, Hajdu MA. Mechanics and composition of cerebral arterioles in renal and spontaneously hypertensive rats. *Hypertension*. 1993;21(6 Pt 1):816-26.
211. Okamoto K YY, Nagaoka A. Establishment of a stroke-prone spontaneously hypertensive rat (SHR). *Circ Res*. 1974;34/35:1143-153.
212. Yamori Y, Horie R, Tanase H, Fujiwara K, Nara Y, Lovenberg W. Possible role of nutritional factors in the incidence of cerebral lesions in stroke-prone spontaneously hypertensive rats. *Hypertension*. 1984;6(1):49-53.
213. Smeda JS. Hemorrhagic stroke development in spontaneously hypertensive rats fed a North American, Japanese-style diet. *Stroke; a journal of cerebral circulation*. 1989;20(9):1212-8.
214. Slemmer JE, Shaughnessy KS, Scanlan AP, Sweeney MI, Gottschall-Pass KT. Choice of diet impacts the incidence of stroke-related symptoms in the spontaneously hypertensive stroke-prone rat model. *Can J Physiol Pharmacol*. 2012;90(2):243-8.
215. Yamori Y, Horie R, Handa H, Sato M, Fukase M. Pathogenetic similarity of strokes in stroke-prone spontaneously hypertensive rats and humans. *Stroke; a journal of cerebral circulation*. 1976;7(1):46-53.
216. Yamori Y, Horie R. Developmental course of hypertension and regional cerebral blood flow in stroke-prone spontaneously hypertensive rats. *Stroke; a journal of cerebral circulation*. 1977;8(4):456-61.
217. Ogata J, Fujishima M, Tamaki K, Nakatomi Y, Ishitsuka T, Omae T. Vascular changes underlying cerebral lesions in stroke-prone spontaneously hypertensive rats. A serial section study. *Acta neuropathologica*. 1981;54(3):183-8.
218. Smeda JS, McGuire JJ, Daneshtalab N. Protease-activated receptor 2 and bradykinin-mediated vasodilation in the cerebral arteries of stroke-prone rats. *Peptides*. 2010;31(2):227-37.
219. Goldkuhl R, Jacobsen KR, Kalliokoski O, Hau J, Abelson KS. Plasma concentrations of corticosterone and buprenorphine in rats subjected to jugular vein catheterization. *Lab Anim*. 2010;44(4):337-43.
220. Hall TJ, Jagher B, Schaeublin M, Wiesenberg I. The analgesic drug buprenorphine inhibits osteoclastic bone resorption in vitro, but is proinflammatory in rat adjuvant arthritis. *Inflamm Res*. 1996;45(6):299-302.
221. Ilback NG, Siller M, Stalhandske T. Effects of buprenorphine on body temperature, locomotor activity and cardiovascular function when assessed by telemetric monitoring in rats. *Lab Anim*. 2008;42(2):149-60.

222. Udaka K, Takeuchi Y, Movat HZ. Simple method for quantitation of enhanced vascular permeability. *Proc Soc Exp Biol Med.* 1970;133(4):1384-7.
223. Baumbach GL, Faraci FM, Heistad DD. Effects of local reduction in pressure on endothelium-dependent responses of cerebral arterioles. *Stroke; a journal of cerebral circulation.* 1994;25(7):1456-61; discussion 61-2.
224. Baumbach GL, Heistad DD. Remodeling of cerebral arterioles in chronic hypertension. *Hypertension.* 1989;13(6 Pt 2):968-72.
225. Yamori Y. The development of Spontaneously Hypertensive Rat (SHR) and of various spontaneous rat models, and their implications. *Handbook of Hypertension Vol 4 Experimental and genetic models of hypertension.* 4. Amsterdam, New York, Oxford: Elsevier; 1984. p. 224-39.
226. Takeichi N, Suzuki K, Okayasu T, Kobayashi H. Immunological depression in spontaneously hypertensive rats. *Clin Exp Immunol.* 1980;40(1):120-6.
227. Reece AS, Hulse GK. Lifetime opiate exposure as an independent and interactive cardiovascular risk factor in males: a cross-sectional clinical study. *Vascular health and risk management.* 2013;9:551-61.
228. Martinez EA, Hartsfield SM, Melendez LD, Matthews NS, Slater MR. Cardiovascular effects of buprenorphine in anesthetized dogs. *American journal of veterinary research.* 1997;58(11):1280-4.
229. Stanescu R, Lider O, van Eden W, Holoshitz J, Cohen IR. Histopathology of arthritis induced in rats by active immunization to mycobacterial antigens or by systemic transfer of T lymphocyte lines. A light and electron microscopic study of the articular surface using cationized ferritin. *Arthritis and rheumatism.* 1987;30(7):779-92.
230. Bugatti S, Manzo A, Bombardieri M, Vitolo B, Humby F, Kelly S, et al. Synovial tissue heterogeneity and peripheral blood biomarkers. *Current rheumatology reports.* 2011;13(5):440-8.
231. Chu CQ, Field M, Feldmann M, Maini RN. Localization of tumor necrosis factor alpha in synovial tissues and at the cartilage-pannus junction in patients with rheumatoid arthritis. *Arthritis and rheumatism.* 1991;34(9):1125-32.
232. Matsuno H, Yudoh K, Katayama R, Nakazawa F, Uzuki M, Sawai T, et al. The role of TNF-alpha in the pathogenesis of inflammation and joint destruction in rheumatoid arthritis (RA): a study using a human RA/SCID mouse chimera. *Rheumatology (Oxford, England).* 2002;41(3):329-37.
233. Cannon GW, Woods ML, Clayton F, Griffiths MM. Induction of arthritis in DA rats by incomplete Freund's adjuvant. *J Rheumatol.* 1993;20(1):7-11.
234. Cremer MA, Townes AS, Kang AH. Adjuvant-induced arthritis in rats. Evidence that autoimmunity to homologous collagens types I, II, IX and XI is not involved in the pathogenesis of arthritis. *Clin Exp Immunol.* 1990;82(2):307-12.
235. Kohashi O, Pearson M, Beck FJ, Alexander M. Effect of oil composition on both adjuvant-induced arthritis and delayed hypersensitivity to purified protein derivative and peptidoglycans in various rat strains. *Infect Immun.* 1977;17(2):244-9.
236. Pan K, Xia X, Guo WH, Kong LY. Suppressive effects of total alkaloids of *Lycopodium casuarinoides* on adjuvant-induced arthritis in rats. *Journal of ethnopharmacology.* 2015;159:17-22.

237. Fukuda S, Hashimoto N, Naritomi H, Nagata I, Nozaki K, Kondo S, et al. Prevention of rat cerebral aneurysm formation by inhibition of nitric oxide synthase. *Circulation*. 2000;101(21):2532-8.
238. Hosaka K, Hoh BL. Inflammation and cerebral aneurysms. *Transl Stroke Res*. 2014;5(2):190-8.
239. Kataoka H. Molecular mechanisms of the formation and progression of intracranial aneurysms. *Neurol Med Chir (Tokyo)*. 2015;55(3):214-29.
240. Penn DL, Witte SR, Komotar RJ, Sander Connolly E, Jr. The role of vascular remodeling and inflammation in the pathogenesis of intracranial aneurysms. *Journal of clinical neuroscience : official journal of the Neurosurgical Society of Australasia*. 2014;21(1):28-32.
241. Edwards DG, Farquhar WB. Vascular effects of dietary salt. *Current opinion in nephrology and hypertension*. 2015;24(1):8-13.
242. Drenjancevic-Peric I, Frisbee JC, Lombard JH. Skeletal muscle arteriolar reactivity in SS.BN13 consomic rats and Dahl salt-sensitive rats. *Hypertension*. 2003;41(5):1012-5.
243. Zhu J, Drenjancevic-Peric I, McEwen S, Friesema J, Schulta D, Yu M, et al. Role of superoxide and angiotensin II suppression in salt-induced changes in endothelial Ca<sup>2+</sup> signaling and NO production in rat aorta. *American journal of physiology Heart and circulatory physiology*. 2006;291(2):H929-38.
244. Choi HY, Park HC, Ha SK. Salt Sensitivity and Hypertension: A Paradigm Shift from Kidney Malfunction to Vascular Endothelial Dysfunction. *Electrolyte & blood pressure : E & BP*. 2015;13(1):7-16.
245. Kleinewietfeld M, Manzel A, Titze J, Kvakana H, Yosef N, Linker RA, et al. Sodium chloride drives autoimmune disease by the induction of pathogenic TH17 cells. *Nature*. 2013;496(7446):518-22.
246. Arora P. Salt, immune function, and the risk of autoimmune diseases. *Circ Cardiovasc Genet*. 2013;6(6):642-3.
247. Binger KJ, Linker RA, Muller DN, Kleinewietfeld M. Sodium chloride, SGK1, and Th17 activation. *Pflugers Arch*. 2015;467(3):543-50.
248. Croxford AL, Waisman A, Becher B. Does dietary salt induce autoimmunity? *Cell Res*. 2013;23(7):872-3.
249. Zampeli E, Vlachoyiannopoulos PG, Tzioufas AG. Treatment of rheumatoid arthritis: Unraveling the conundrum. *Journal of autoimmunity*. 2015.
250. Siebert S, Tsoukas A, Robertson J, McInnes I. Cytokines as therapeutic targets in rheumatoid arthritis and other inflammatory diseases. *Pharmacol Rev*. 2015;67(2):280-309.
251. Saklatvala J. Tumour necrosis factor alpha stimulates resorption and inhibits synthesis of proteoglycan in cartilage. *Nature*. 1986;322(6079):547-9.
252. Brennan FM, Feldmann M. Cytokines in autoimmunity. *Curr Opin Immunol*. 1992;4(6):754-9.
253. Feldmann M, Maini SR. Role of cytokines in rheumatoid arthritis: an education in pathophysiology and therapeutics. *Immunol Rev*. 2008;223:7-19.
254. Cawthorn WP, Sethi JK. TNF-alpha and adipocyte biology. *FEBS Lett*. 2008;582(1):117-31.

255. Guzik TJ, Hoch NE, Brown KA, McCann LA, Rahman A, Dikalov S, et al. Role of the T cell in the genesis of angiotensin II induced hypertension and vascular dysfunction. *J Exp Med*. 2007;204(10):2449-60.
256. Elmarakby AA, Quigley JE, Pollock DM, Imig JD. Tumor necrosis factor alpha blockade increases renal Cyp2c23 expression and slows the progression of renal damage in salt-sensitive hypertension. *Hypertension*. 2006;47(3):557-62.
257. Fahmy Wahba MG, Shehata Messiha BA, Abo-Saif AA. Ramipril and haloperidol as promising approaches in managing rheumatoid arthritis in rats. *Eur J Pharmacol*. 2015.
258. Ferreri NR, Zhao Y, Takizawa H, McGiff JC. Tumor necrosis factor-alpha-angiotensin interactions and regulation of blood pressure. *Journal of hypertension*. 1997;15(12 Pt 1):1481-4.
259. Henke N, Schmidt-Ullrich R, Dechend R, Park JK, Qadri F, Wellner M, et al. Vascular endothelial cell-specific NF-kappaB suppression attenuates hypertension-induced renal damage. *Circ Res*. 2007;101(3):268-76.
260. Izawa-Ishizawa Y, Ishizawa K, Sakurada T, Imanishi M, Miyamoto L, Fujii S, et al. Angiotensin II receptor blocker improves tumor necrosis factor-alpha-induced cytotoxicity via antioxidative effect in human glomerular endothelial cells. *Pharmacology*. 2012;90(5-6):324-31.
261. Zhang J, Patel MB, Griffiths R, Mao A, Song YS, Karlovich NS, et al. Tumor necrosis factor-alpha produced in the kidney contributes to angiotensin II-dependent hypertension. *Hypertension*. 2014;64(6):1275-81.
262. Schreiber S, Bueche CZ, Garz C, Kropf S, Kuester D, Amann K, et al. Kidney pathology precedes and predicts the pathological cascade of cerebrovascular lesions in stroke prone rats. *PloS one*. 2011;6(10):e26287.
263. Feng W, Ying WZ, Aaron KJ, Sanders PW. Transforming Growth Factor-beta Mediates Endothelial Dysfunction in Rats During High Salt Intake. *American journal of physiology Renal physiology*. 2015:ajprenal.00328.2015.
264. Durand MJ, Raffai G, Weinberg BD, Lombard JH. Angiotensin-(1-7) and low-dose angiotensin II infusion reverse salt-induced endothelial dysfunction via different mechanisms in rat middle cerebral arteries. *American journal of physiology Heart and circulatory physiology*. 2010;299(4):H1024-33.
265. Santoni G, Cardinali C, Morelli MB, Santoni M, Nabissi M, Amantini C. Danger- and pathogen-associated molecular patterns recognition by pattern-recognition receptors and ion channels of the transient receptor potential family triggers the inflammasome activation in immune cells and sensory neurons. *Journal of neuroinflammation*. 2015;12:21.
266. Kastbom A, Arlestig L, Rantapaa-Dahlqvist S. Genetic Variants of the NLRP3 Inflammasome Are Associated with Stroke in Patients with Rheumatoid Arthritis. *J Rheumatol*. 2015;42(10):1740-5.
267. Numata T, Takahashi K, Inoue R. "TRP inflammation" relationship in cardiovascular system. *Seminars in immunopathology*. 2015.
268. Chauhan A, Sun Y, Pani B, Quenumzangbe F, Sharma J, Singh BB, et al. Helminth induced suppression of macrophage activation is correlated with inhibition of calcium channel activity. *PloS one*. 2014;9(7):e101023.
269. Neumann P, Gertzberg N, Johnson A. TNF-alpha induces a decrease in eNOS promoter activity. *Am J Physiol Lung Cell Mol Physiol*. 2004;286(2):L452-9.

270. DuPont JJ, Greaney JL, Wenner MM, Lennon-Edwards SL, Sanders PW, Farquhar WB, et al. High dietary sodium intake impairs endothelium-dependent dilation in healthy salt-resistant humans. *Journal of hypertension*. 2013;31(3):530-6.
271. Lee SJ, Kim WJ, Moon SK. TNF-alpha regulates vascular smooth muscle cell responses in genetic hypertension. *International immunopharmacology*. 2009;9(7-8):837-43.
272. Pires PW, Girgla SS, Moreno G, McClain JL, Dorrance AM. Tumor necrosis factor-alpha inhibition attenuates middle cerebral artery remodeling but increases cerebral ischemic damage in hypertensive rats. *American journal of physiology Heart and circulatory physiology*. 2014;307(5):H658-69.
273. Thibonnier M. Signal transduction of V1-vascular vasopressin receptors. *Regulatory peptides*. 1992;38(1):1-11.
274. Sengupta P. The Laboratory Rat: Relating Its Age With Human's. *Int J Prev Med*. 2013;4(6):624-30.
275. Wu C, Yosef N, Thalhamer T, Zhu C, Xiao S, Kishi Y, et al. Induction of pathogenic TH17 cells by inducible salt-sensing kinase SGK1. *Nature*. 2013;496(7446):513-7.
276. Mrhova O, Albrecht I, Urbanova D. Vessel wall metabolism in SHR rats in relation to atherosclerosis. *Annals of the New York Academy of Sciences*. 1976;275:302-10.